Neutral Pion Multiplicity Studies

Marshall B. C. Scott

https://www.linkedin.com/in/marshall-scott-ph-d-17ab191b9

U.S. DEPARTMENT OF ENERGY

Argonne National Laboratory is a U.S. Department of Energy laboratory managed by UChicago Argonne, LLC.

This work is supported in part by the U.S. Department of Energy, Office of Nuclear Physics under contract No. DE-AC02-06CH11357.

Semi-Inclusive Deep Inelastic Scattering

- Our analysis is centered on the study of neutral pion hadronization.
- The SIDIS channel of interest involves the detection of the scattered electron and photons coming from neutral pion decays.
- **SIDIS variables of interest**
  - $Q^2 = -q^2 = -(l' - l)^2$: the square of the momentum transferred from the electron to the parton
  - $x_B = Q^2/2P\cdot q$: the fraction of target momentum the struck parton contained
  - $z = P\cdot P_h/P\cdot q$: the fraction of transferred momentum the resultant hadron contained
  - p_T : the transverse hadron momentum
  - $\varphi_h = \arccos[(q \times l)\cdot(q \times P_h)/(|q \times l|\cdot|q \times P_h|)]$: angle between the lepton scattering plane and the hadron plane

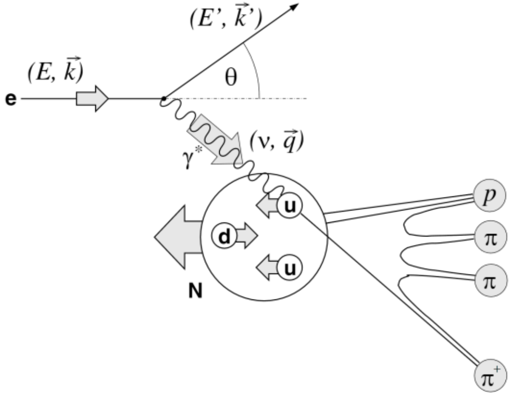

https://doi.org/10.1103/PhysRevD.71.012003

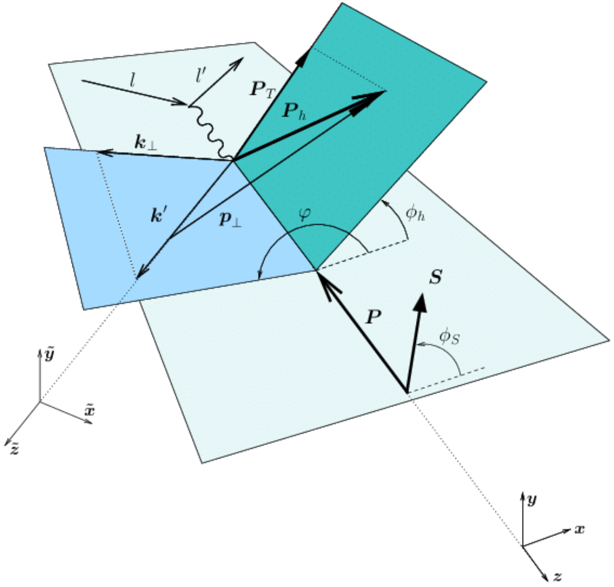

https://doi.org/10.1103/PhysRevD.75.054032

SIDIS Multiplicities

- **Goal**
  - Measure neutral pion multiplicities

$$M_h = \frac{d\sigma^h}{dxdQ^2dzdp_T^2} / \frac{d\sigma^{DIS}}{dxdQ^2}$$

  - Related to the non-perturbative proton structure, i.e., PDFs and FFs

$$\sigma^{\pi^0} \approx \sigma^{DIS} \otimes f^p(x, Q^2) \otimes D^{p\to\pi^0}(z, Q^2)$$

  - Connected to charged pion multiplicities

$$D_1^{\pi^0/q} = \frac{1}{2}\left(D_1^{\pi^+/q} + D_1^{\pi^-/q}\right)$$

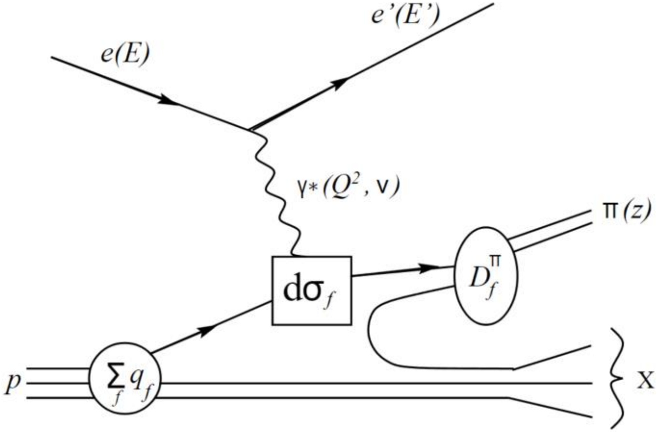

https://doi.org/10.1007/s100520100765

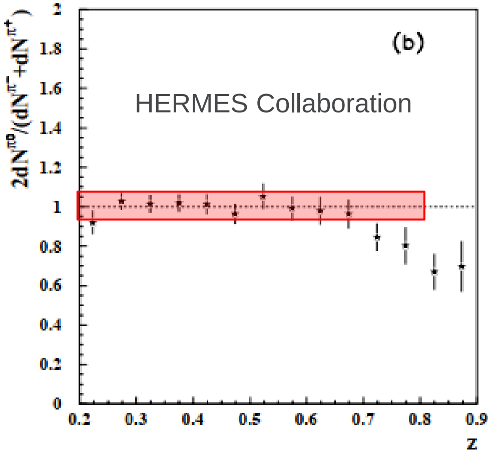

https://doi.org/10.1007/s100520100765

Data Selection

- Fall 2018 data taking period, which used a 10.6 GeV polarized election beam scattering off an unpolarized liquid hydrogen target.
- Zero net electron polarization over this run period.
- **General quality cuts**
  – Data quality cuts
  – Fiducial cuts for better data-mc agreement
  – Exactly 1 electron in Forward Detector
  – At least 2 photons in Forward Detector

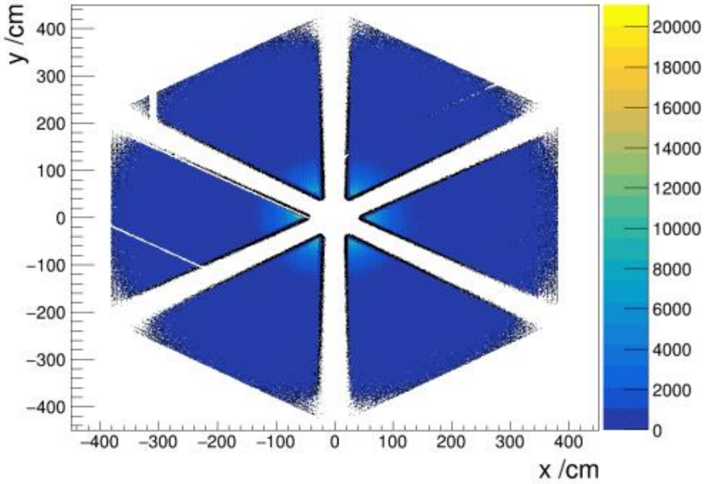

Preshower Calorimeter (PCAL) hit plane for electrons. Black points show hits before fiducial cuts were made and the overlayed colored points show the surviving hits after the cut (Internal Documentation : RG-A Analysis note).

Selection Cuts for Electrons and Photons

- **Electron**
  - $2 < p_e < 8$ GeV
  - $Q^2 > 2$ GeV^2
  - W > 2 GeV [W = |q + P|]
  - y < 0.75 [y = q•P/l•P] : remove events with large radiative effects
  - l_v & l_w > 9 cm (constant sampling fraction region)
- **Photon**
  - $E_\gamma > 0.5$ GeV : background removal
  - e-γ opening angle > 8 deg : remove radiative γs
  - 0.9 < β < 1.1 : γs with β > 1.1 are not associated with π^0s
  - l_v & l_w > 15 cm (constant sampling fraction region)

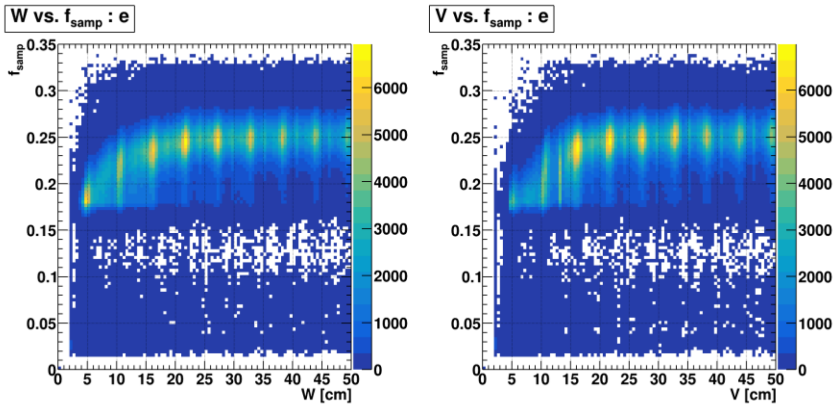

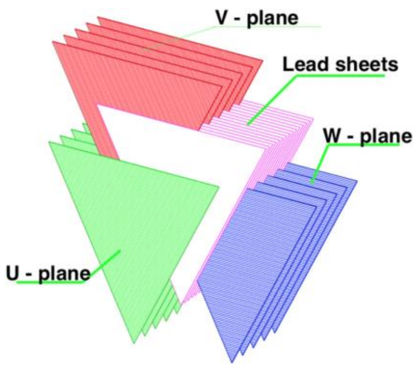

https://www.sciencedirect.com/science/article/pii/S0168900220300309

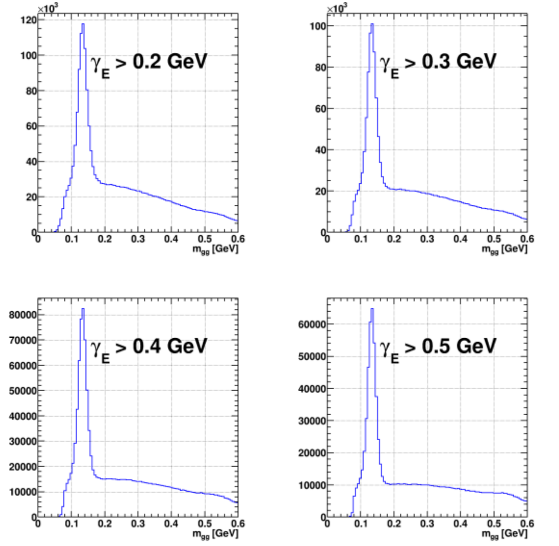

Selection Cuts for Neutral Pions

- π^0 candidates are reconstructed from photon pairs.
- The resulting invariant mass distribution shows a characteristic peak around the π^0 mass of 0.135 GeV.
- **Cuts**
  - $x_F > 0$ [$x_F = 2P_{h,L}/\sqrt{s}$] : current fragmentation region
  - $M_x > 1.5$ GeV [$M_x = |q + P - P_h|$] : remove exclusive events
  - $\alpha_{\gamma\gamma} > 6 \cdot Exp(1 - p_\pi) + 0.5$: background removal

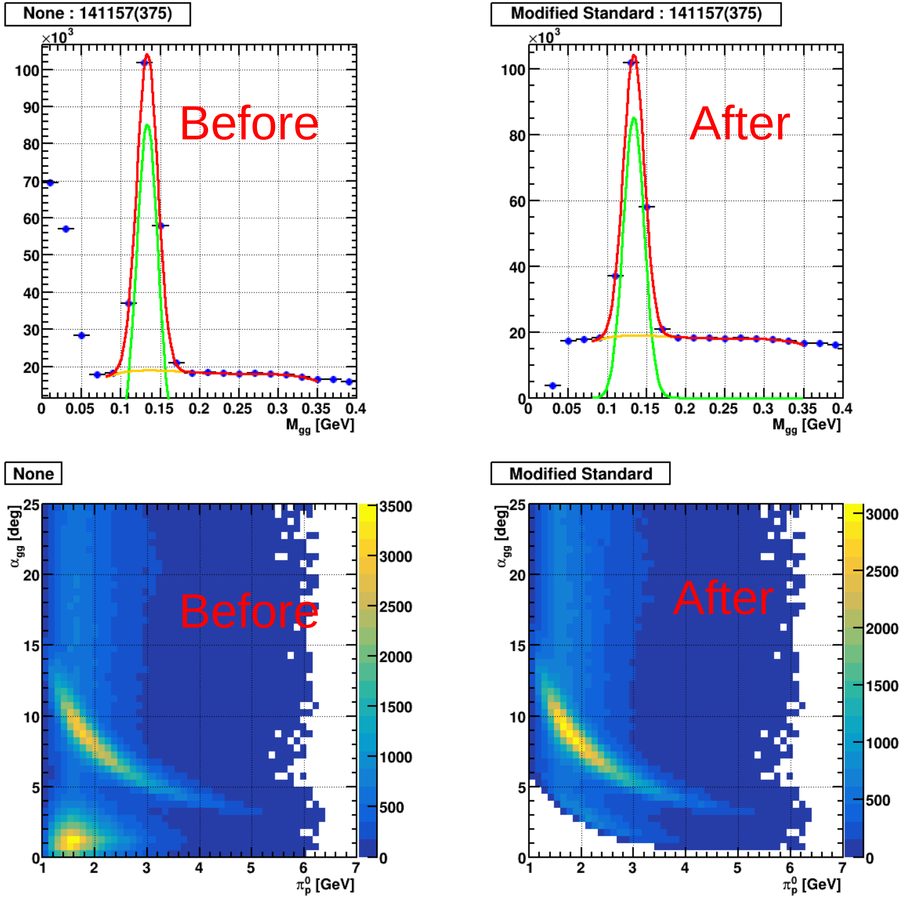

Data & Monte Carlo

- The monte carlo is created from a SIDIS generator based on LEPTO.
- The momenta, θ, and φ distributions of the electron and the two photons between the data and monte carlo agree well.

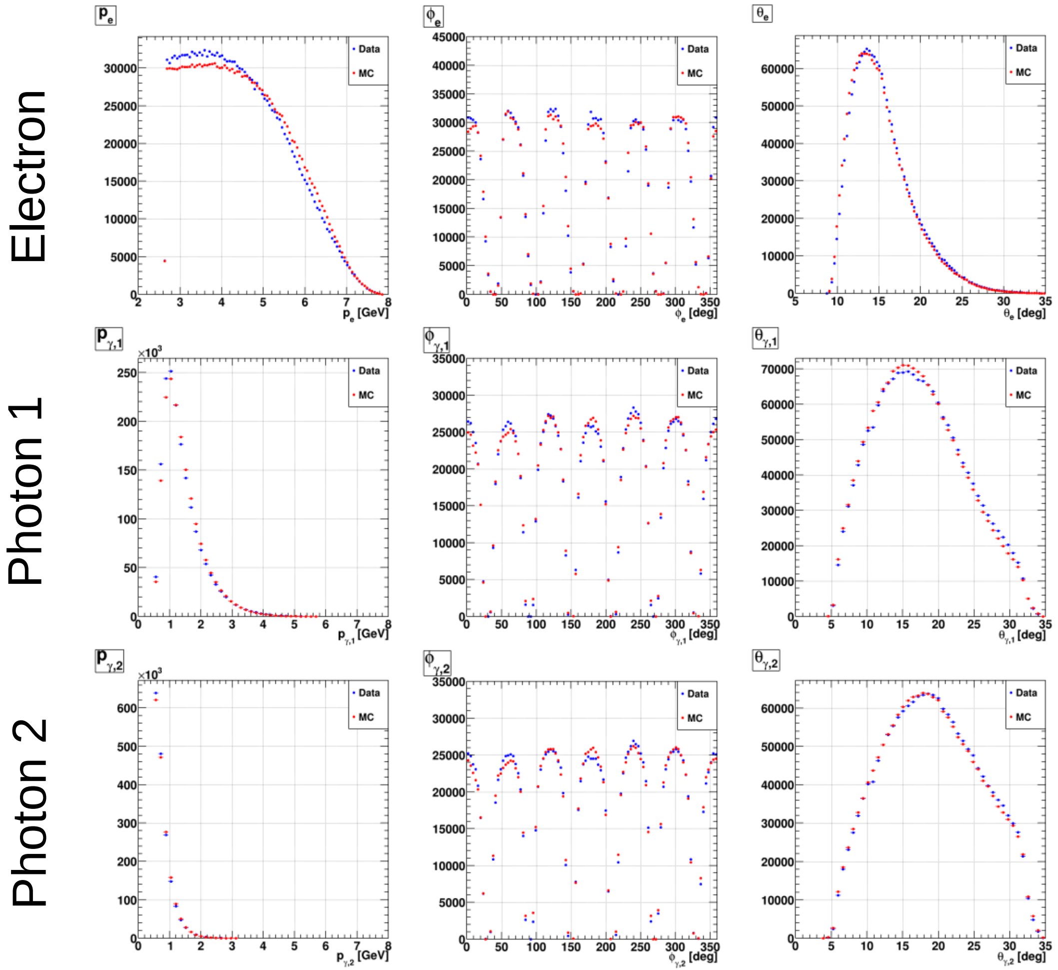

Data & Monte Carlo

- The data and monte carlo also show agreement in the x_B, Q^2, z, p_T^2, φ_h, and $m_{\gamma\gamma}$ distributions.

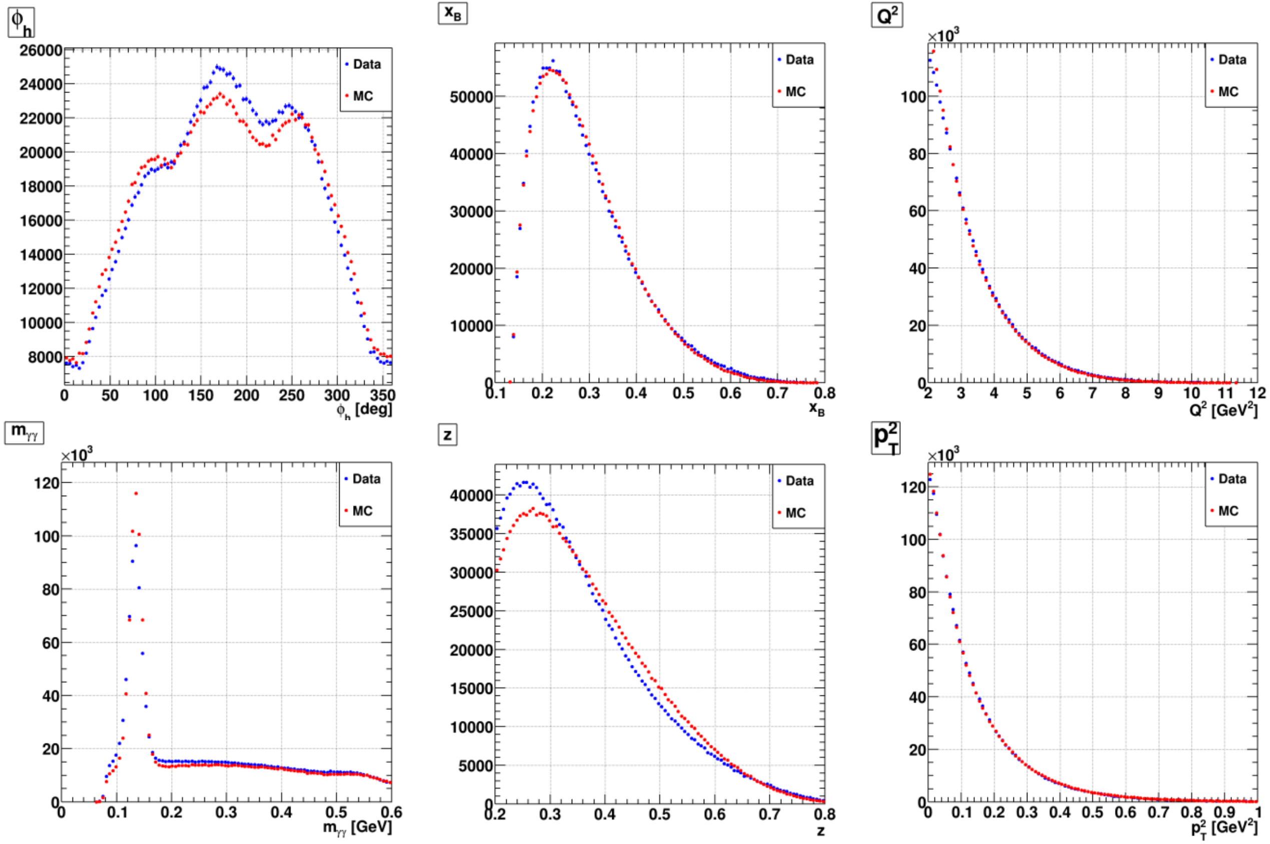

π^0 Extraction

- All photons within an event are combined into unique pairs, which become our neutral pion candidates.
- The resulting invariant mass distributions are fit, and the number of pions is extracted.
- **π^0 extraction**
  – 20 bins : 0 – 0.4 GeV
  – Fit range : 0.08 - 0.35 GeV
  – Fit function : Gaussian + pol4
  – Signal range : 5.5σ
  – Error : derived from covariance matrix of fit

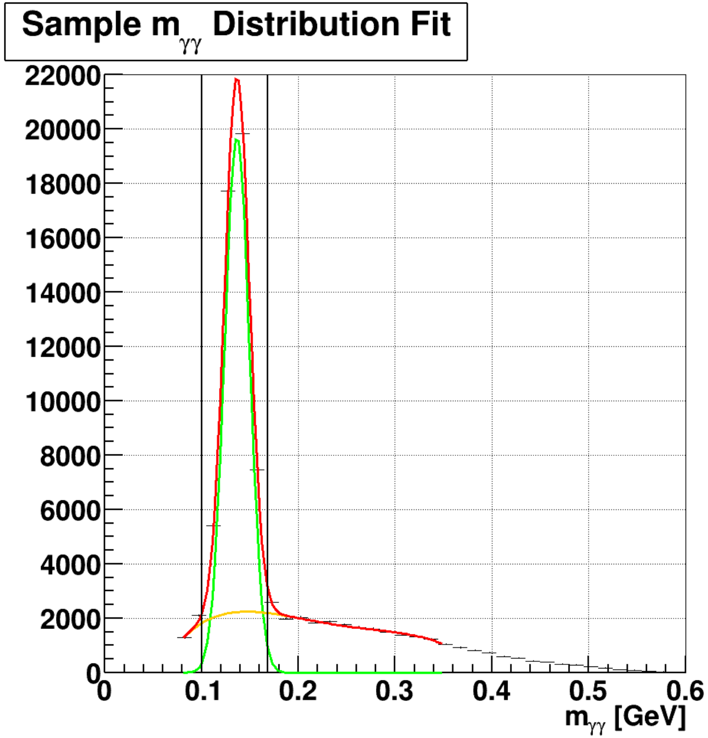

Phase space

8 z bins & 8 p_T^2 bins ∈ 13 x_B-Q^2 bins ; Integration over φ_h

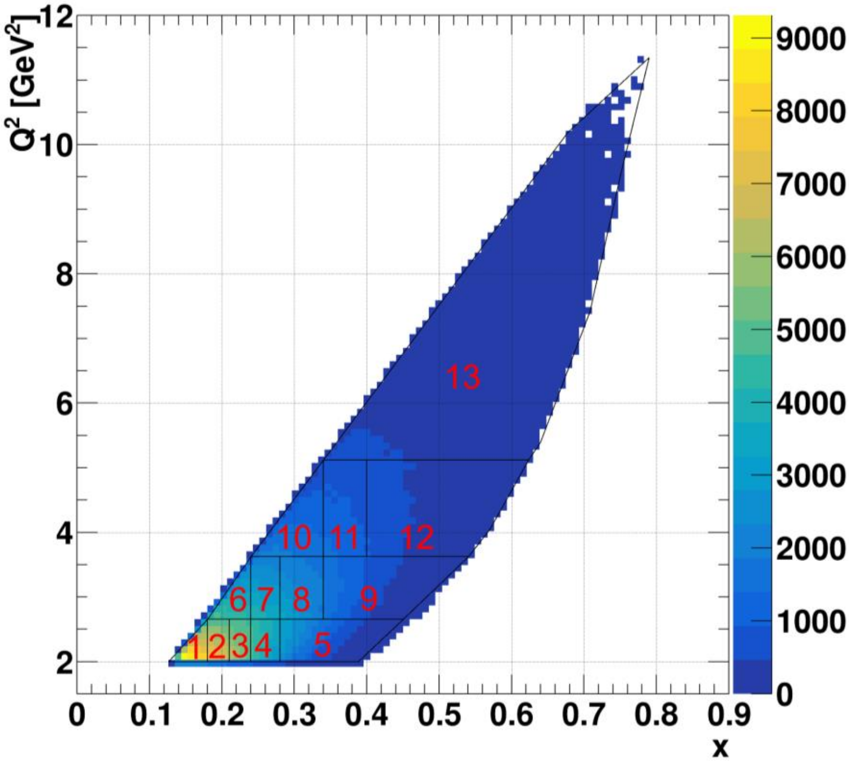

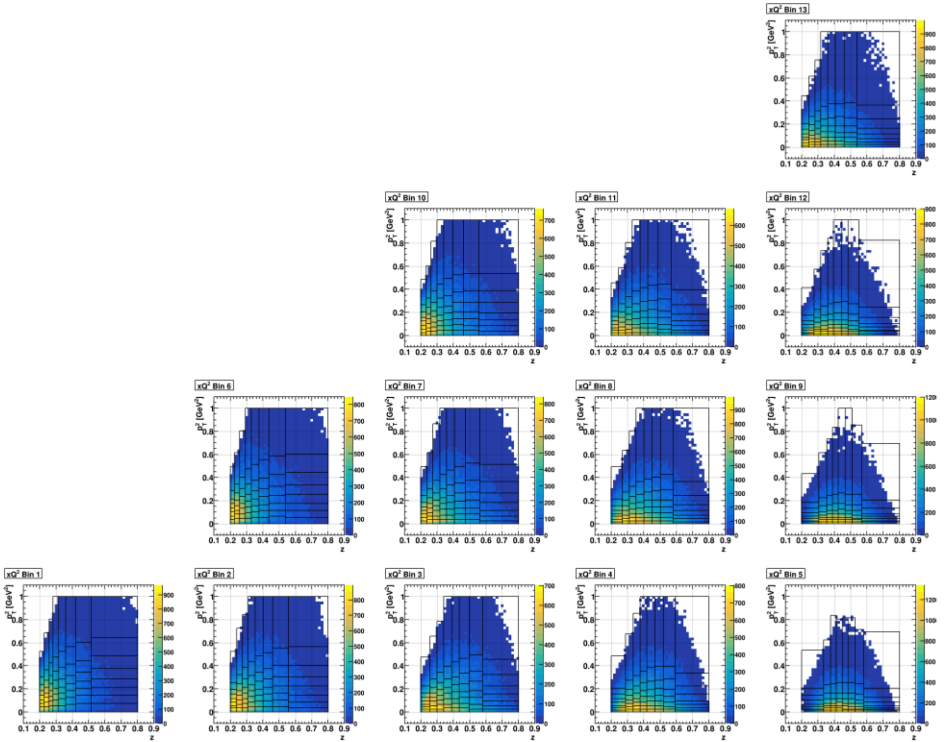

MULTIPLICITIES

- 5D multiplicity

$$M_h = \frac{d\sigma}{dxQ^2dzdp_T^2d\phi_h} / \frac{d\sigma}{dxdQ^2}$$

$$= A(1 + Bcos(\phi_h) + Ccos(2\phi_h)) / \frac{d\sigma}{dxdQ^2}$$

- For the results in this presentation, φ_h was averaged over, so the 4D multiplicity was measured, which is the ratio of the neutral pion production to the DIS cross section :

$$M_h = \frac{d\sigma}{dxQ^2dzdp_T^2} / \frac{d\sigma}{dxdQ^2}$$

Raw Multiplicities and Acceptance

- Raw multiplicity

$$M_{h,raw} = \frac{dN^{\pi^0}}{dxQ^2dzdp_T^2} \Big/ \frac{dN^{DIS}}{dxdQ^2}$$

- For the bin-by-bin acceptance*efficiency we divide the reconstructed mc by the generated mc, with the understanding that the generated mc stemmed from an event where the reconstructed electron passed all the DIS cuts.

$$A_h = \frac{dN^{\pi^0}_{rec}}{dxdQ^2dzdp_T^2} \Big/ \frac{dN^{\pi^0}_{gen}}{dxdQ^2dzdp_T^2}$$

- The final multiplicity is the raw multiplicity divided by the acceptance.

$$M_h = M_{h,raw}/A_h$$

$A_H(z, p_T^2)$ & $M_H(z, p_T^2)$ for xQ^2 Bin 1

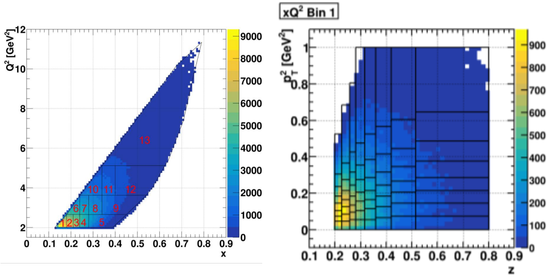

x-Q² Bin 1 : $A_H(p_T^2)$

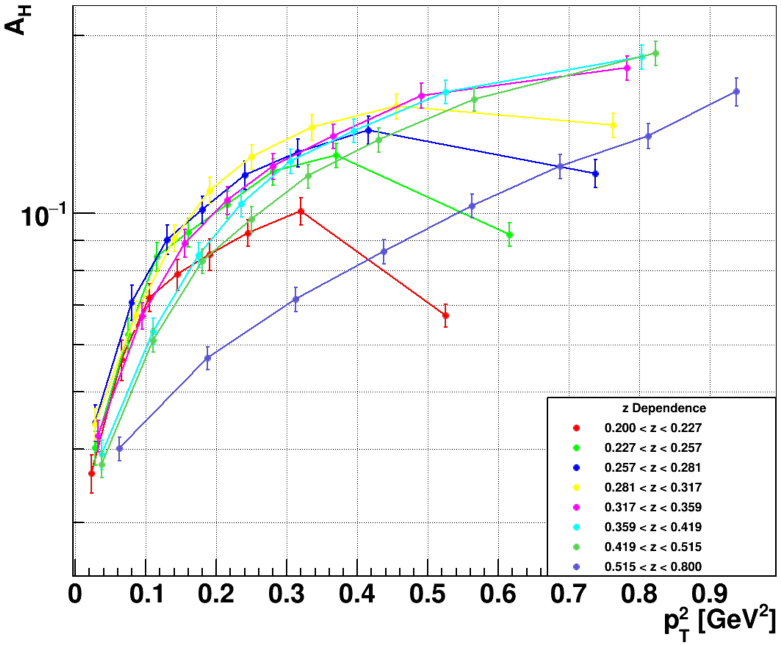

x-Q² Bin 1 : $M_H(p_T^2)$

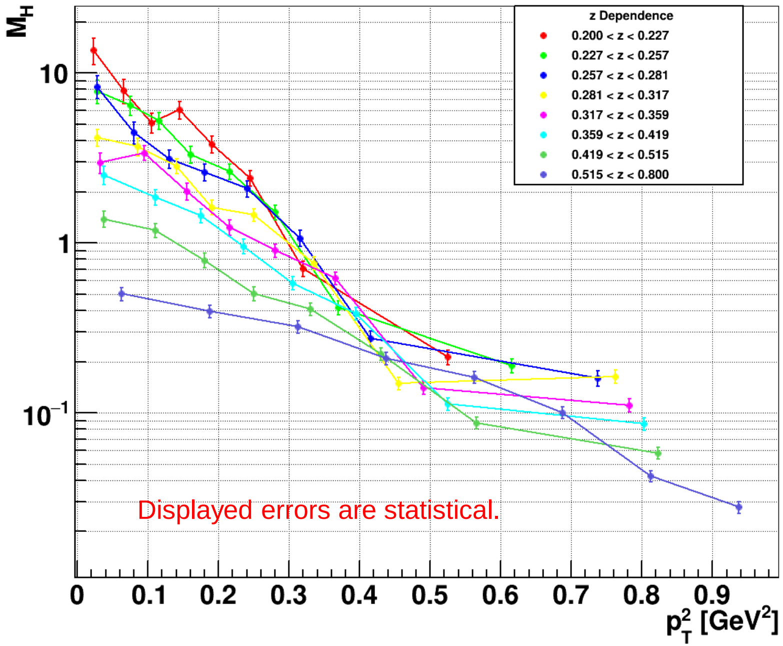

$A_H(z, p_T^2)$ & $M_H(z, p_T^2)$ for xQ^2 Bin 7

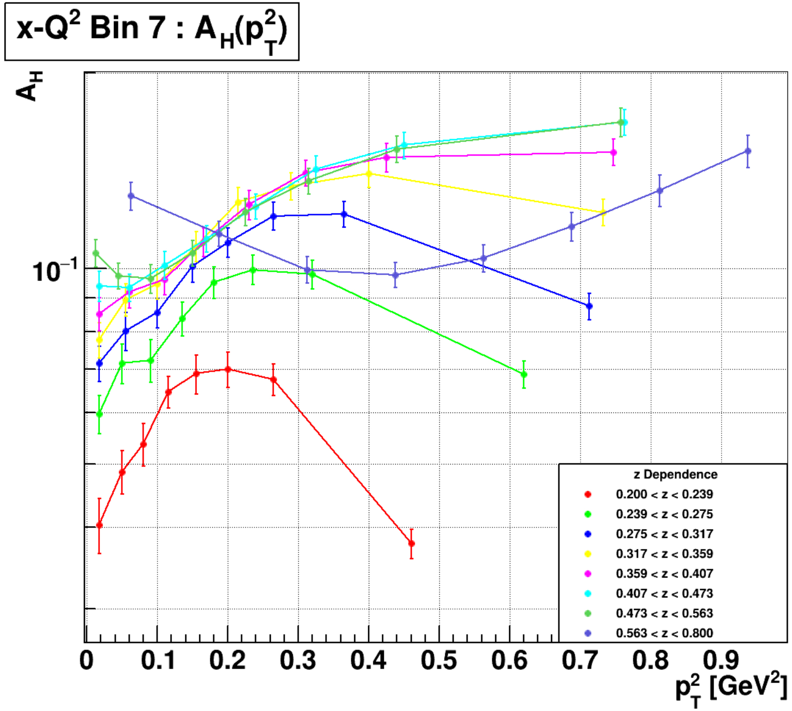

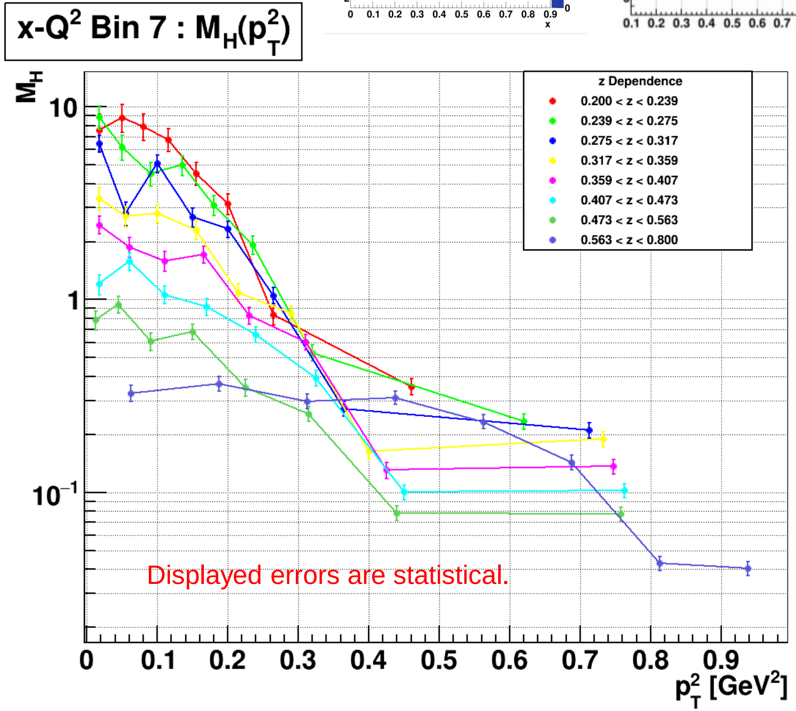

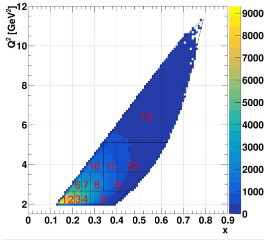

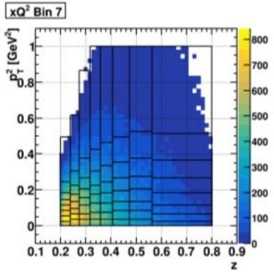

P_T^2 Integrated M_H and Leading Order Theoretical predictions

- The LO predictions used the MAPFF (https://doi.org/10.1103/PhysRevD.104.034007) and NNFF1.1h (https://doi.org/10.48550/arXiv.1807.03310) FFs and the CT10nlo PDF sets.
- The FF plots are drawn with 1σ error bands.
- NNFF contains e^+e^- annihilation and p+p data, whereas MAPFF contains annihilation data and multiplicity data.

$$M_h = \frac{\sum_q e_q^2 f_q(x) D_q(z)}{\sum_q e_q^2 f_q(x)}$$

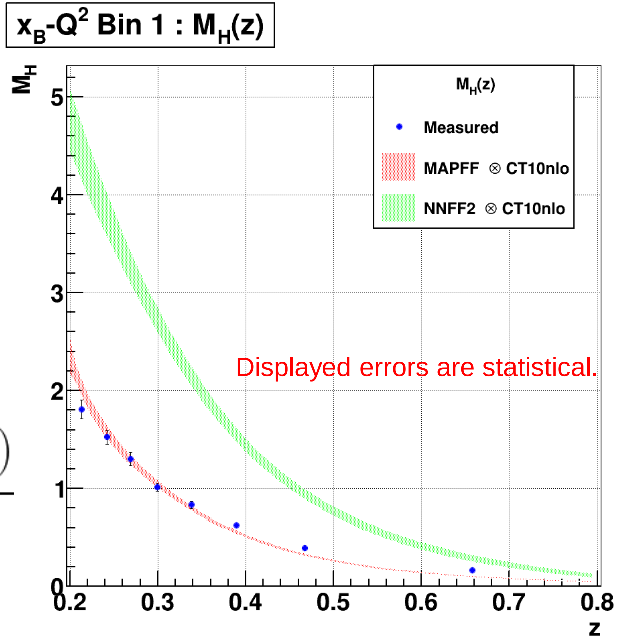

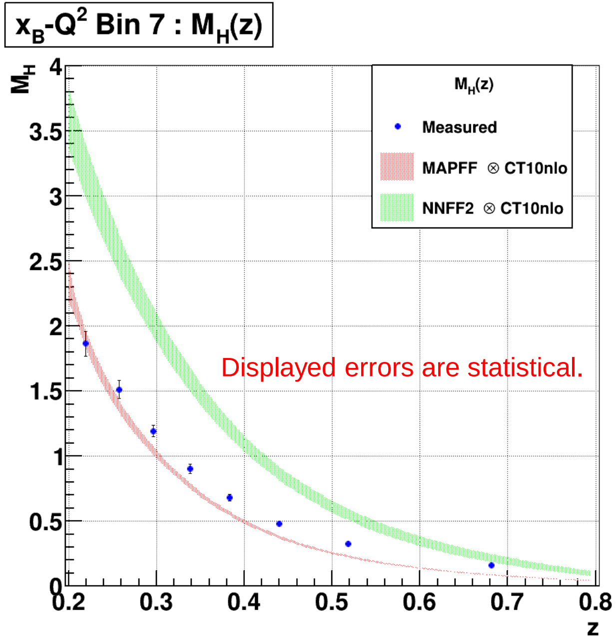

Current work : Incorporating phi trento

- Instead of averaging over the φ_h bins, now the number of pions is fit within each φ_h bin and that distribution is then fit with $A(1 + B\cos(\varphi_h) + C\cos(2\varphi_h))$.
- The resultant number of pions is then the extracted A term.
- The plots to the right show the a preliminary φ_h distribution in x_B-Q^2 1 (in the old binning) with the $A(1 + B\cos(\varphi_h) + C\cos(2\varphi_h))$ fit in red along with a pol0 fit in green.
- They are within error of each other for most bins.
- The plots for all x_B-Q^2 bins are in the backup slides.

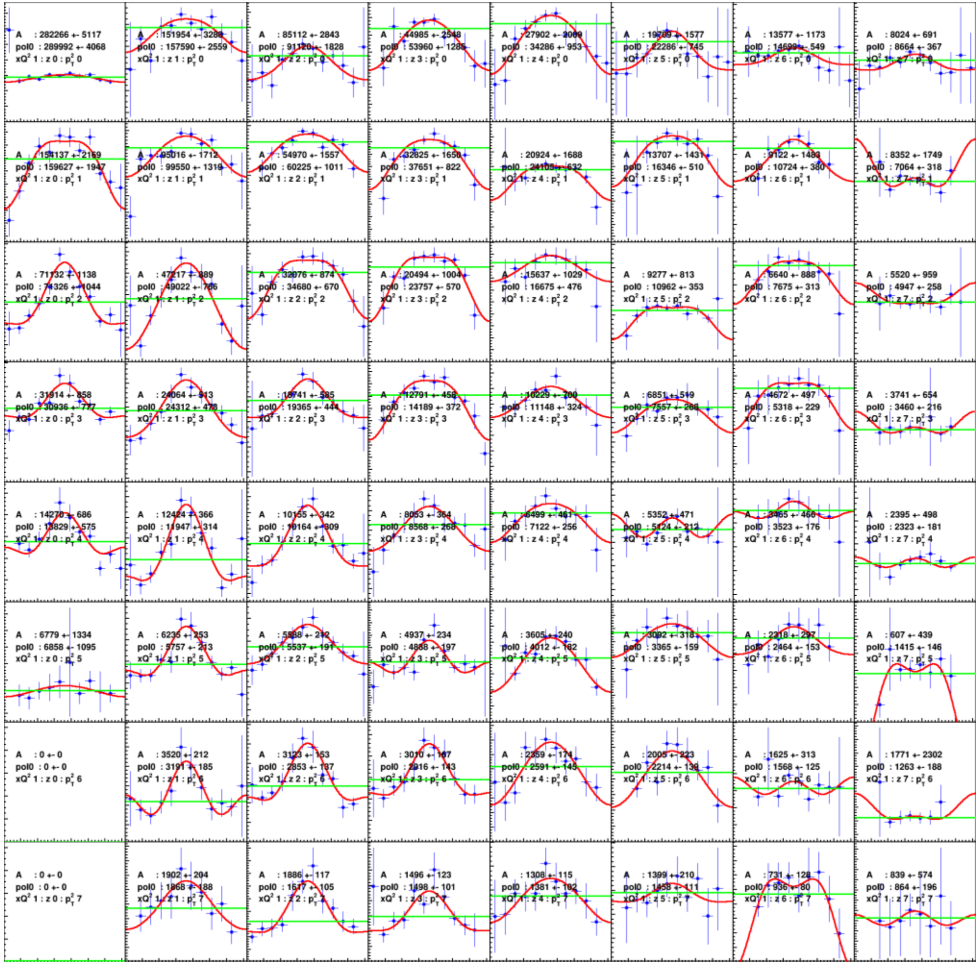

Current work : Unfolding

- Current acceptance work is using Singular Value Decomposition (SVD) and Bayesian unfolding along with the migration matrix for acceptance corrections in all bins.
- The plot to the right is a portion of the x_B-Q^2 Bin 1 3D migration matrix showing φ_h migration in the first x_B-Q^2-z-p_T^2 bin.

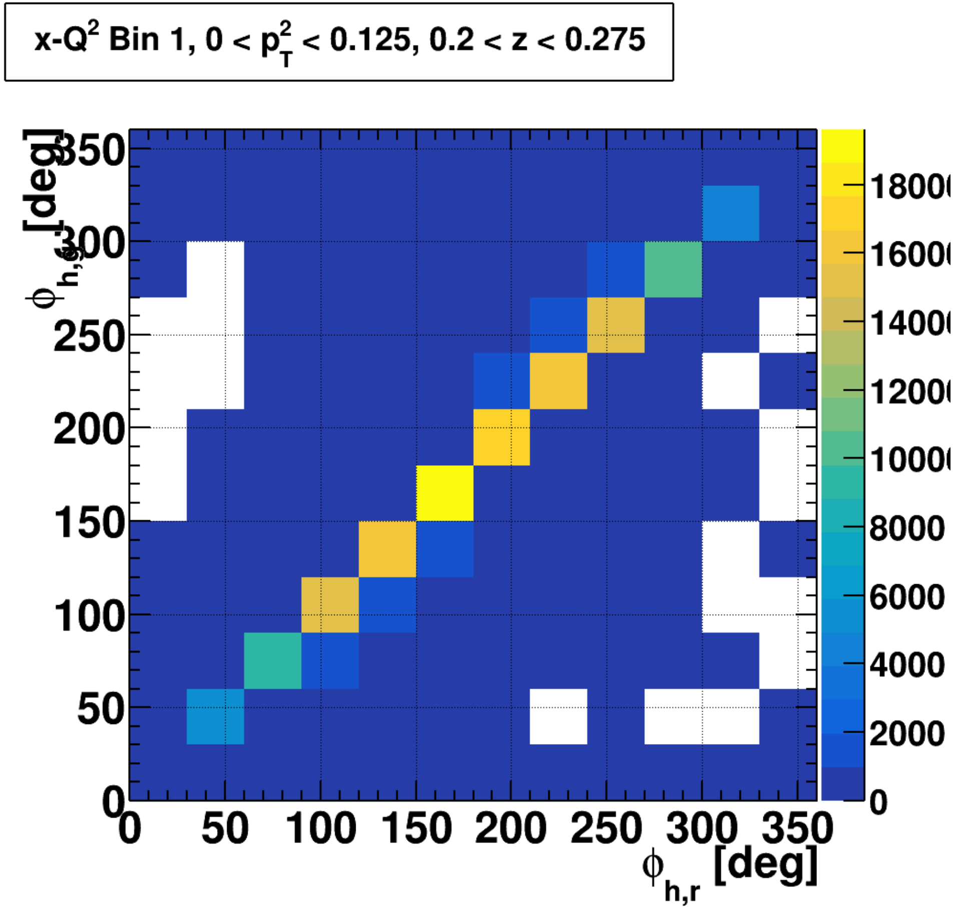

CONCLUSION

- Using the invariant mass distributions of photon pairs, the number of neutral pions has been extracted from the Fall 2018 data taking period.
- From these distributions, correcting for acceptance and efficiency, the neutral pion multiplicities was measured in the x_B-Q^2-z-p_T^2, four-dimensional kinematic phase space.
- The p_T^2 integrated multiplicities have also been extracted and shown to be inline with the MAPFF$\otimes$CT10nlo leading order predictions.
- Ongoing work is fitting the φ_h distributions for pion extraction and utilizing the migration matrix with Bayesian and SVD unfolding for acceptance corrections.
- Future work is studying radiative effects.

THANK YOU FOR YOUR ATTENTION

BACKUP SLIDES

- SIDIS CROSS SECTION
- ACCEPTANCES AND MULTIPLICITIES FOR ALL X_B-Q^2 BINS
- P_T^2 INTEGRATED MULTIPLICITIES FOR ALL X_B-Q^2 BINS
- Φ_H DISTRIBUTIONS
- M_X STUDIES

SIDIS Cross Section

$$\frac{d\sigma}{dxQ^2dzdP_{hT}^2d\phi_h} = \frac{\pi\alpha_e^2}{xQ^4}\frac{y^2}{(1-\varepsilon)}\left(1+\frac{\gamma^2}{2x}\right)\times$$
$$\left\{F_{UU,T}+\varepsilon F_{UU,L}+\sqrt{2\varepsilon(1+\varepsilon)}cos(\phi_h)F_{UU}^{cos(\phi_h)}+\varepsilon cos(2\phi_h)F_{UU}^{cos(2\phi_h)}\right\}$$

$$\frac{d\sigma}{dxQ^2dzdP_{hT}^2d\phi_h} = A\left(1+Bcos(\phi_h)+Ccos(2\phi_h)\right)$$

$$A = \frac{\pi\alpha_e^2}{xQ^4}\frac{y^2}{(1-\varepsilon)}\left(1+\frac{\gamma^2}{2x}\right)\left(F_{UU,T}+\varepsilon F_{UU,L}\right),$$
$$B = \frac{\sqrt{2\varepsilon(1+\varepsilon)}F_{UU}^{cos(\phi_h)}}{F_{UU,T}+\varepsilon F_{UU,L}}, and$$
$$C = \frac{\varepsilon cos(2\phi_h)F_{UU}^{cos(2\phi_h)}}{F_{UU,T}+\varepsilon F_{UU,L}}.$$

ACCEPTANCES AND MULTIPLICITIES FOR ALL x_B-Q^2 BINS AS FUNCTIONS OF Z

$A_H(z, p_T^2)$ & $M_H(z, p_T^2)$ for xQ^2 Bin 1

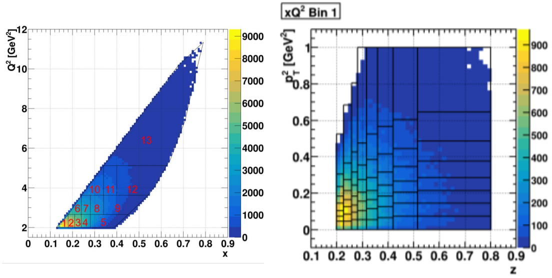

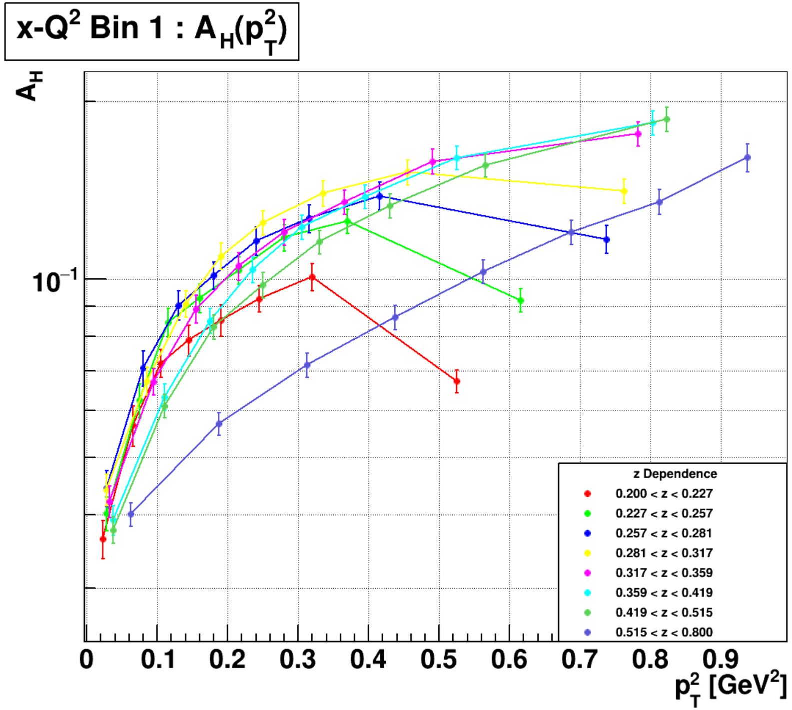

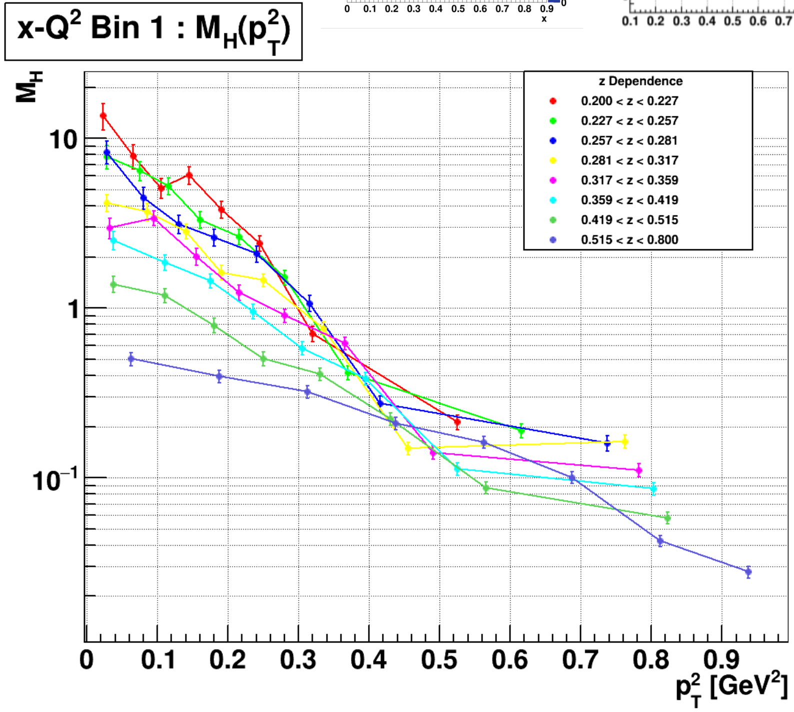

$A_H(z, p_T^2)$ & $M_H(z, p_T^2)$ for xQ^2 Bin 2

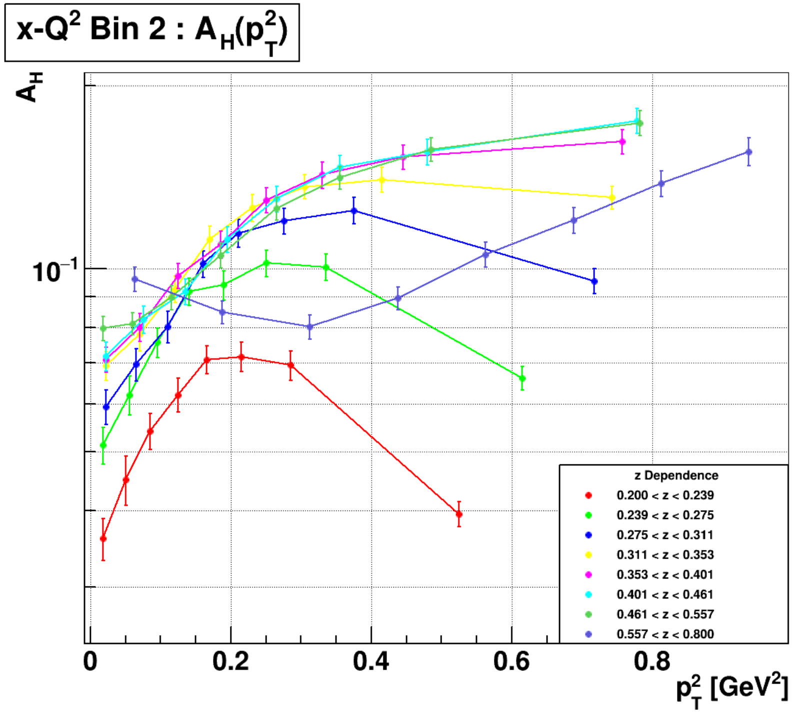

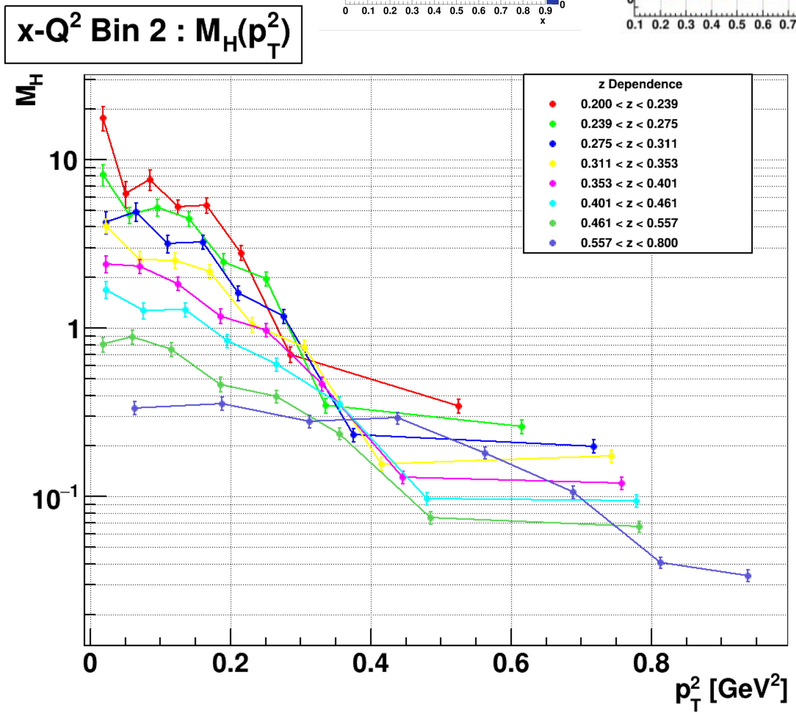

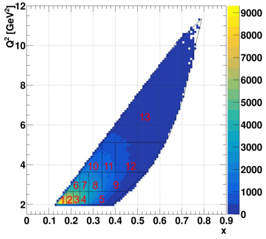

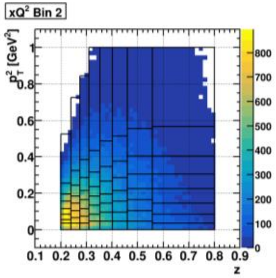

$A_H(z, p_T^2)$ & $M_H(z, p_T^2)$ for xQ^2 Bin 3

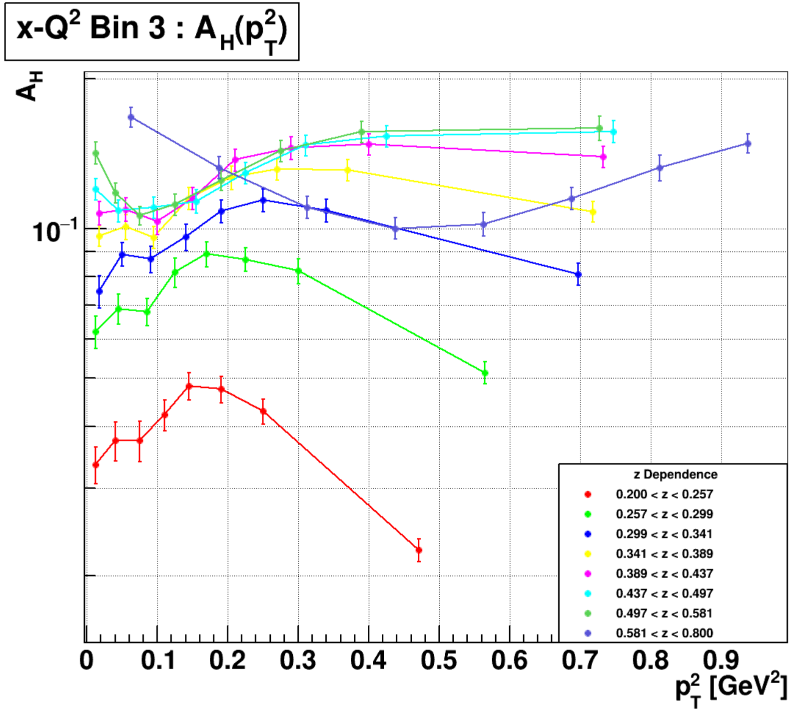

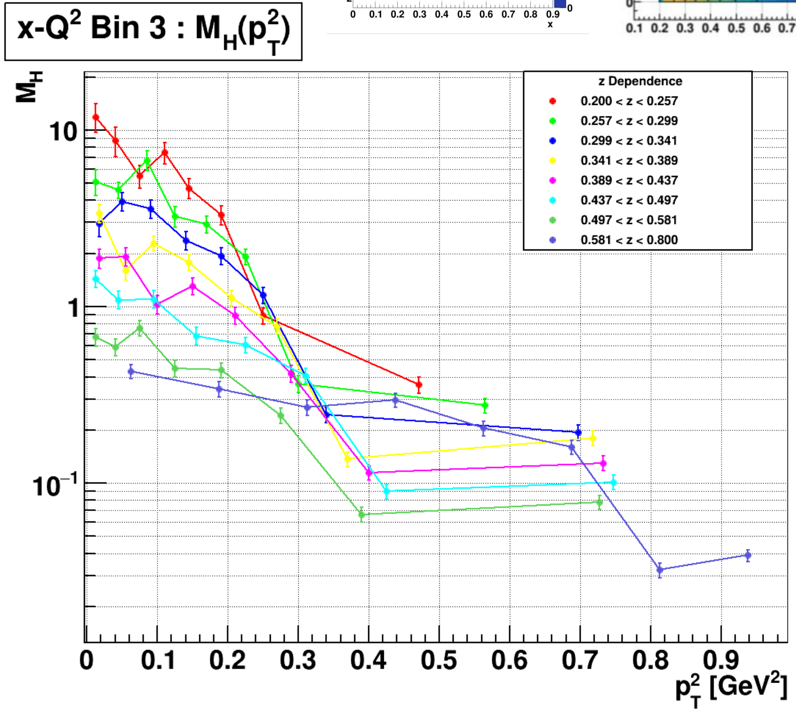

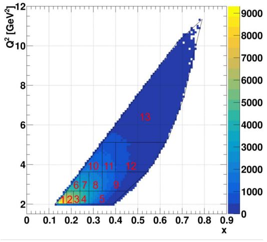

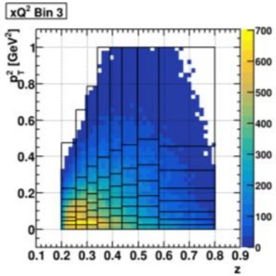

$A_H(z, p_T^2)$ & $M_H(z, p_T^2)$ for xQ^2 Bin 4

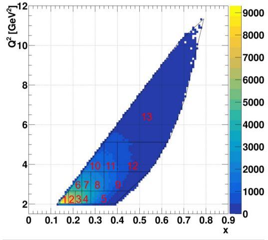

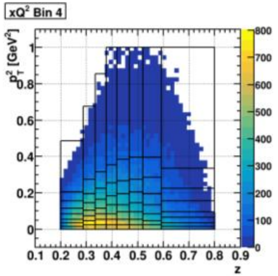

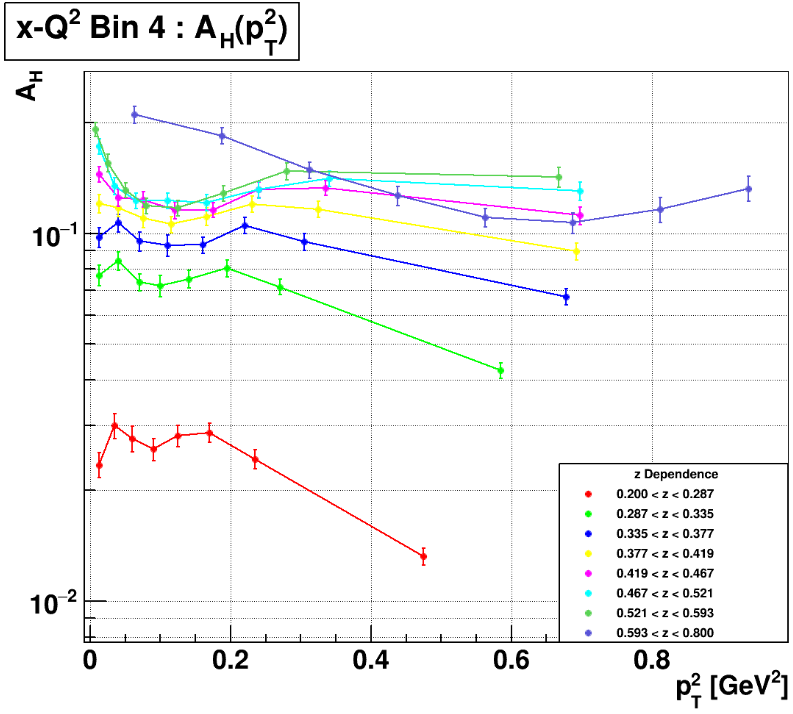

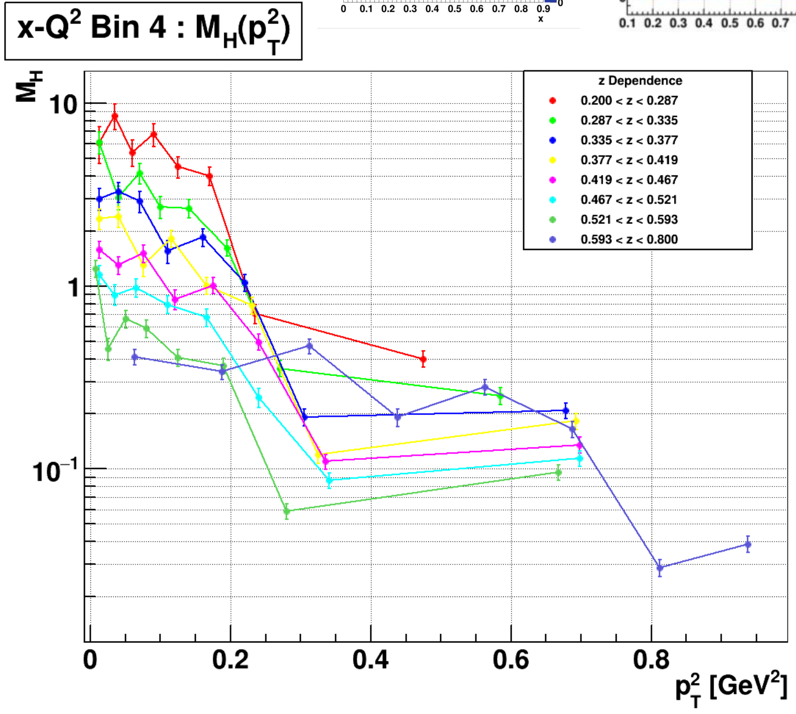

$A_H(z, p_T^2)$ & $M_H(z, p_T^2)$ for xQ^2 Bin 5

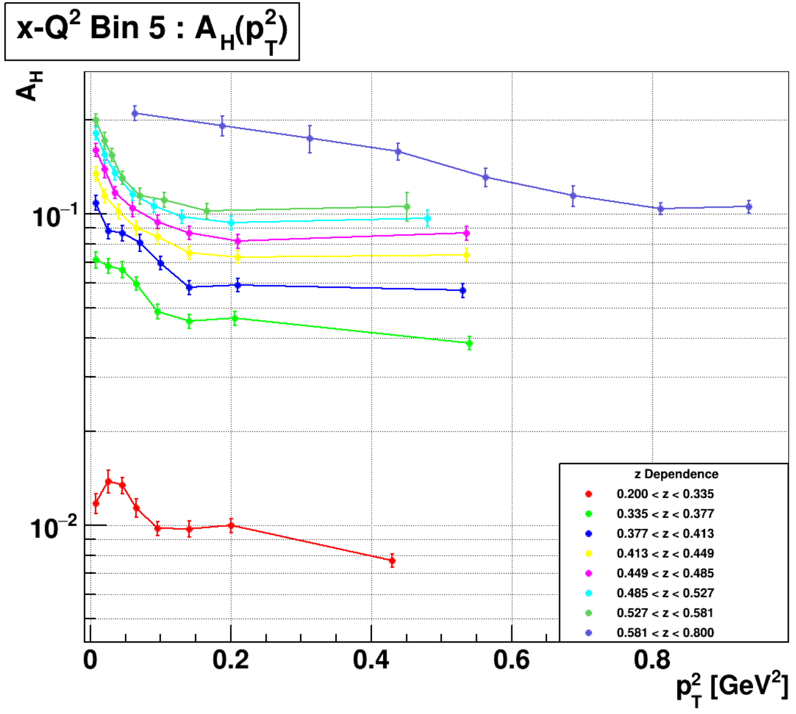

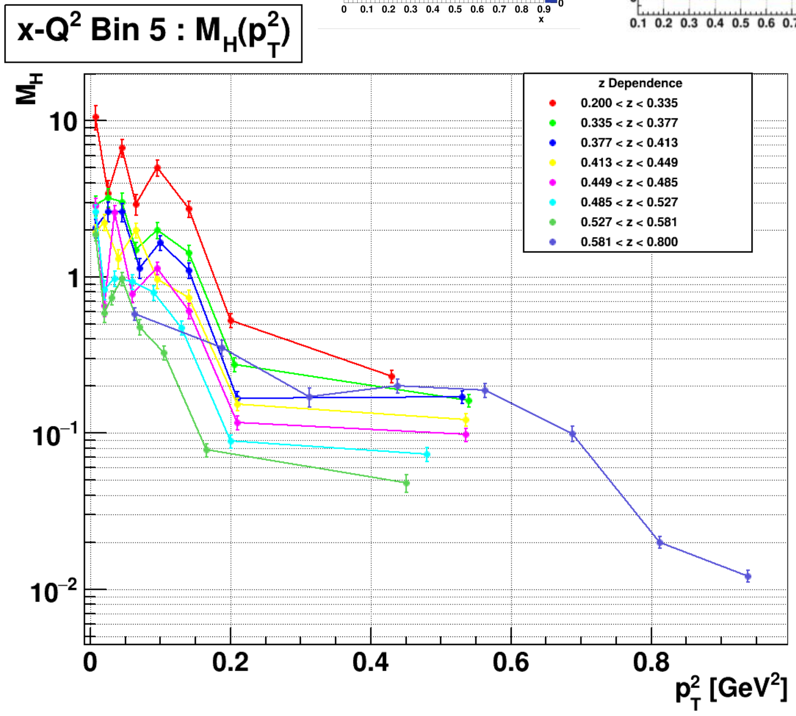

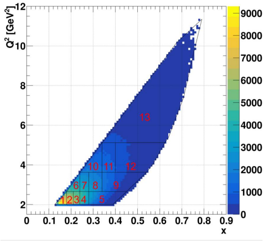

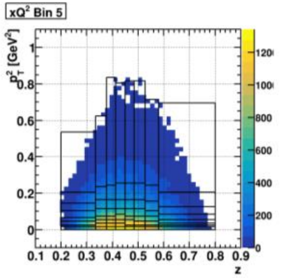

$A_H(z, p_T^2)$ & $M_H(z, p_T^2)$ for xQ^2 Bin 6

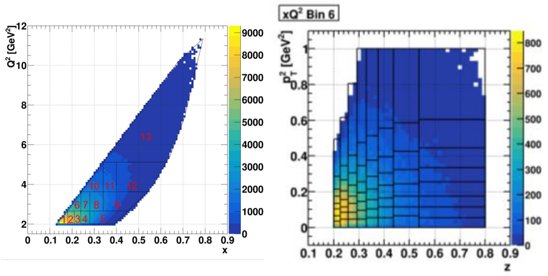

x-Q^2 Bin 6 : $A_H(p_T^2)$

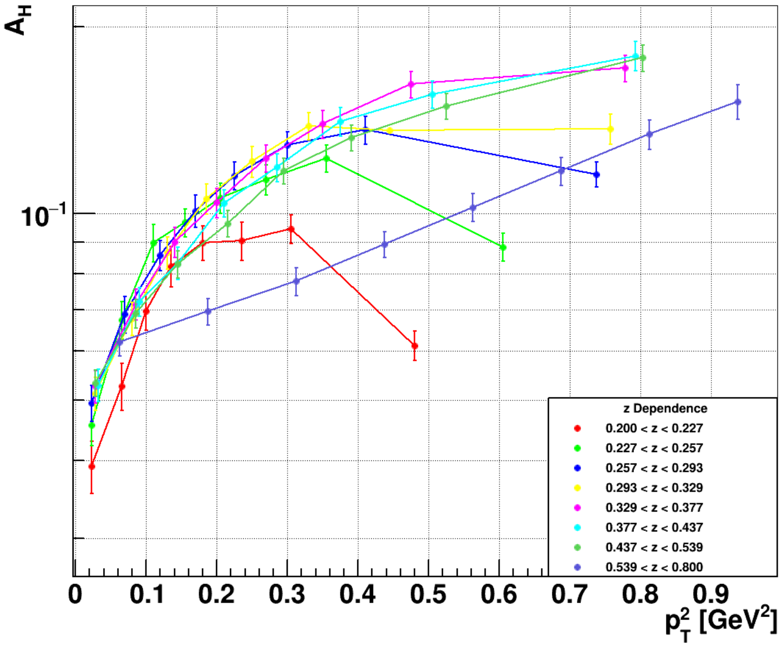

x-Q^2 Bin 6 : $M_H(p_T^2)$

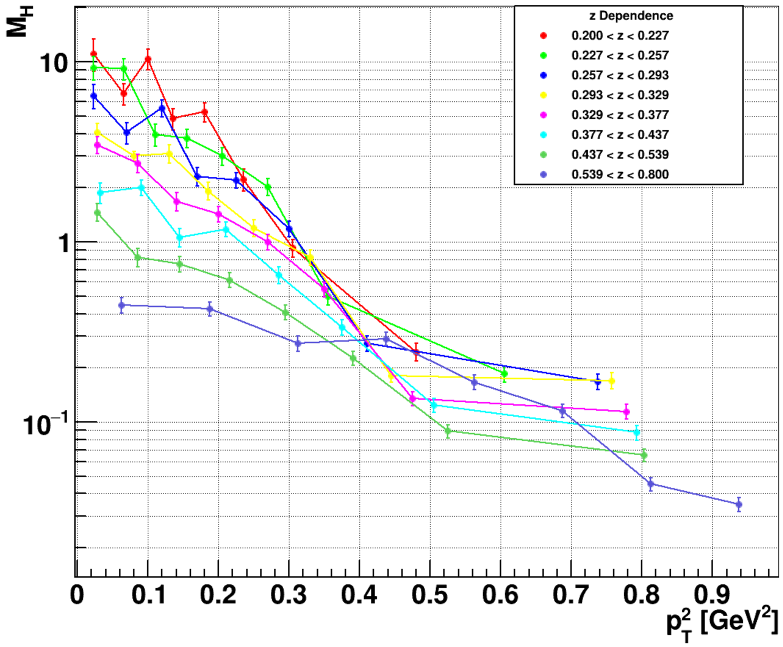

$A_H(z, p_T^2)$ & $M_H(z, p_T^2)$ for xQ^2 Bin 7

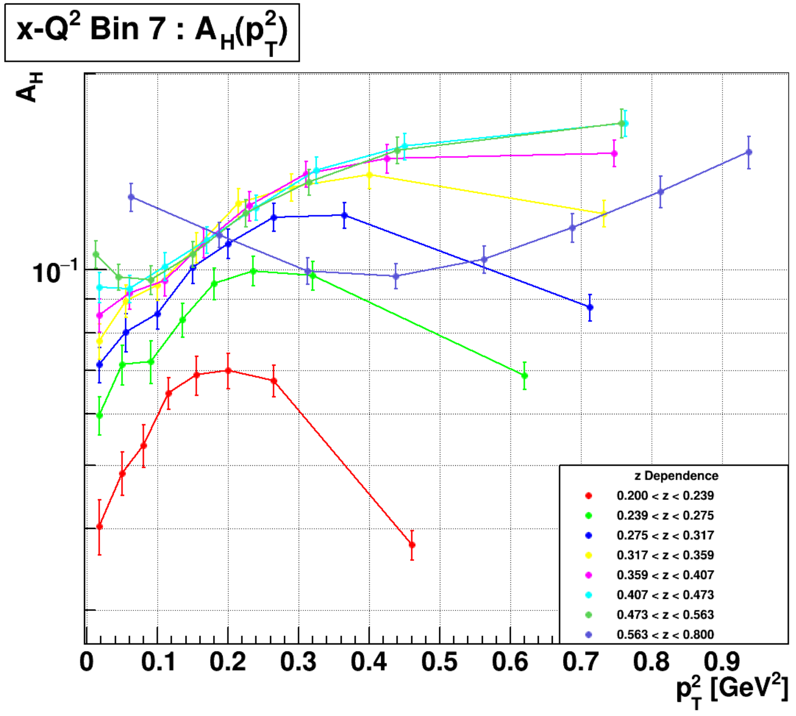

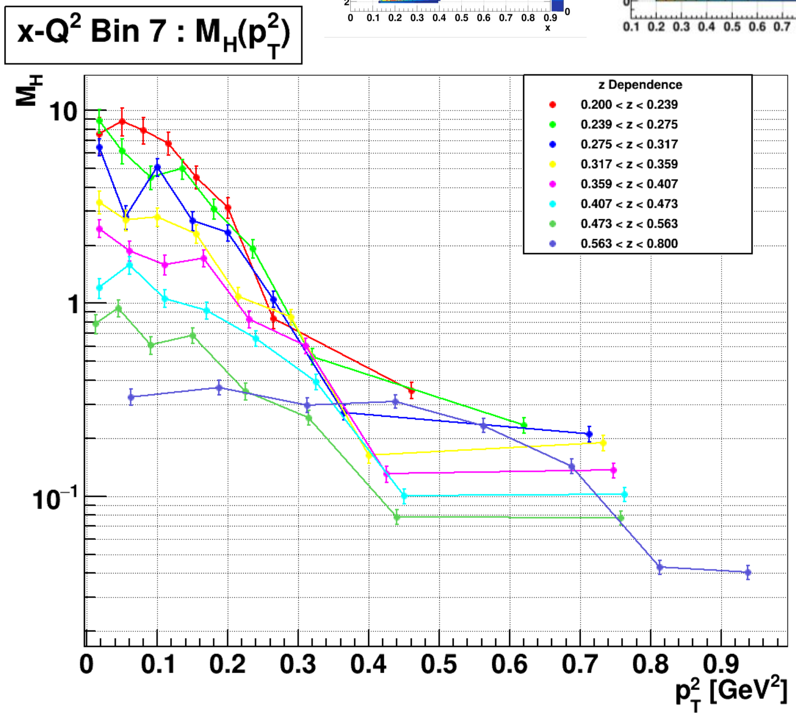

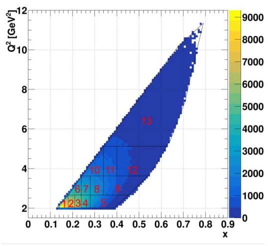

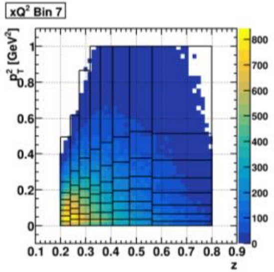

$A_H(z, p_T^2)$ & $M_H(z, p_T^2)$ for xQ^2 Bin 8

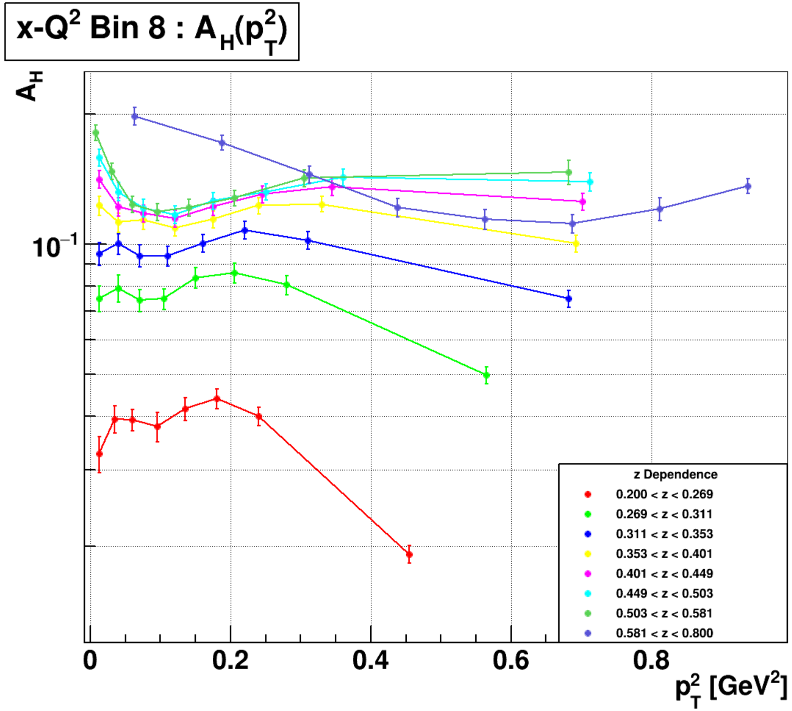

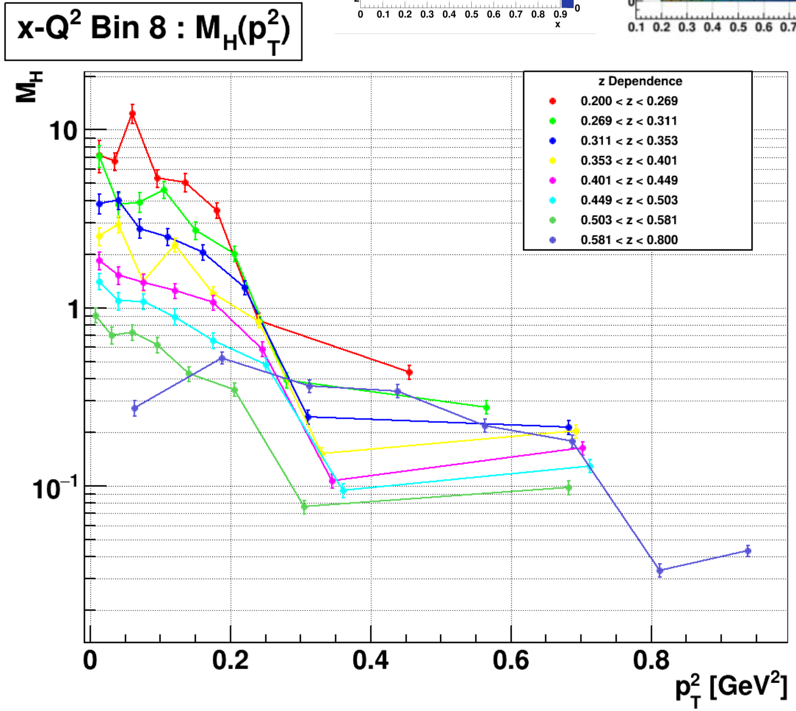

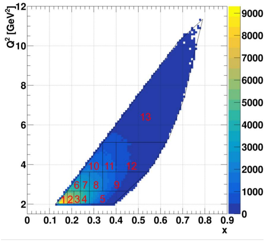

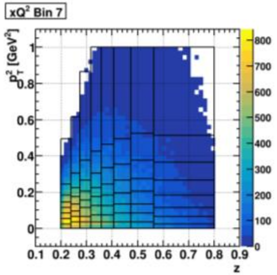

$A_H(z, p_T^2)$ & $M_H(z, p_T^2)$ for xQ^2 Bin 9

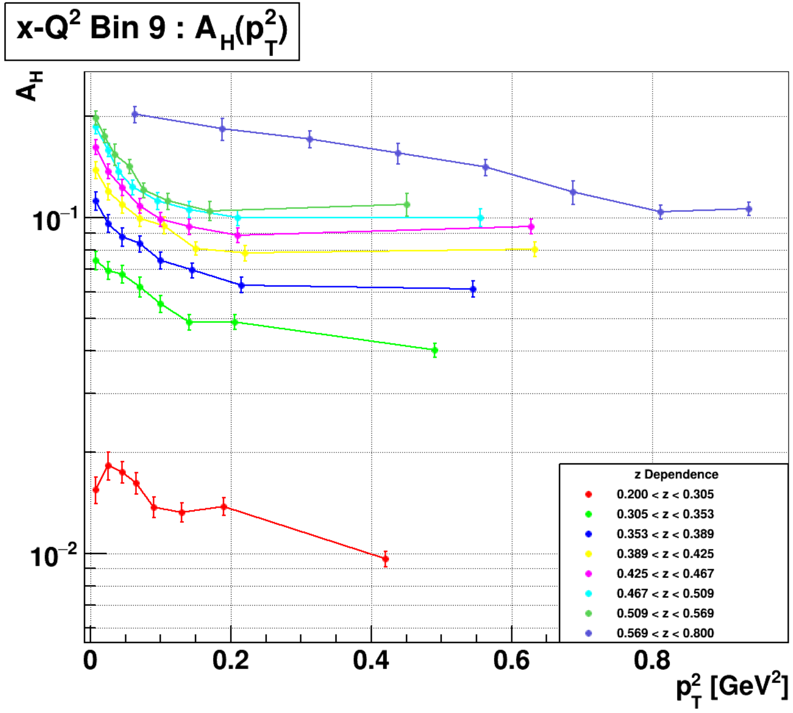

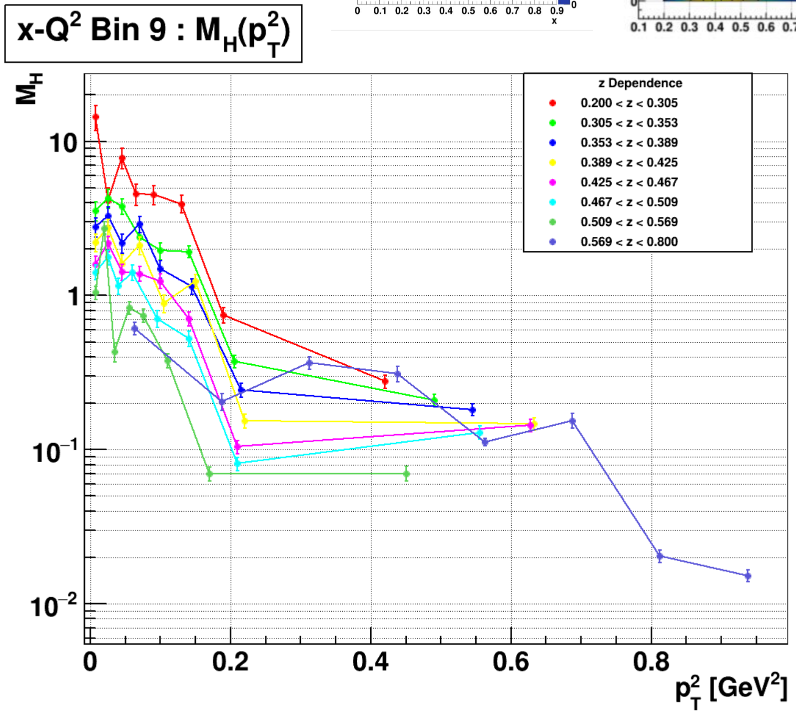

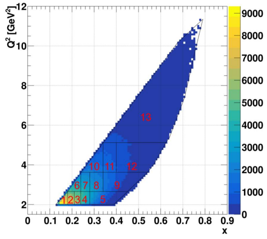

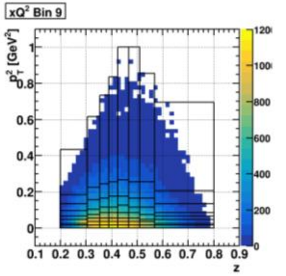

$A_H(z, p_T^2)$ & $M_H(z, p_T^2)$ for xQ^2 Bin 10

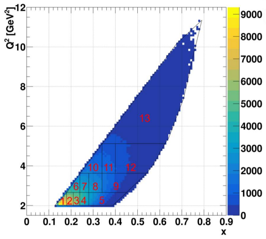

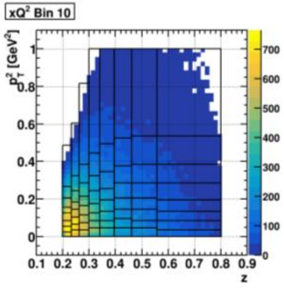

x-Q^2 Bin 10 : $A_H(p_T^2)$

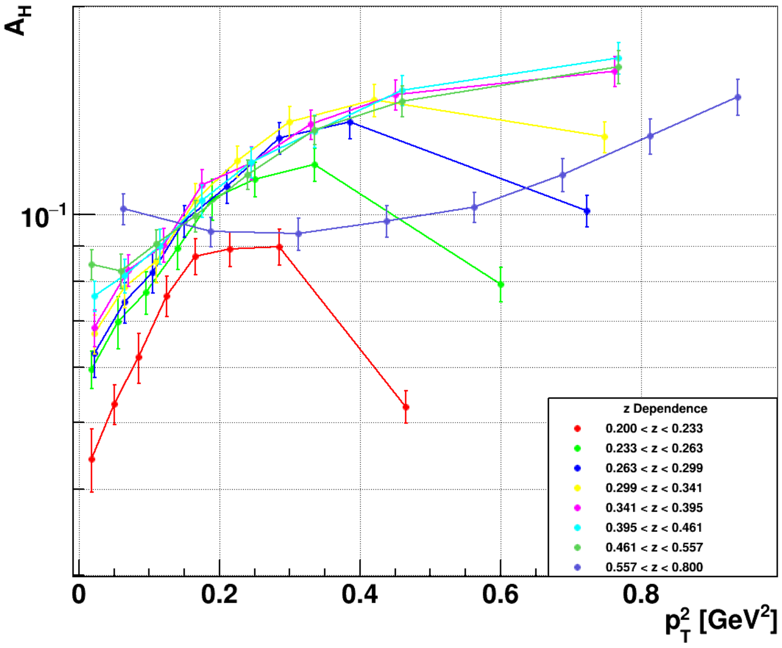

x-Q^2 Bin 10 : $M_H(p_T^2)$

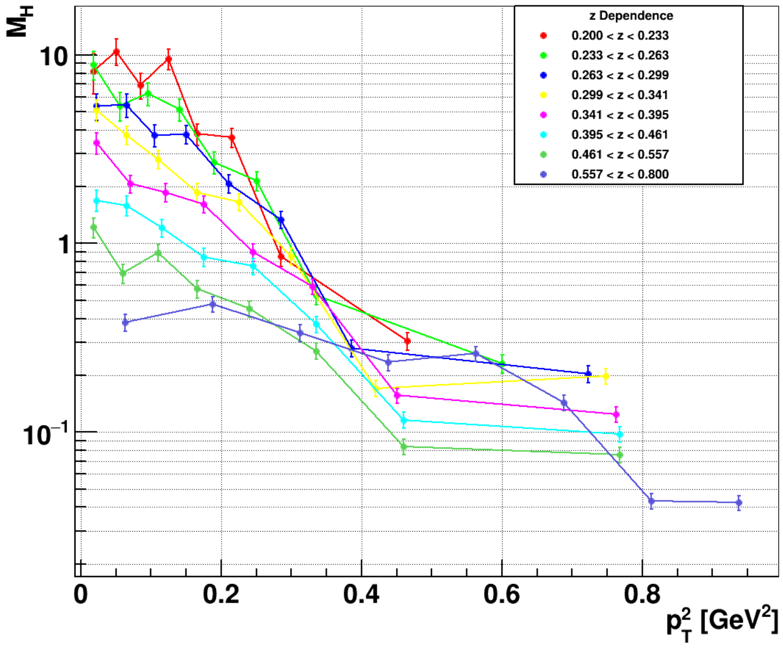

$A_H(z, p_T^2)$ & $M_H(z, p_T^2)$ for xQ^2 Bin 11

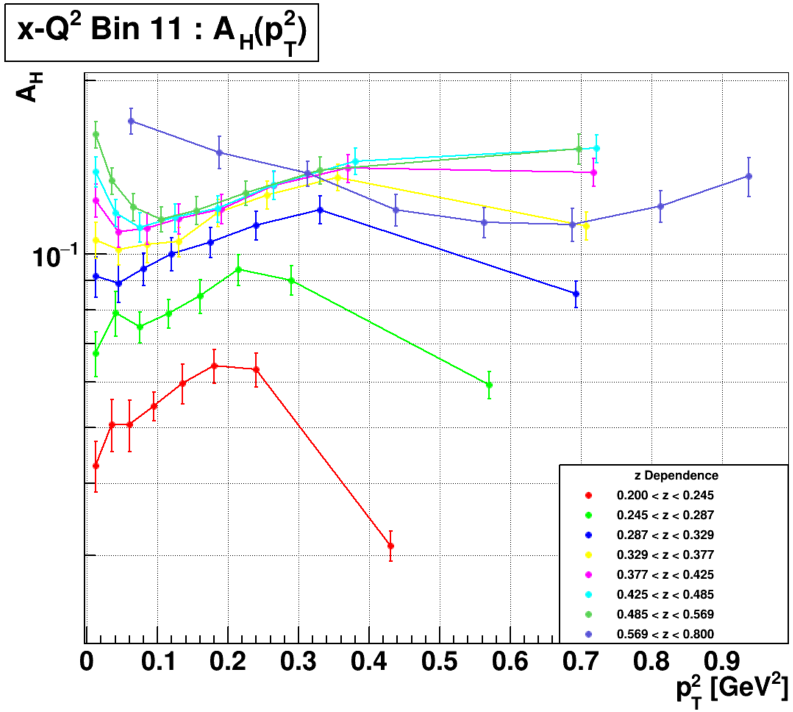

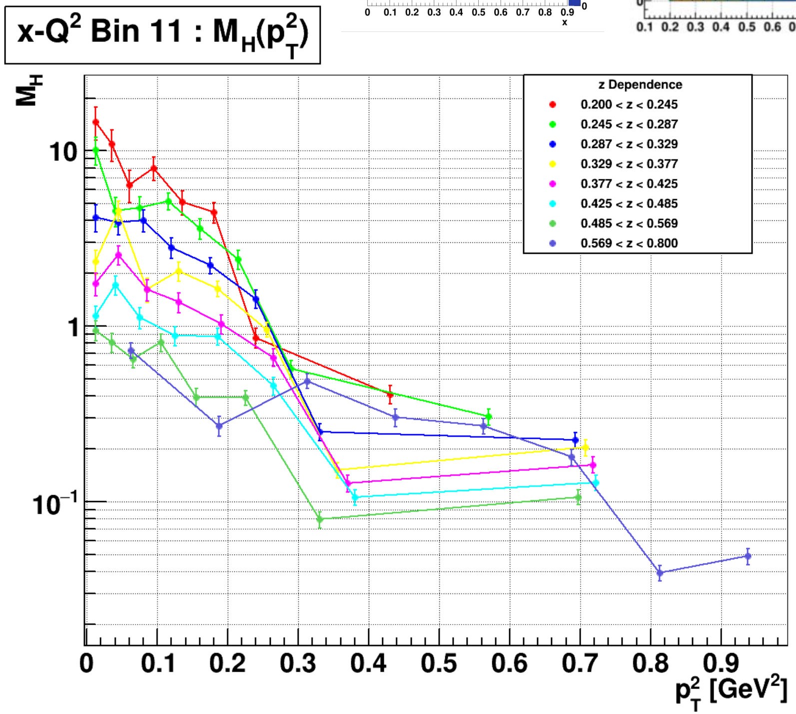

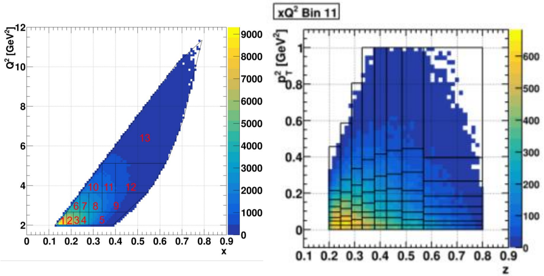

$A_H(z, p_T^2)$ & $M_H(z, p_T^2)$ for xQ^2 Bin 12

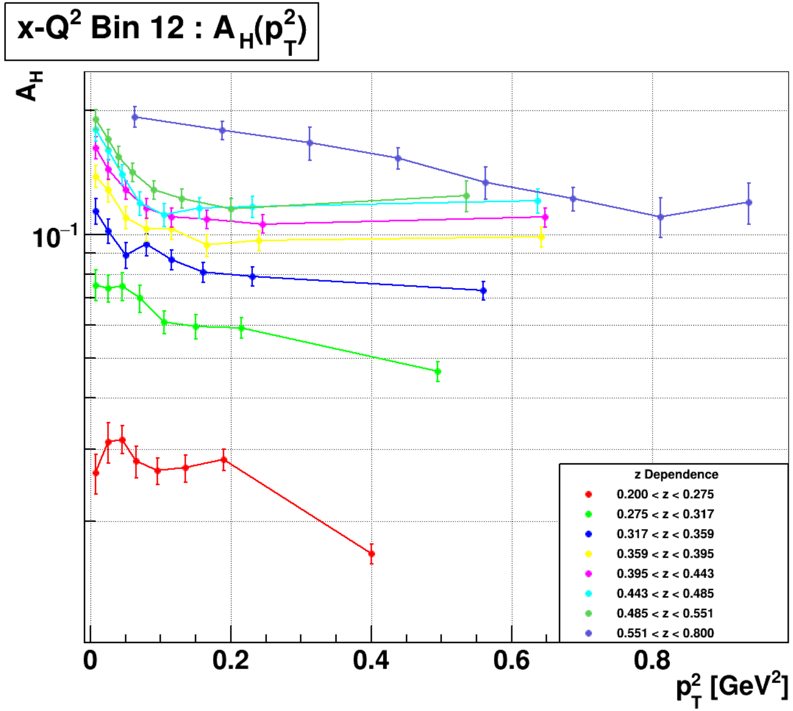

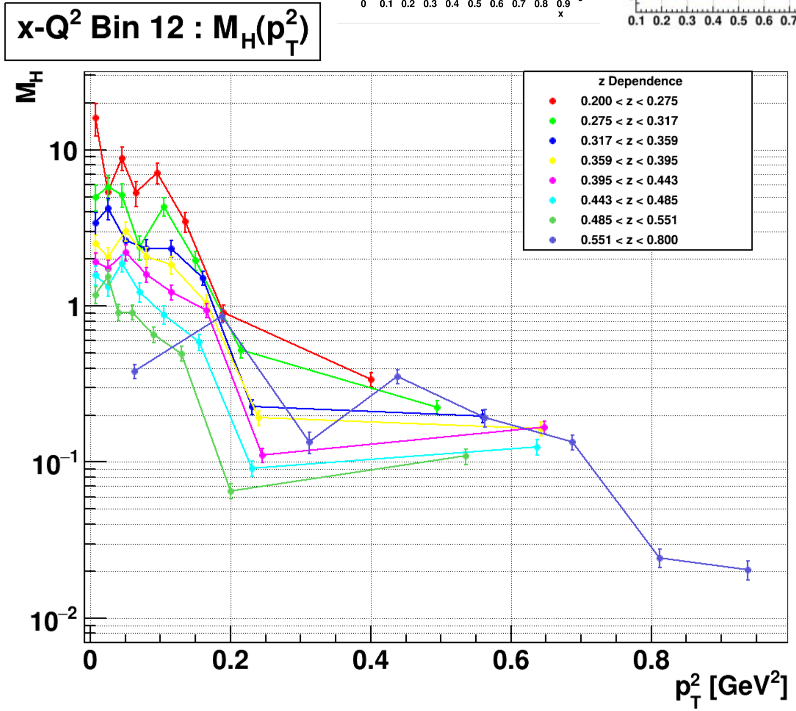

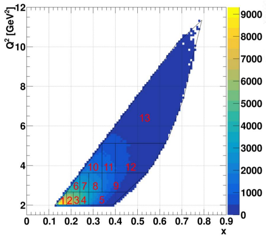

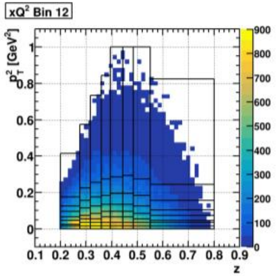

$A_H(z, p_T^2)$ & $M_H(z, p_T^2)$ for xQ^2 Bin 13

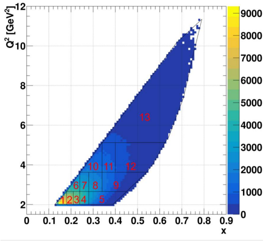

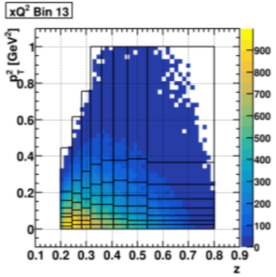

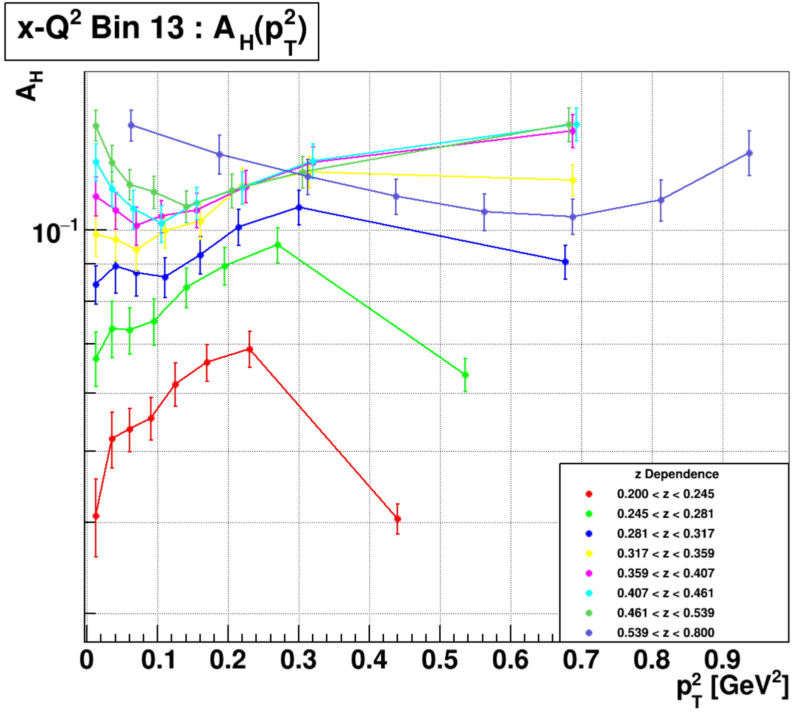

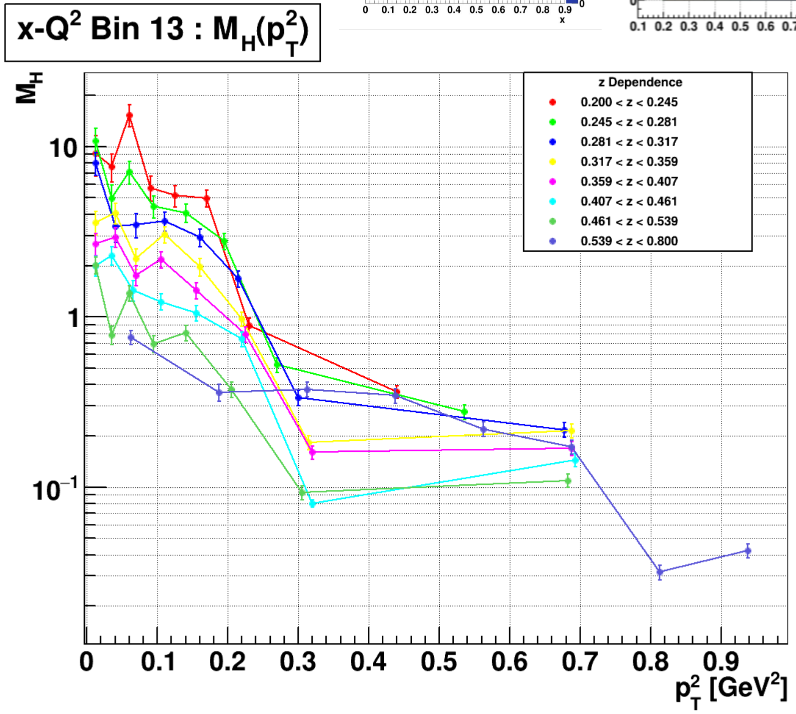

ACCEPTANCES AND MULTIPLICITIES FOR ALL X_B-Q^2 BINS AS FUNCTIONS OF P_T^2

$A_H(z, p_T^2)$ & $M_H(z, p_T^2)$ for xQ^2 Bin 1

x_B-Q^2 Bin 1 : $A_H(z)$

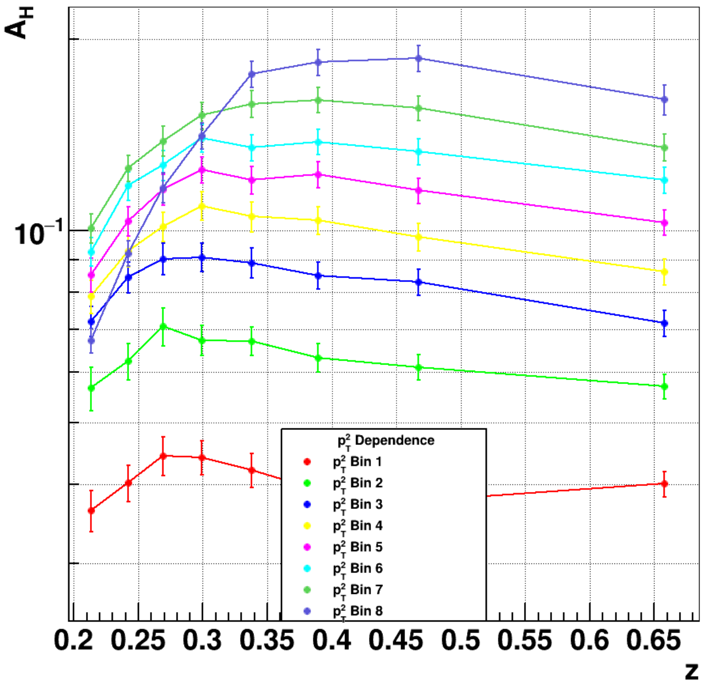

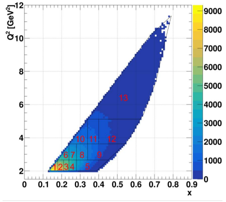

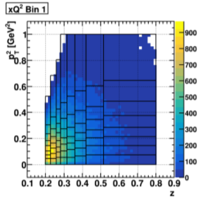

x_B-Q^2 Bin 1 : $M_H(z)$

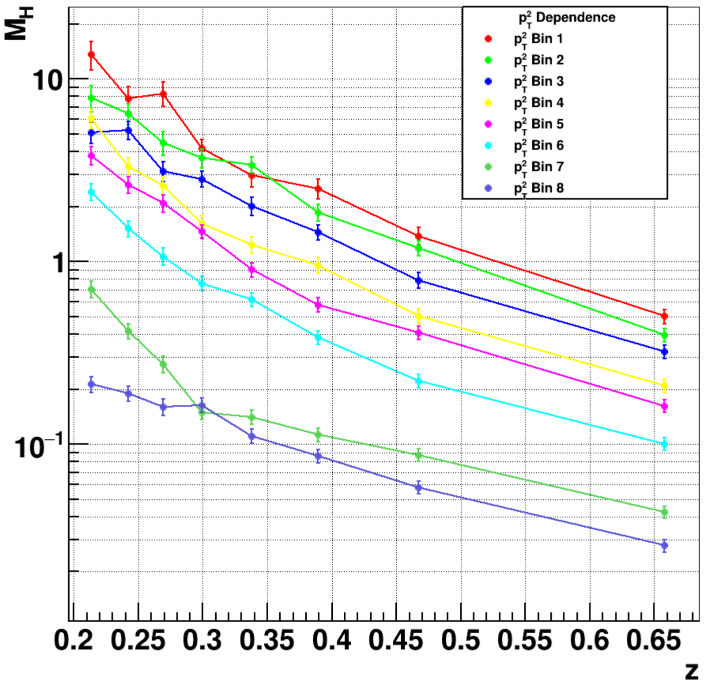

$A_H(z, p_T^2)$ & $M_H(z, p_T^2)$ for xQ^2 Bin 2

x_B-Q^2 Bin 2 : $A_H(z)$

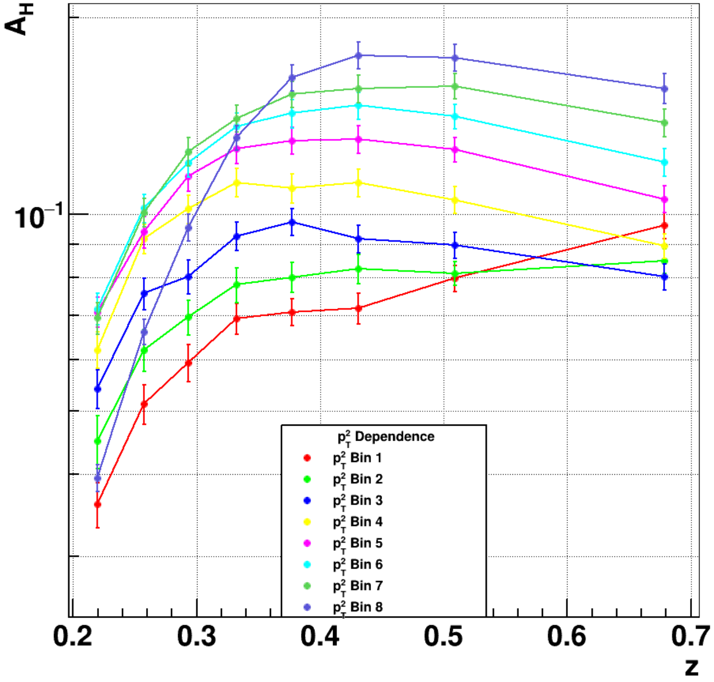

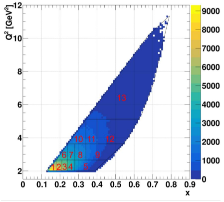

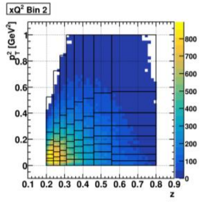

x_B-Q^2 Bin 2 : $M_H(z)$

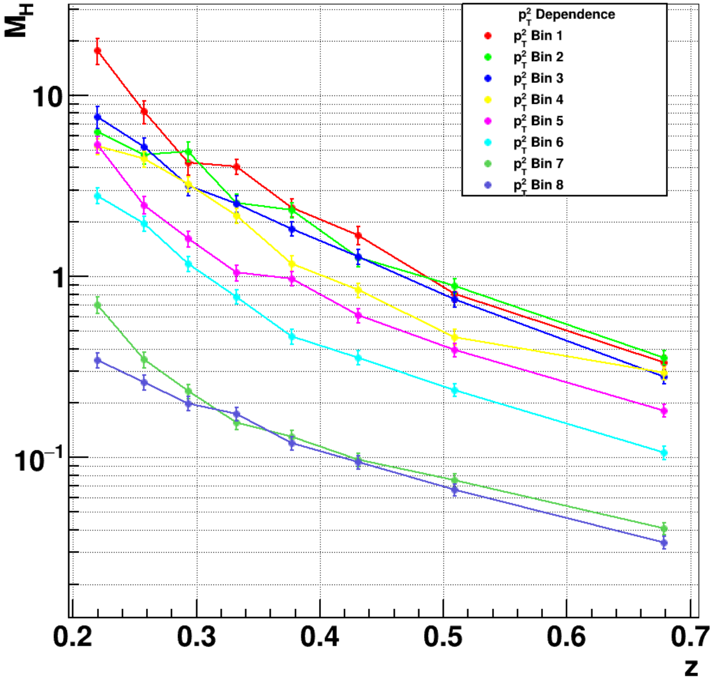

$A_H(z, p_T^2)$ & $M_H(z, p_T^2)$ for xQ^2 Bin 3

x_B-Q^2 Bin 3 : $A_H(z)$

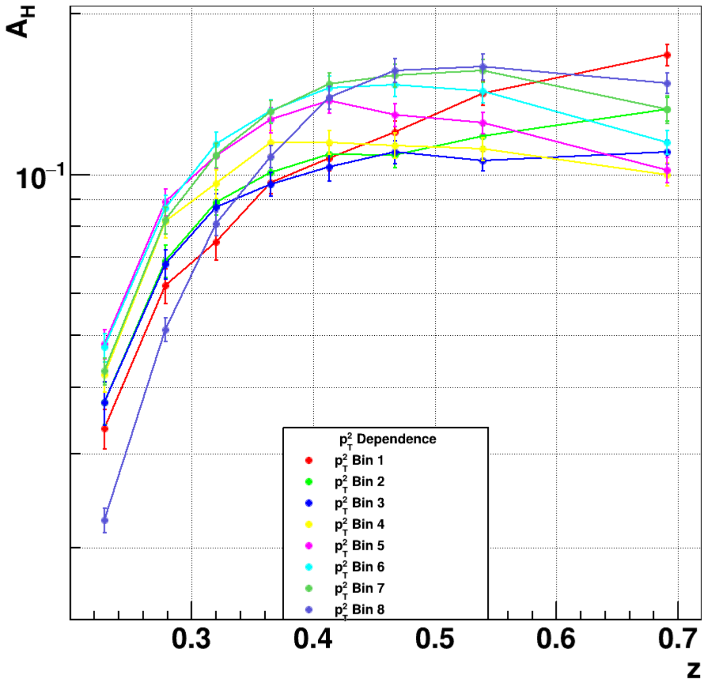

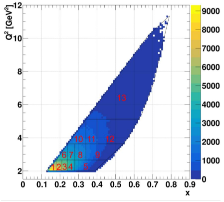

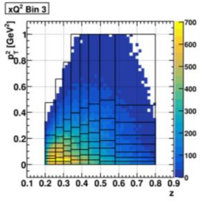

x_B-Q^2 Bin 3 : $M_H(z)$

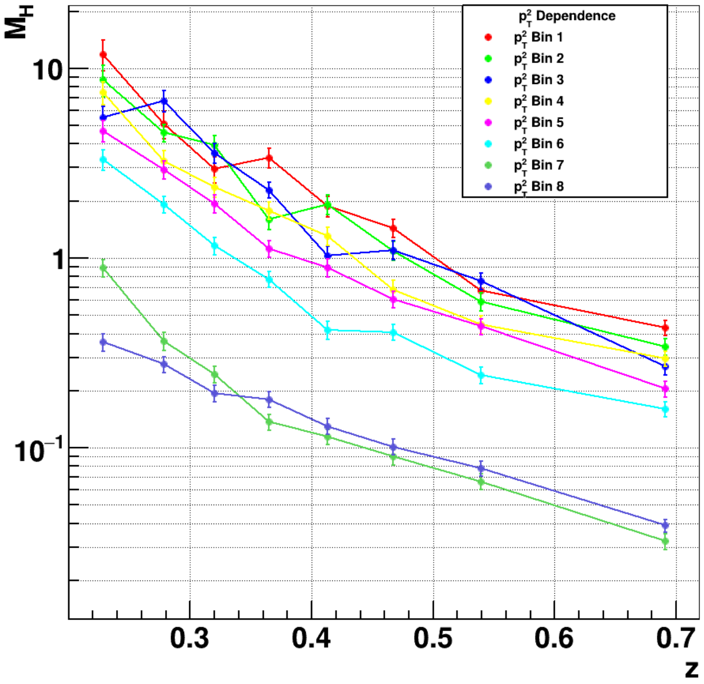

$A_H(z, p_T^2)$ & $M_H(z, p_T^2)$ for xQ^2 Bin 4

x_B-Q^2 Bin 4 : $A_H(z)$

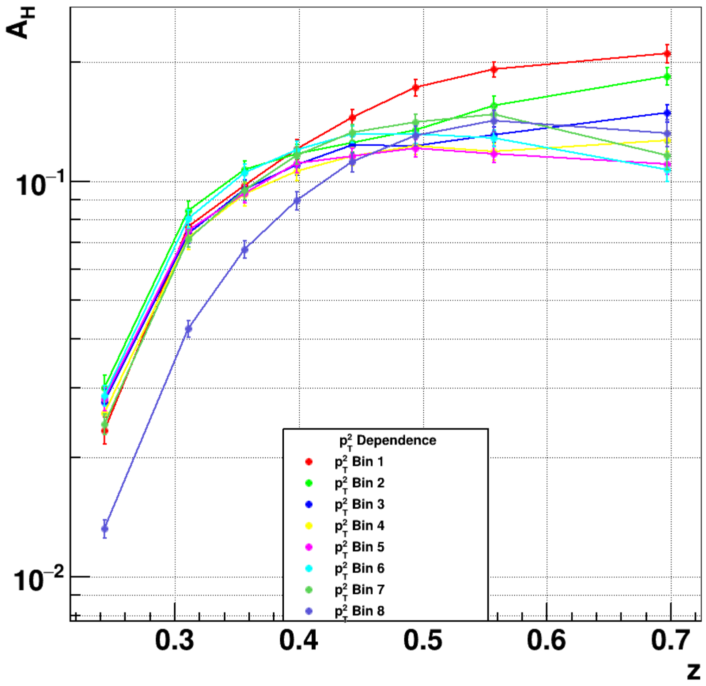

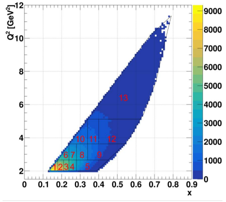

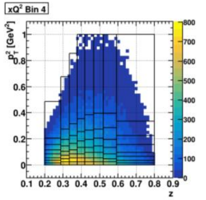

x_B-Q^2 Bin 4 : $M_H(z)$

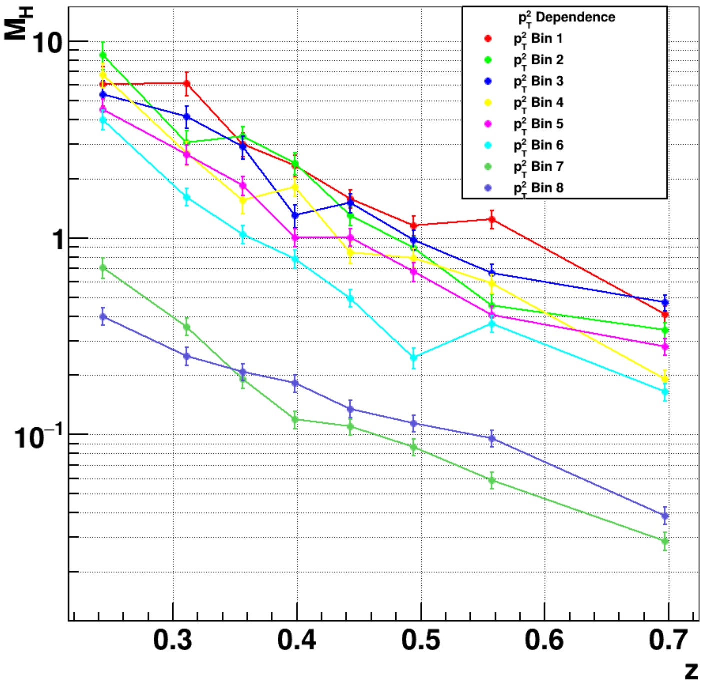

$A_H(z, p_T^2)$ & $M_H(z, p_T^2)$ for xQ^2 Bin 5

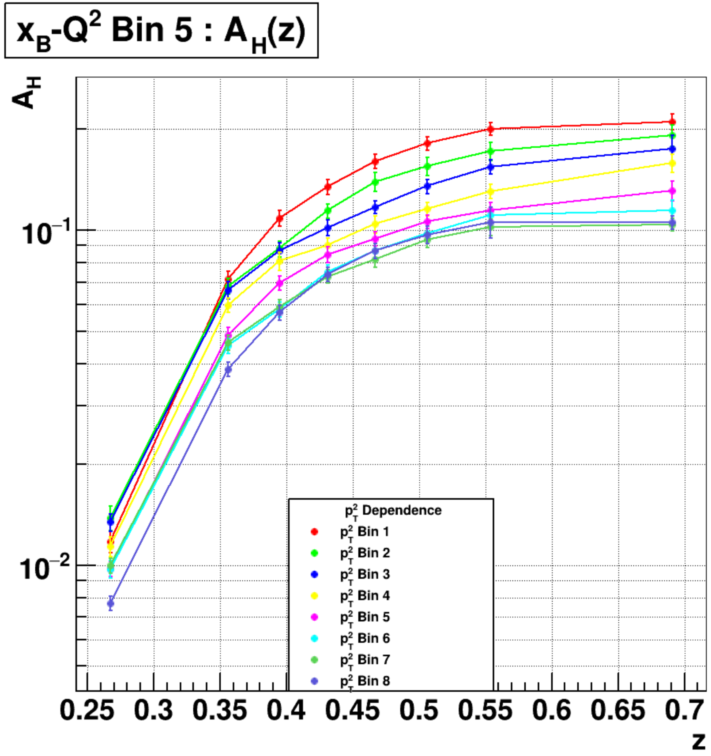

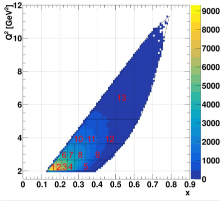

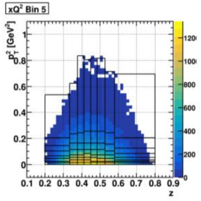

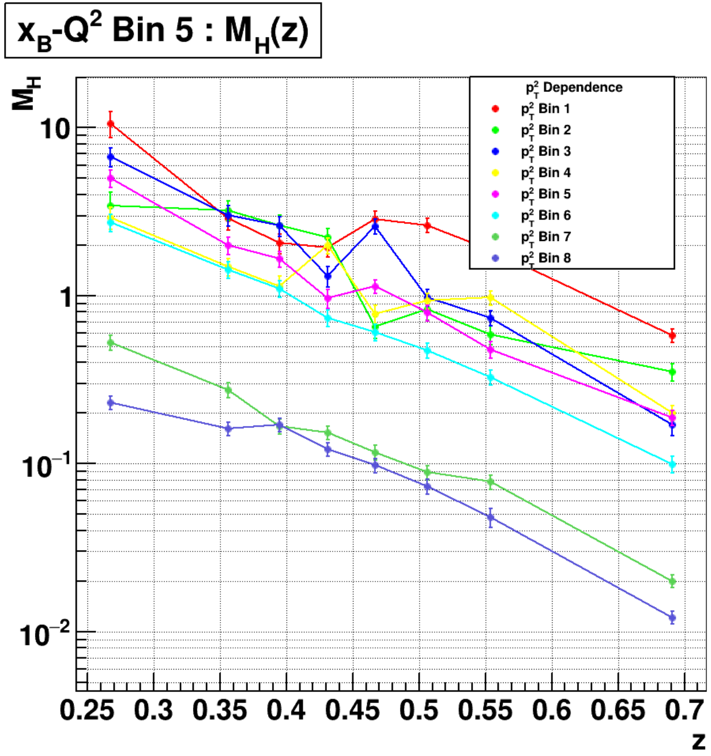

$A_H(z, p_T^2)$ & $M_H(z, p_T^2)$ for xQ^2 Bin 6

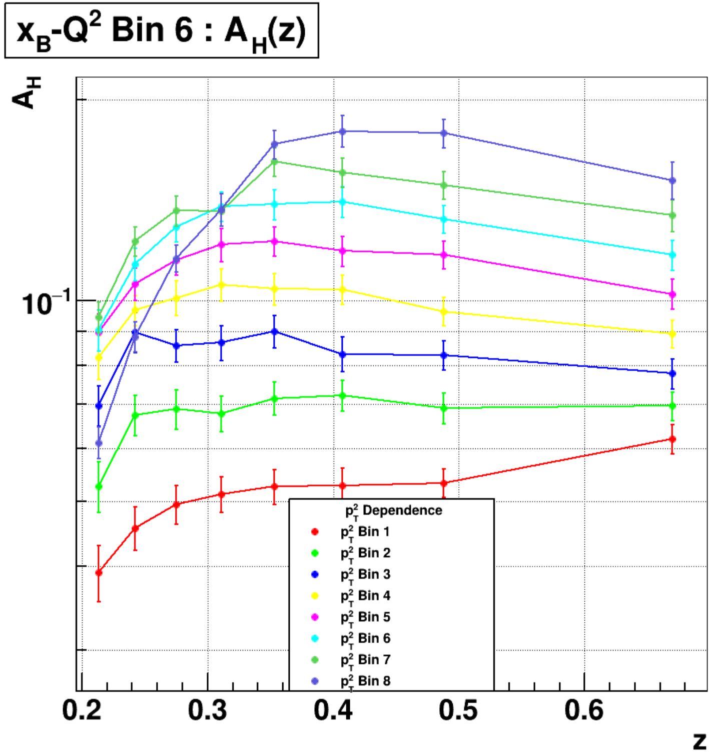

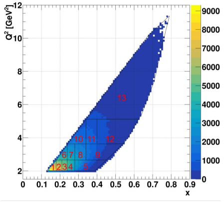

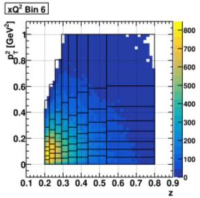

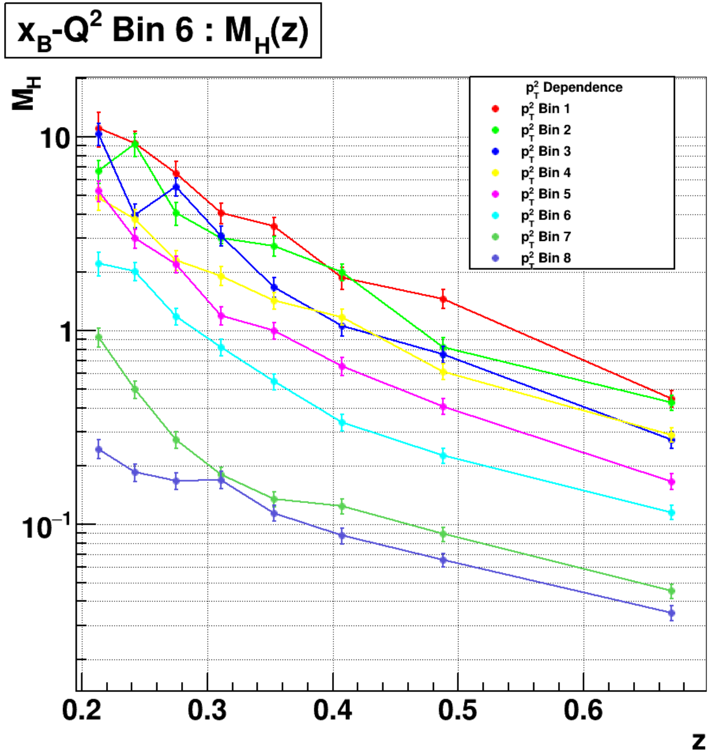

$A_H(z, p_T^2)$ & $M_H(z, p_T^2)$ for xQ^2 Bin 7

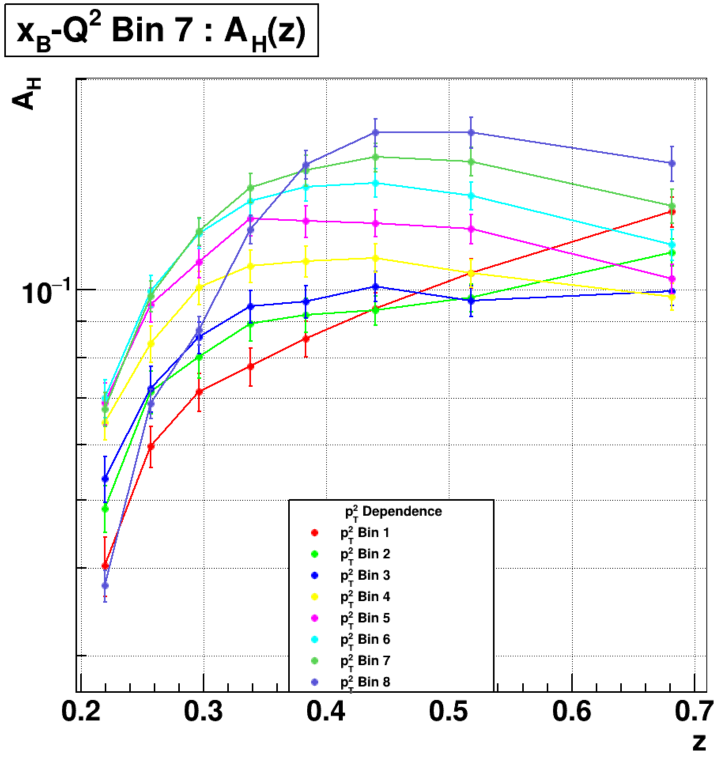

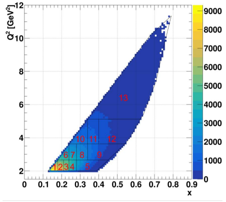

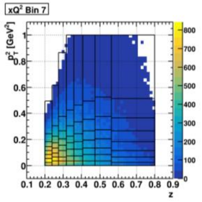

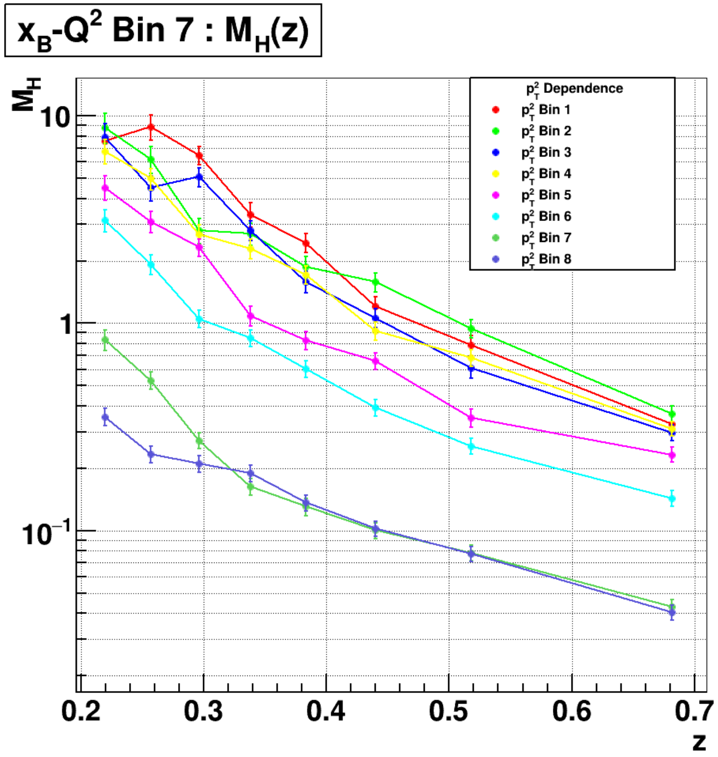

$A_H(z, p_T^2)$ & $M_H(z, p_T^2)$ for xQ^2 Bin 8

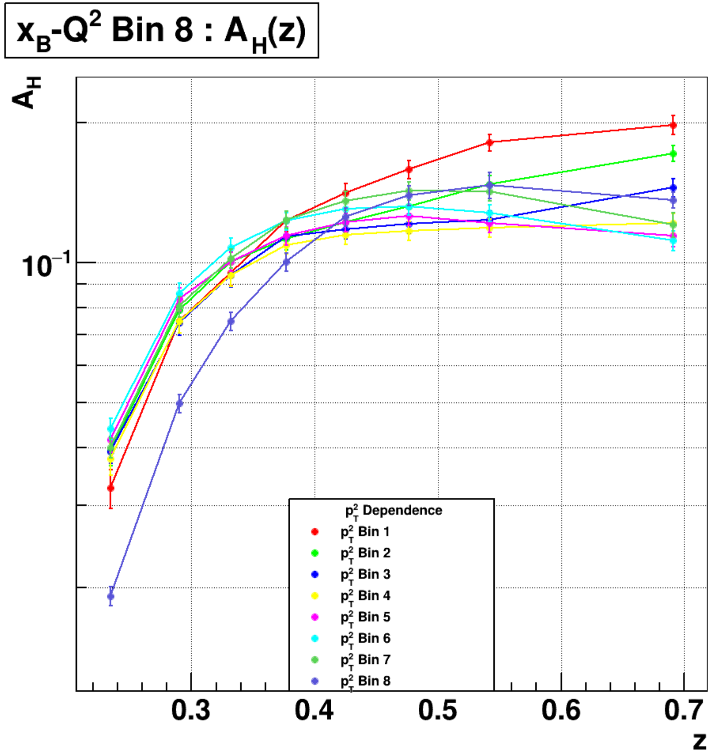

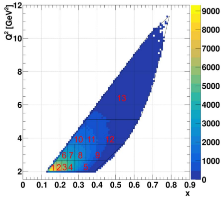

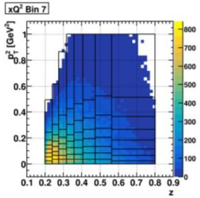

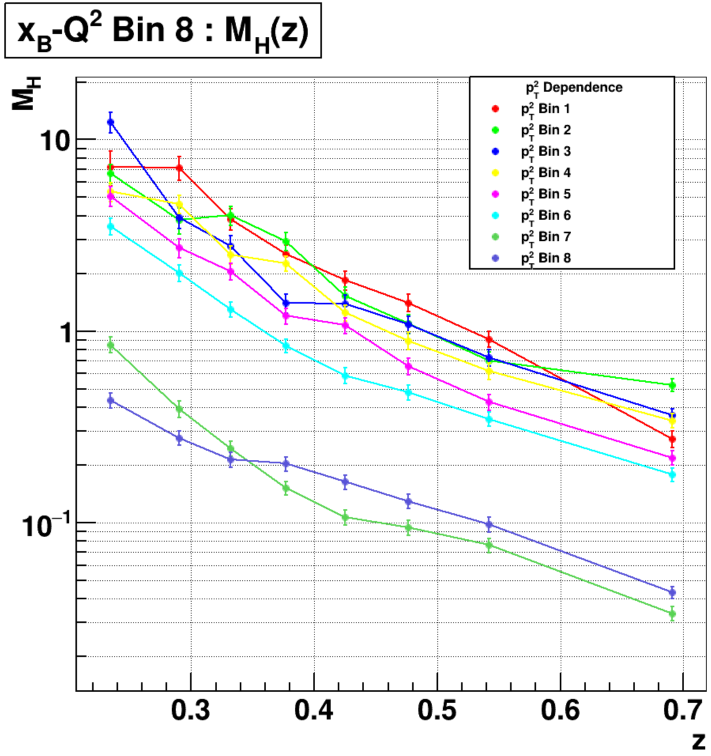

$A_H(z, p_T^2)$ & $M_H(z, p_T^2)$ for xQ^2 Bin 9

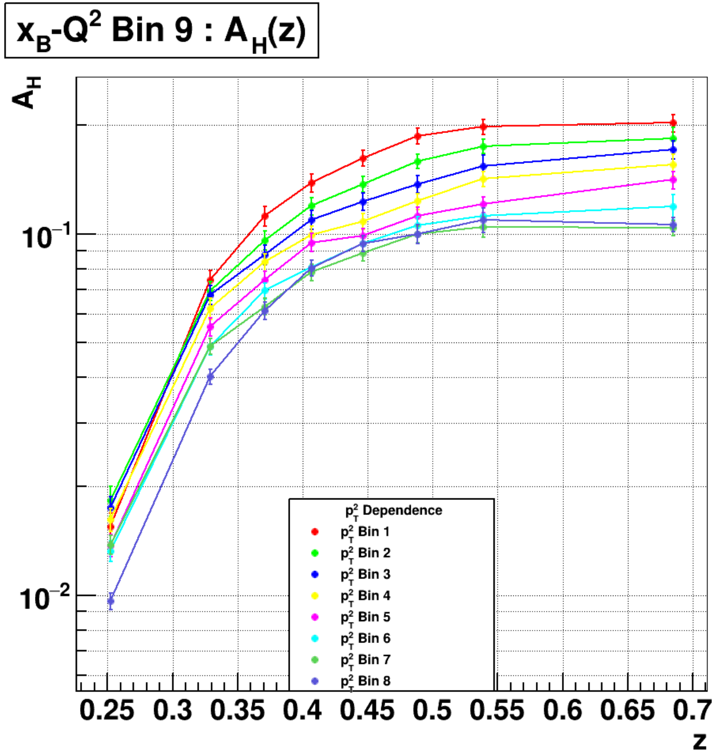

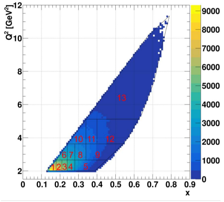

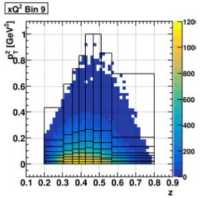

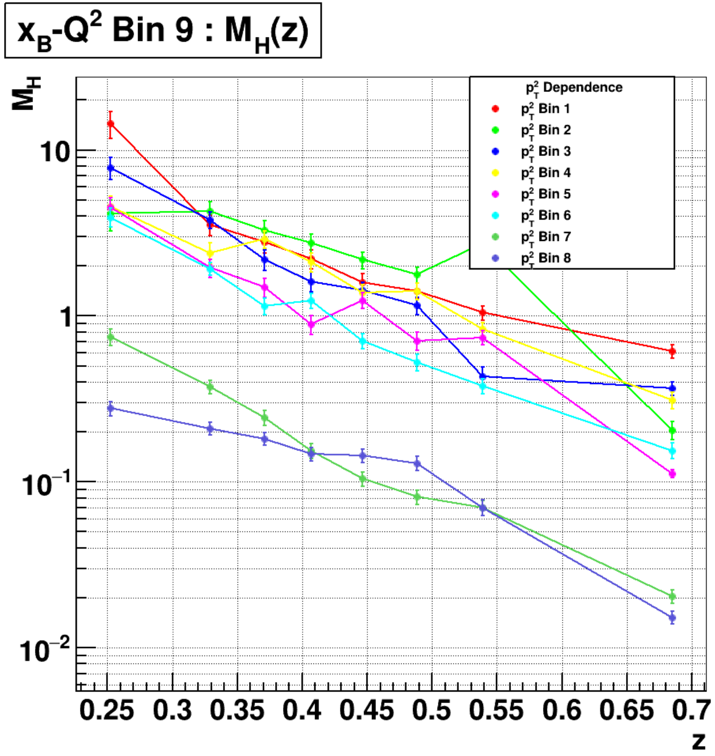

$A_H(z, p_T^2)$ & $M_H(z, p_T^2)$ for xQ^2 Bin 10

x_B-Q^2 Bin 10 : $A_H(z)$

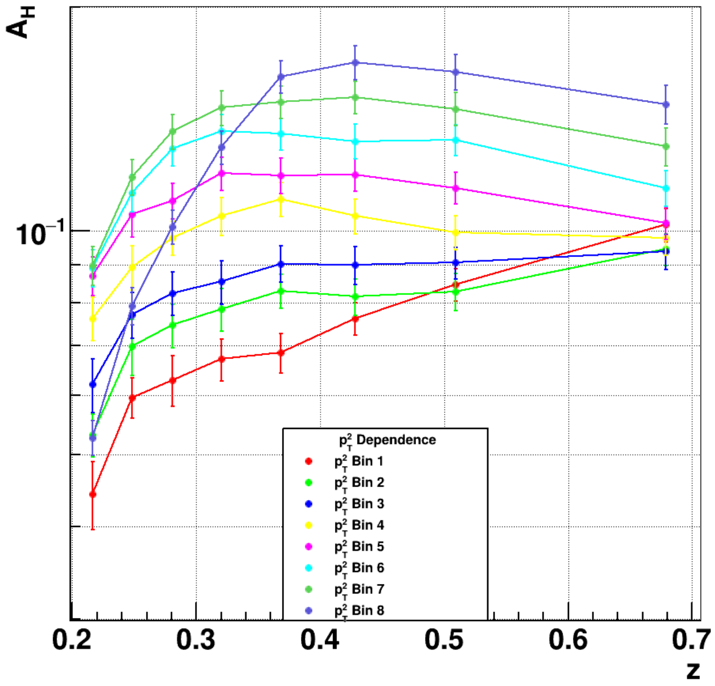

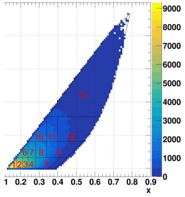

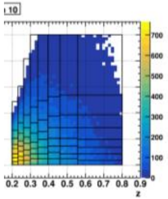

x_B-Q^2 Bin 10 : $M_H(z)$

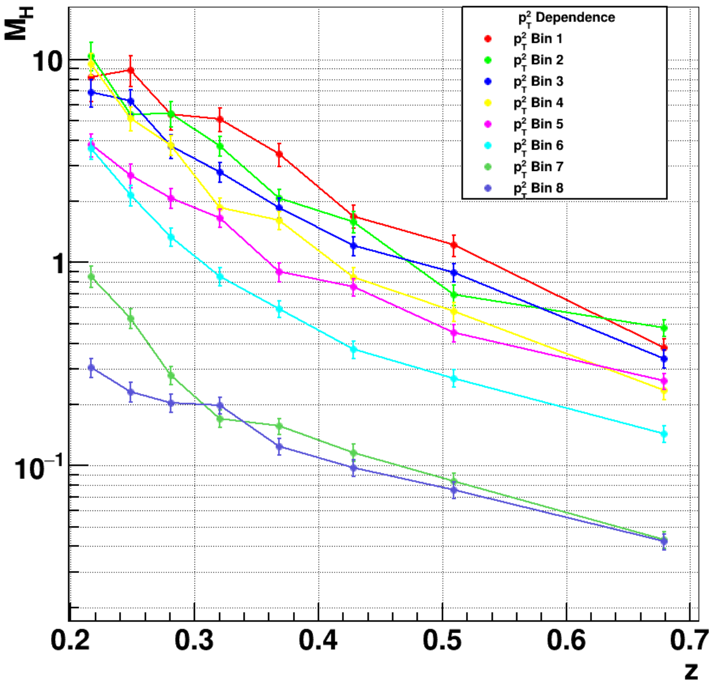

$A_H(z, p_T^2)$ & $M_H(z, p_T^2)$ for xQ^2 Bin 11

x_B-Q^2 Bin 11 : $A_H(z)$

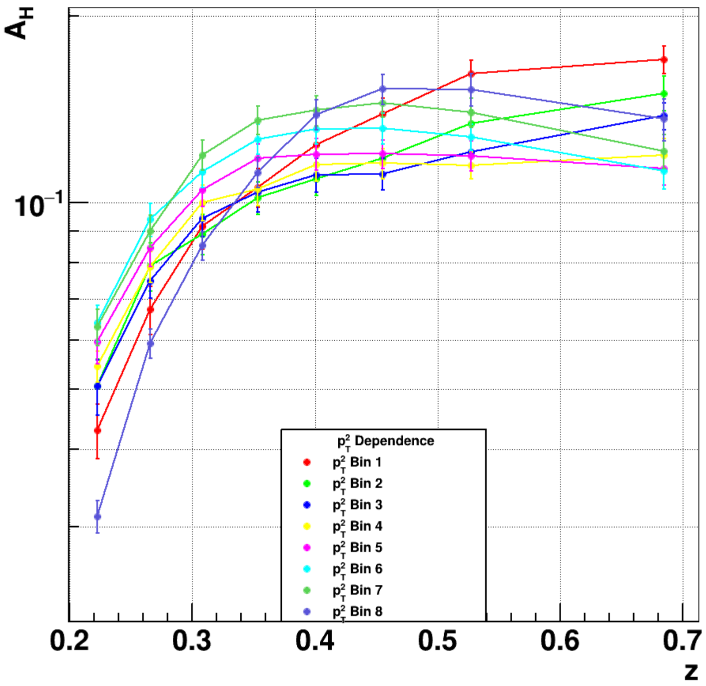

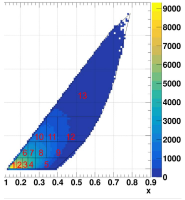

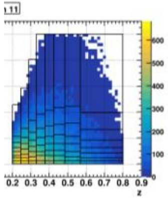

x_B-Q^2 Bin 11 : $M_H(z)$

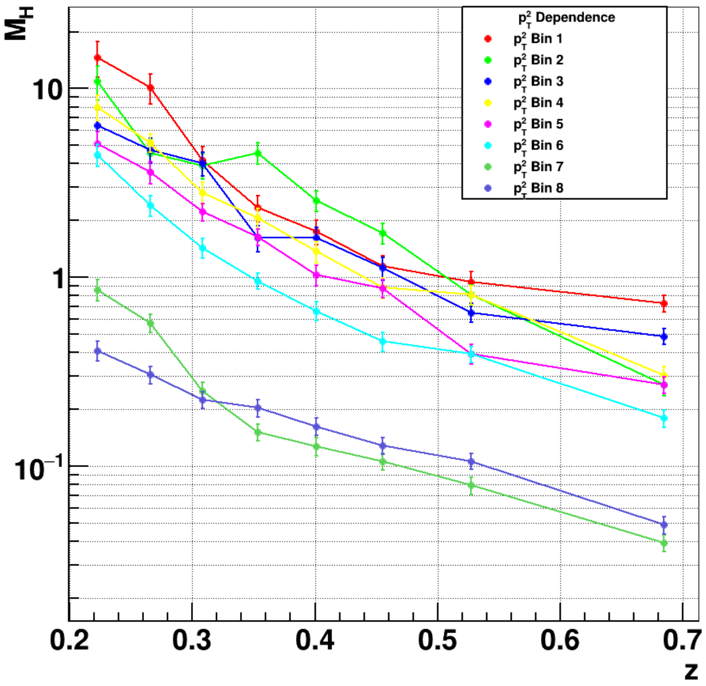

$A_H(z, p_T^2)$ & $M_H(z, p_T^2)$ for xQ^2 Bin 12

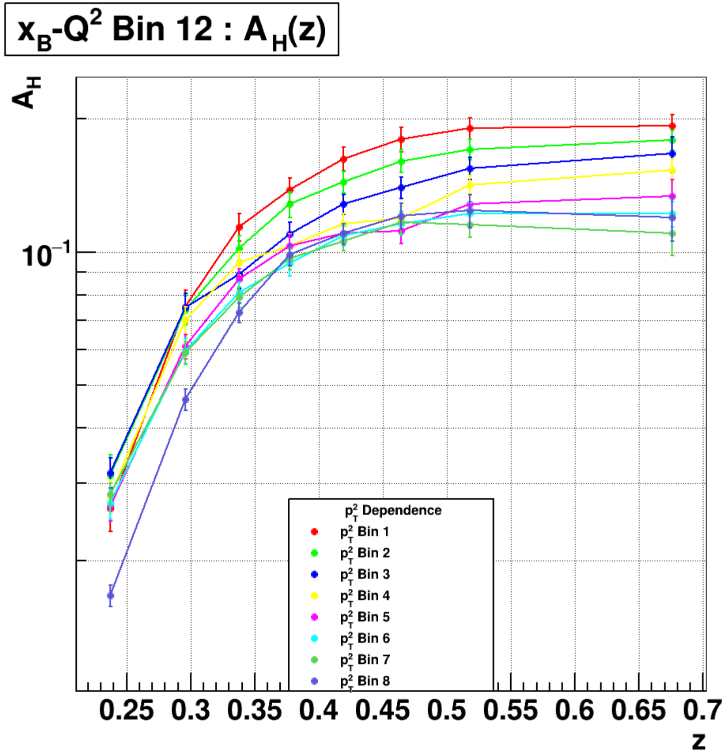

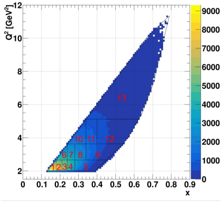

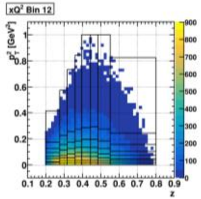

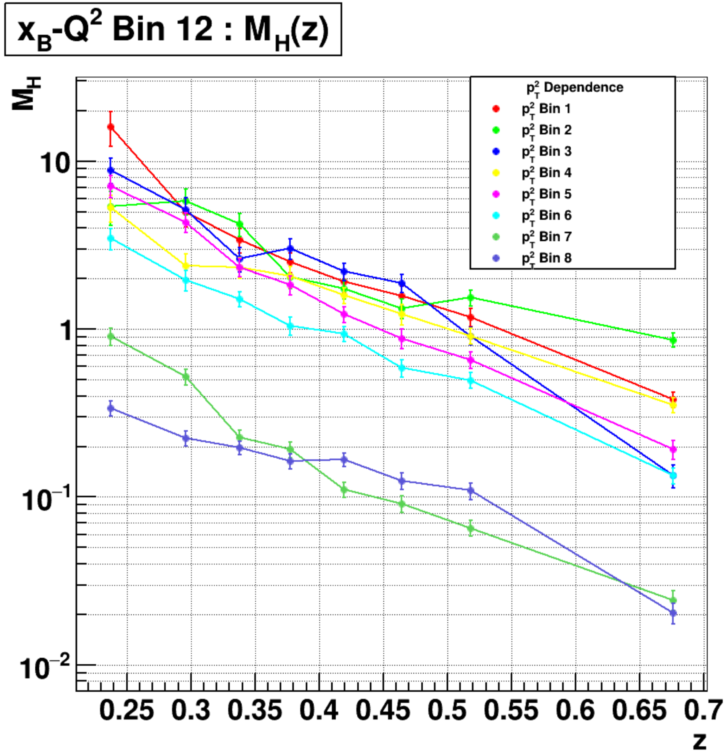

$A_H(z, p_T^2)$ & $M_H(z, p_T^2)$ for xQ^2 Bin 13

x_B-Q^2 Bin 13 : $A_H(z)$

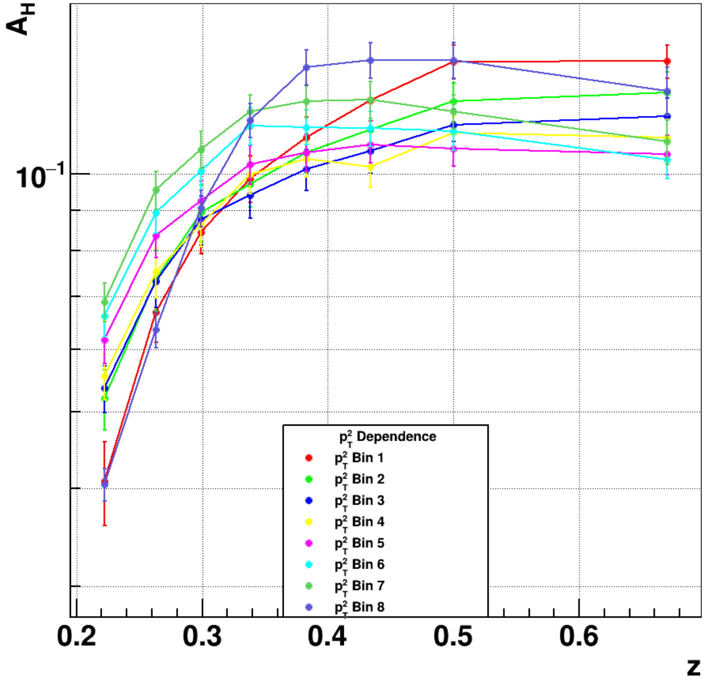

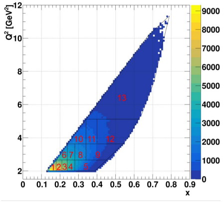

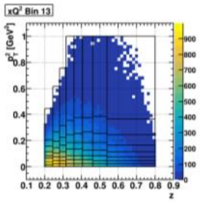

x_B-Q^2 Bin 13 : $M_H(z)$

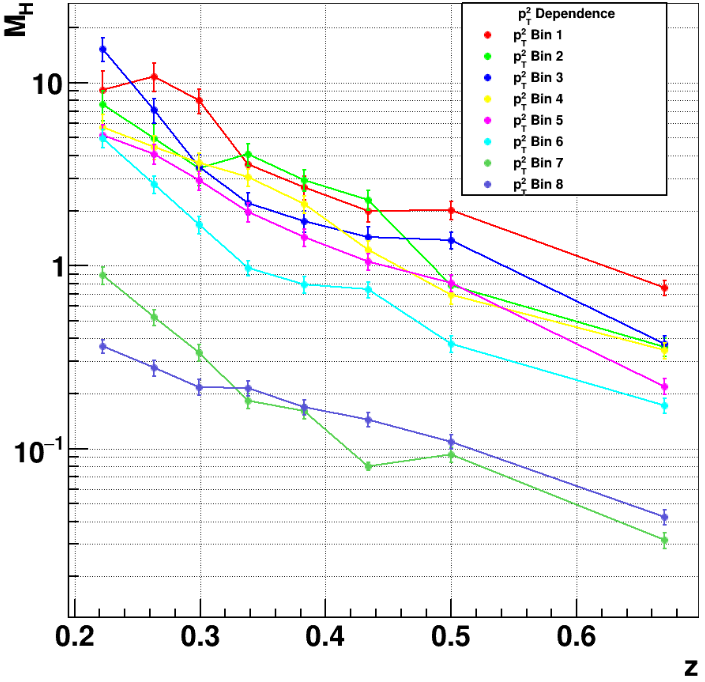

P_T^2 INTEGRATED MULTIPLICITIES

P_T^2 Integrated M_H with LO Theory Predictions : xQ^2 bins 1 & 2

x_B-Q^2 Bin 1 : $M_H(z)$

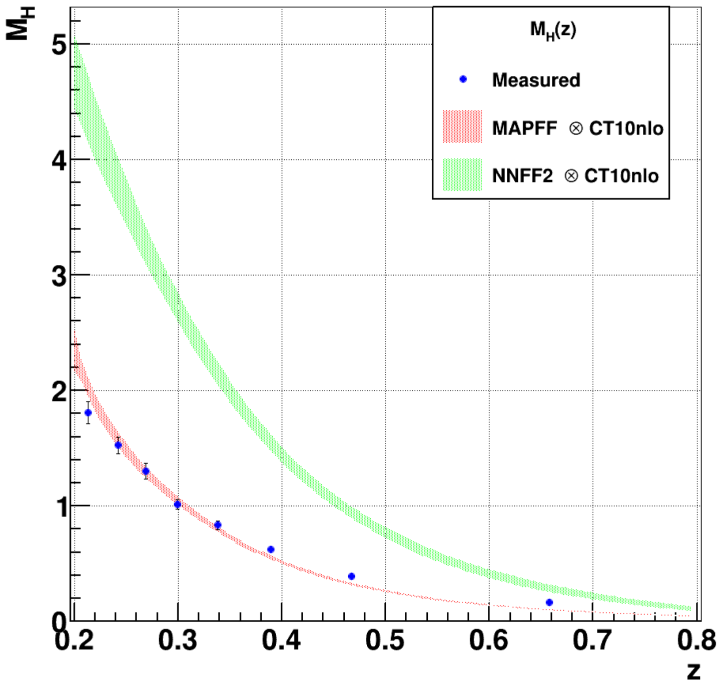

x_B-Q^2 Bin 2 : $M_H(z)$

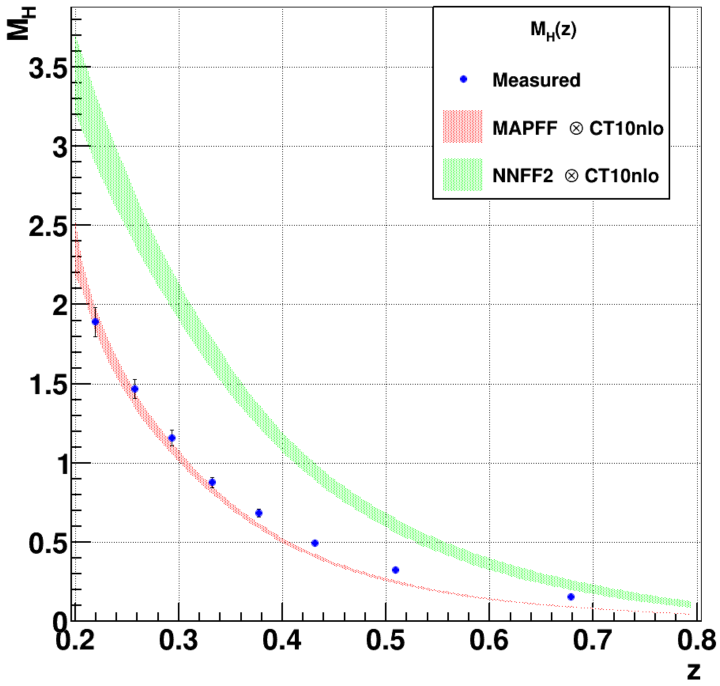

P_T^2 Integrated M_H with LO Theory Predictions : xQ^2 bins 3 & 4

x_B-Q^2 Bin 3 : $M_H(z)$

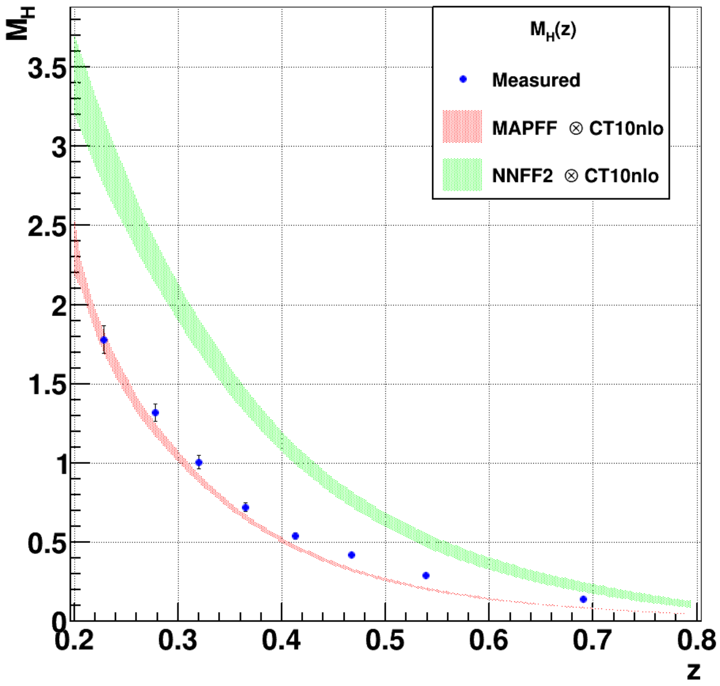

x_B-Q^2 Bin 4 : $M_H(z)$

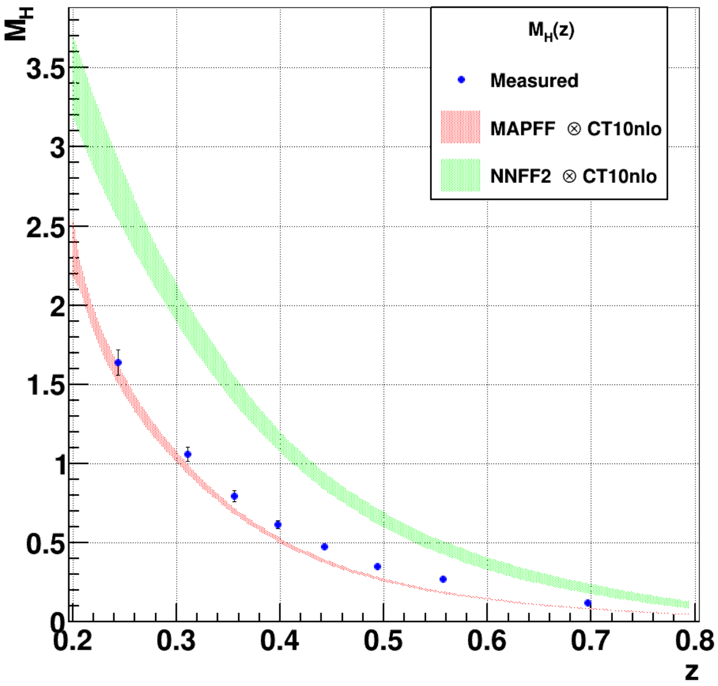

P_T^2 Integrated M_H with LO Theory Predictions : xQ^2 bins 5 & 6

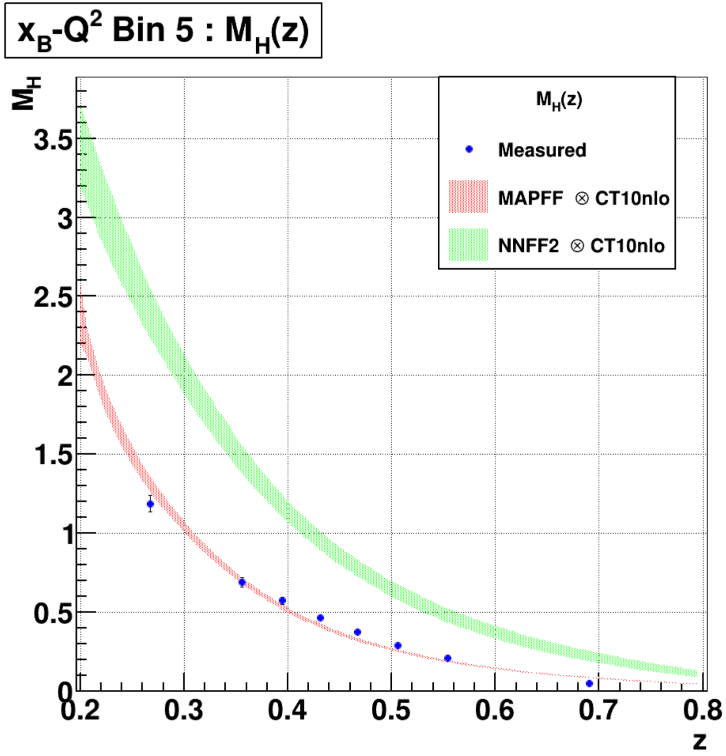

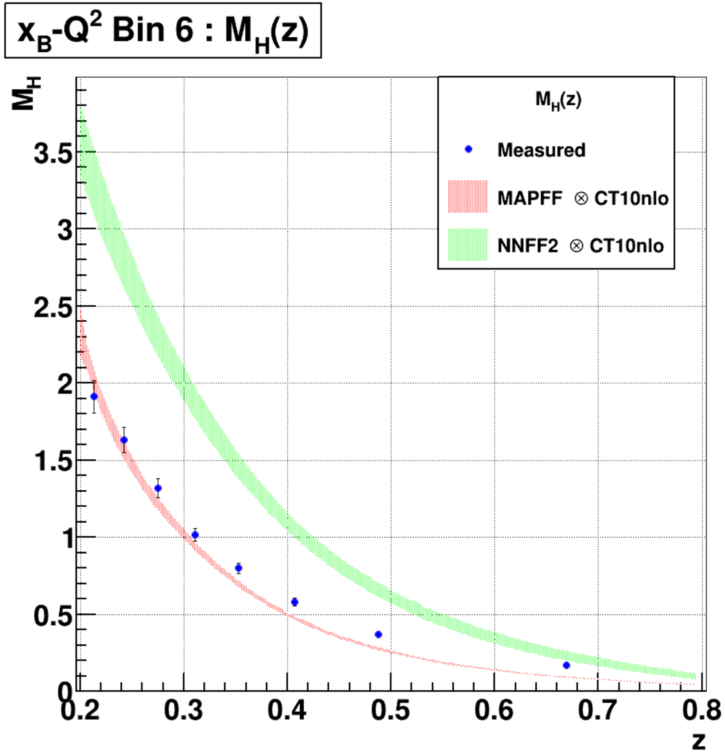

P_T^2 Integrated M_H with LO Theory Predictions : xQ^2 bins 7 & 8

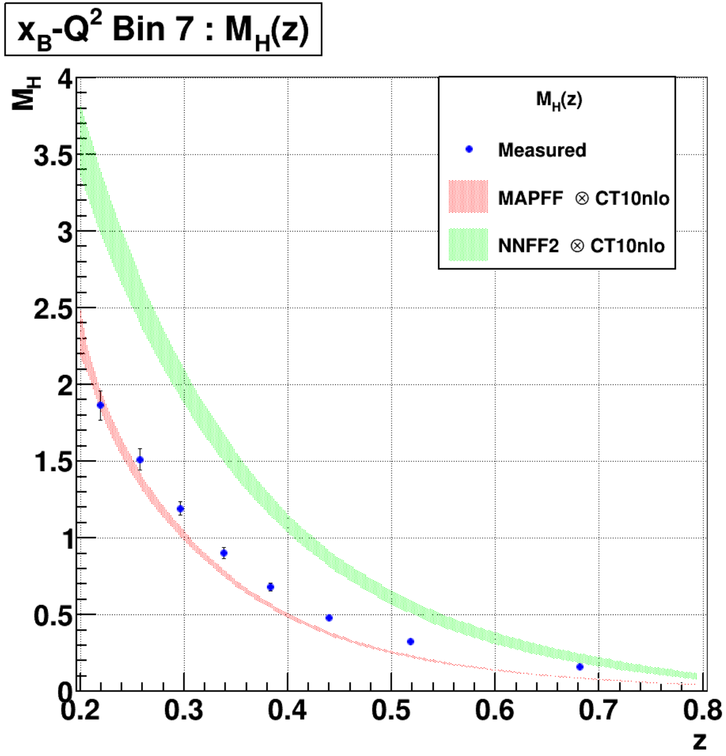

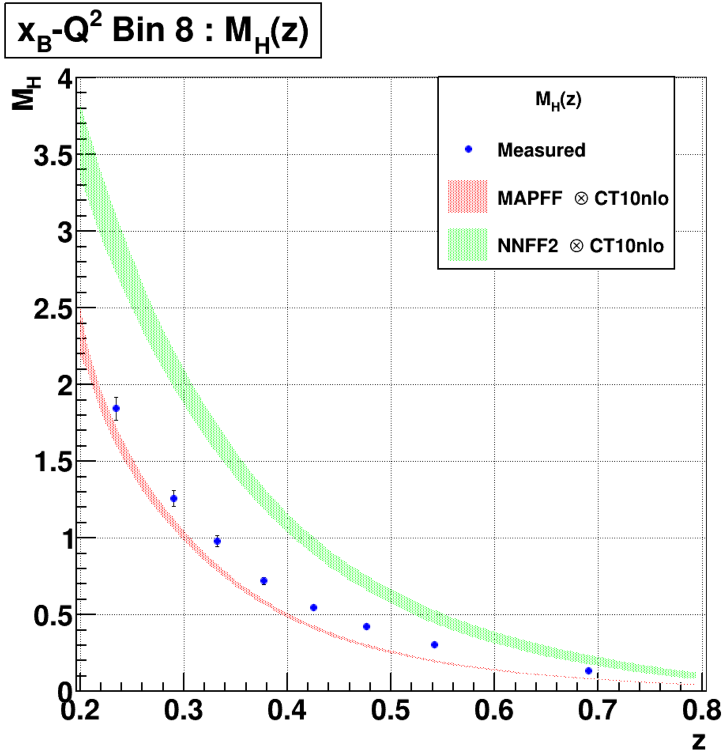

P_T^2 Integrated M_H with LO Theory Predictions : xQ^2 bins 9 & 10

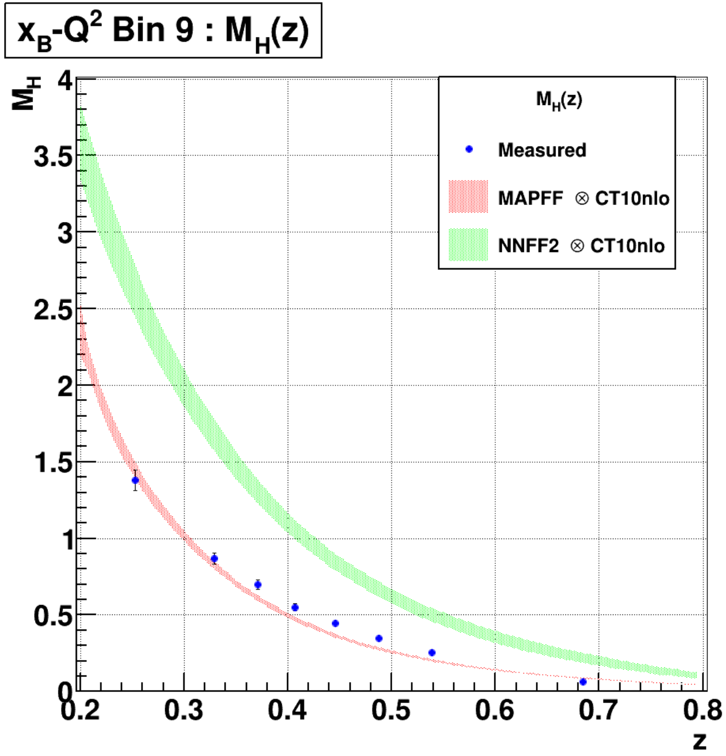

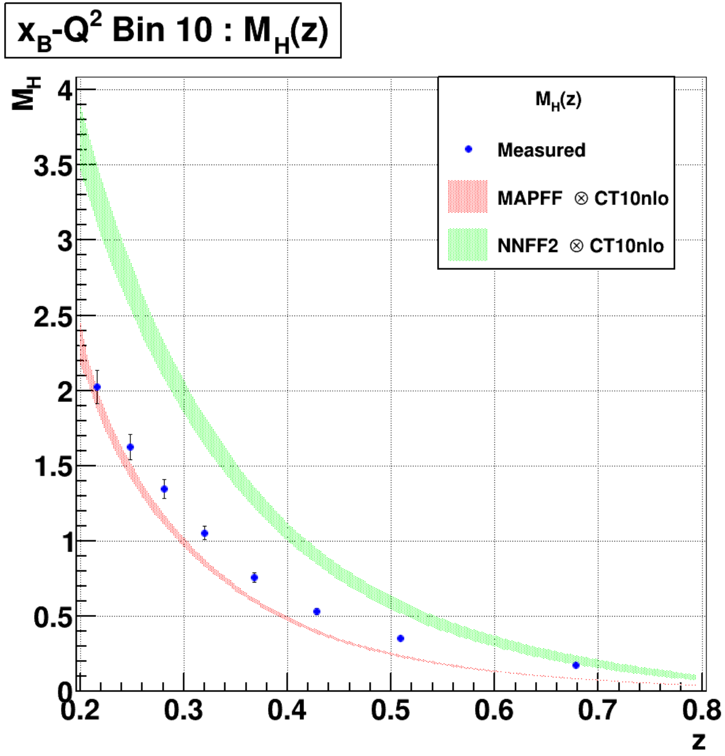

P_T^2 Integrated M_H with LO Theory Predictions : xQ^2 bins 11 & 12

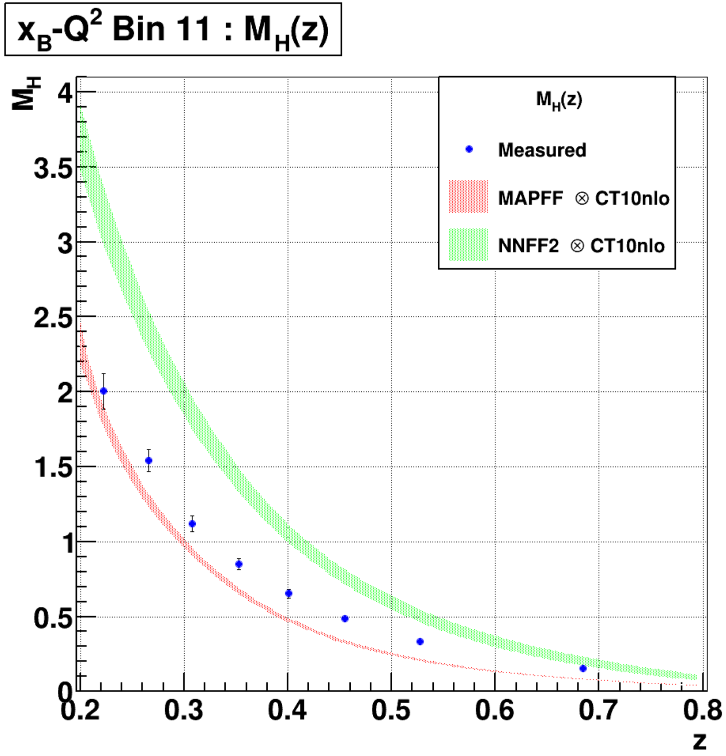

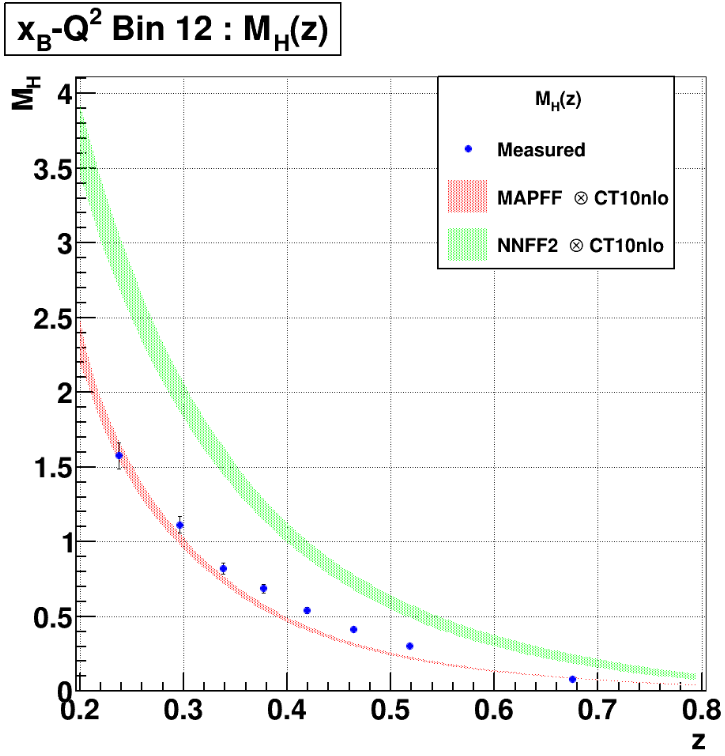

P_T^2 Integrated M_H with LO Theory Predictions : xQ^2 bin 13

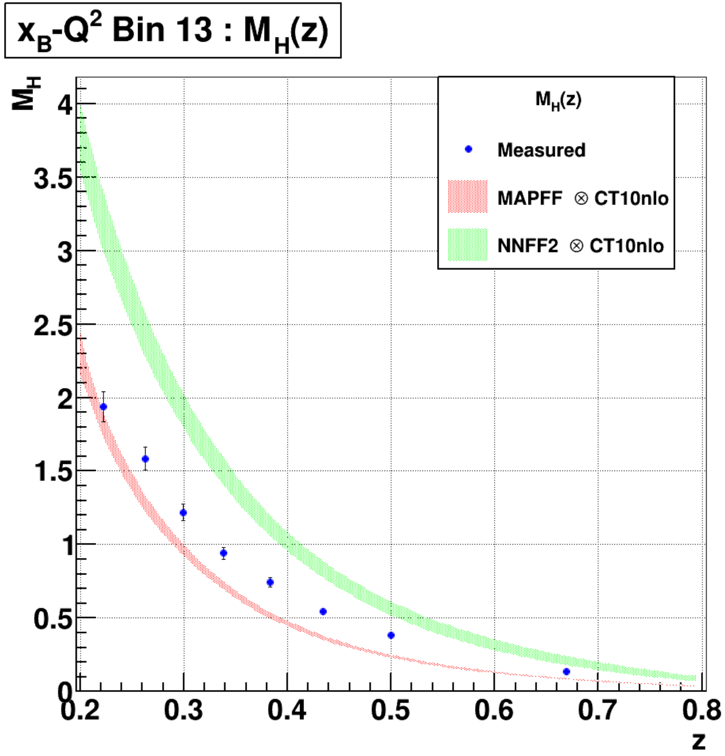

Phi Trento Studies

- The previous results just integrated over φ_h instead of fitting the distributions and extracting the A term.
- The results that follow are a first look at the φ_h distributions within each x-Q^2-z-p_T^2 bin.
- For these results, the binning scheme has been modified
  - Same each x-Q^2-z-p_T^2 binning as before
  - 12 φ_h bins
  - 20 $m_{\gamma\gamma}$ bins
- Within each φ_h bin the $m_{\gamma\gamma}$ distribution is fit and the number of pions and associated error is extracted. The fit range has been extended to 0.03-0.35 GeV, to help bring down the fit on the left side of the mass peak, but the signal region is the same.

PHI TRENTO STUDIES 2

- Within each φ_h bin the $m_{\gamma\gamma}$ distribution is fit and the number of pions and the integral error is extracted.
- 1^{st} Order cuts
  - Bin content > 1 pion
  - Acceptance > 1e-4
  - Bin content > bin error
  - Background ≥ 0
    - Some of the polynomial fits will give negative background in the signal region
    - The polynomial power was decreased and refit if this happened

$\varphi_H(Z, P_T^2)$ DISTRIBUTIONS

- The following results show the φ_h distribution with the $A(1 + B\cos(\varphi_h) + C\cos(2\varphi_h))$ fit in red along with a pol0 fit in green.
- The A and the pol0 terms are also listed.

x-Q² Bin 1 : $\phi_H(z, p_T^2)$

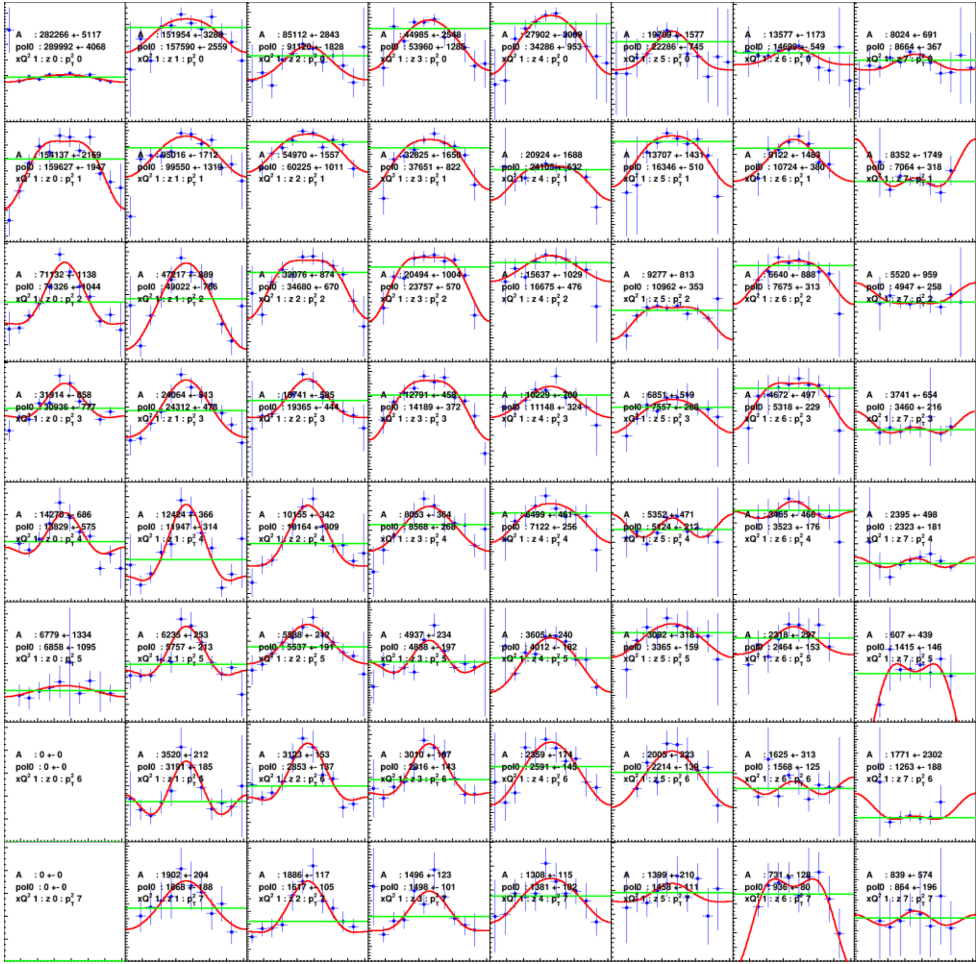

X-Q^2 Bin 2 : $\varphi_H(z, P_T^2)$

X-Q^2 Bin 3 : $\varphi_H(z, P_T^2)$

X-Q^2 Bin 4 : $\varphi_H(z, p_T^2)$

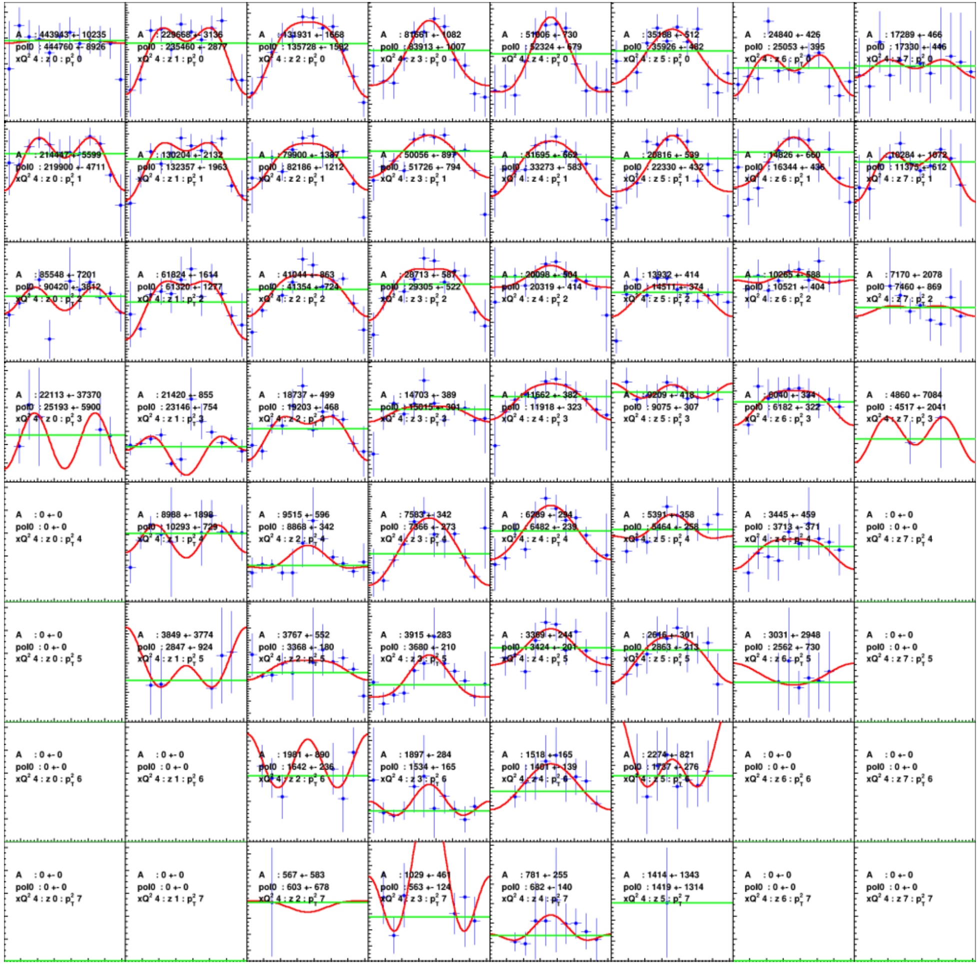

X-Q^2 Bin 5 : $\varphi_H(z, p_T^2)$

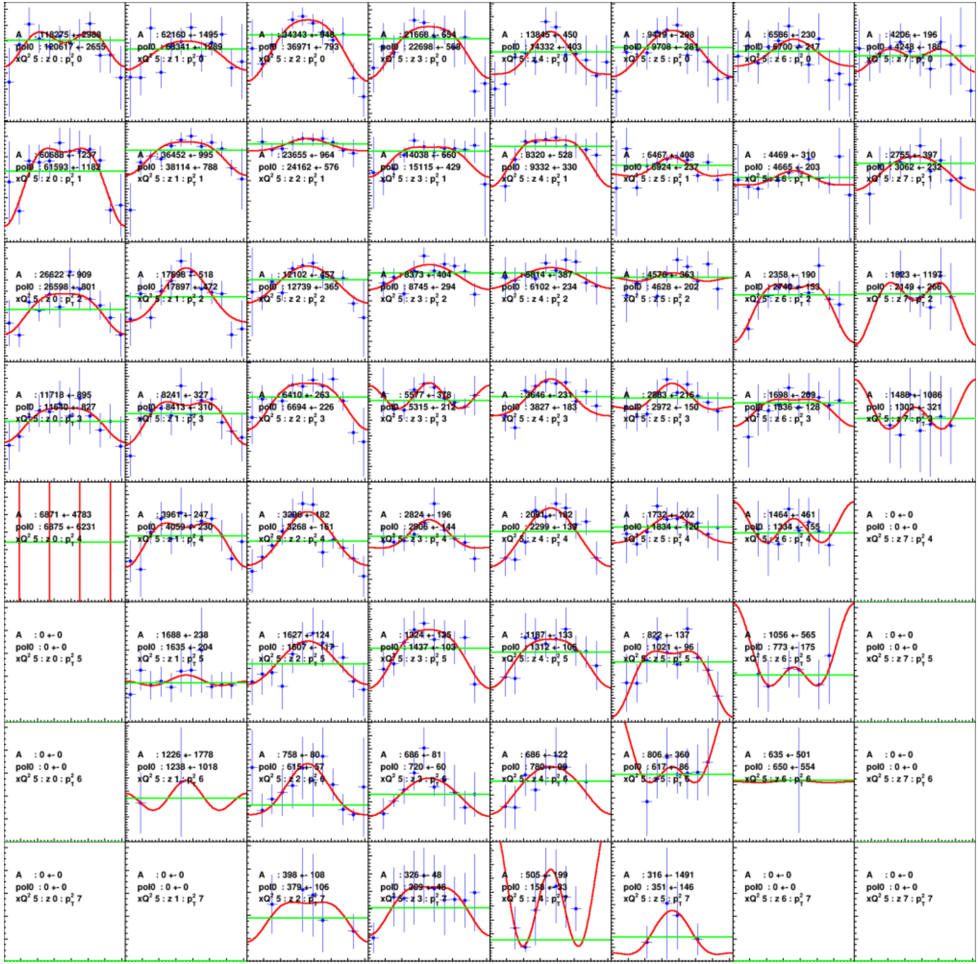

X-Q^2 Bin 6 : $\phi_H(z, p_T^2)$

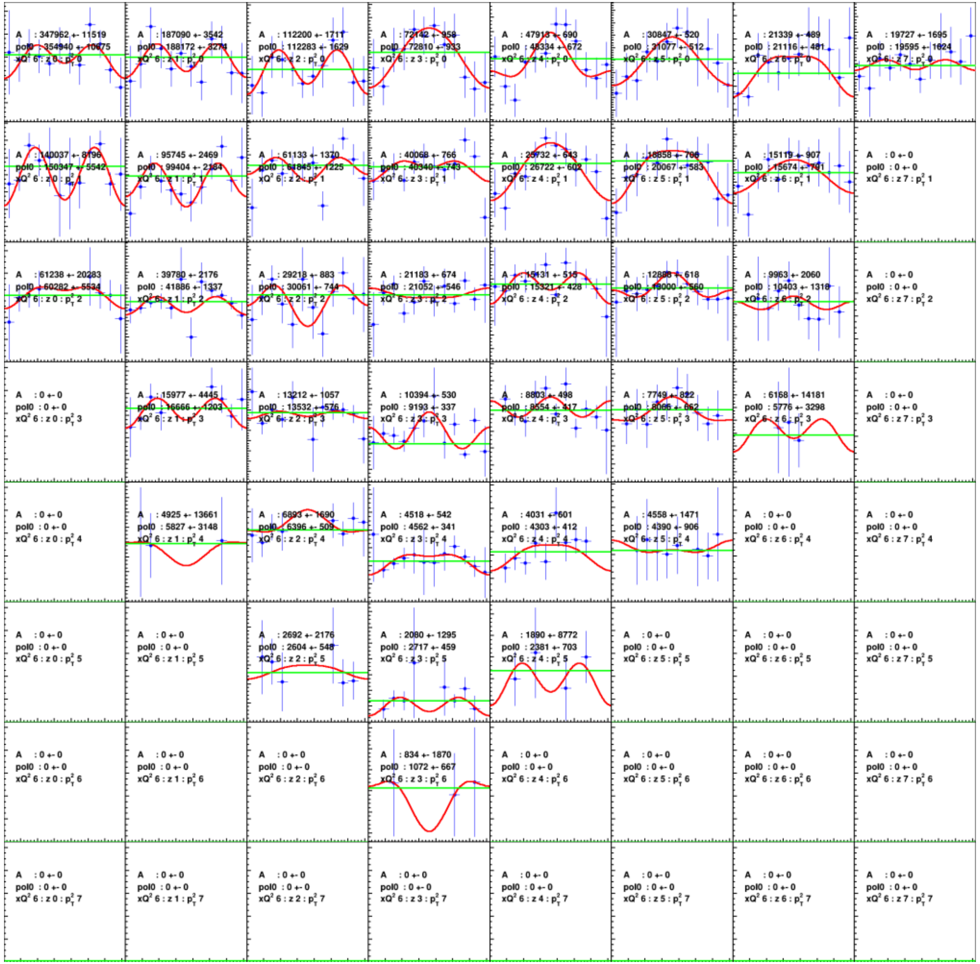

X-Q^2 Bin 7 : $\varphi_H(z, P_T^2)$

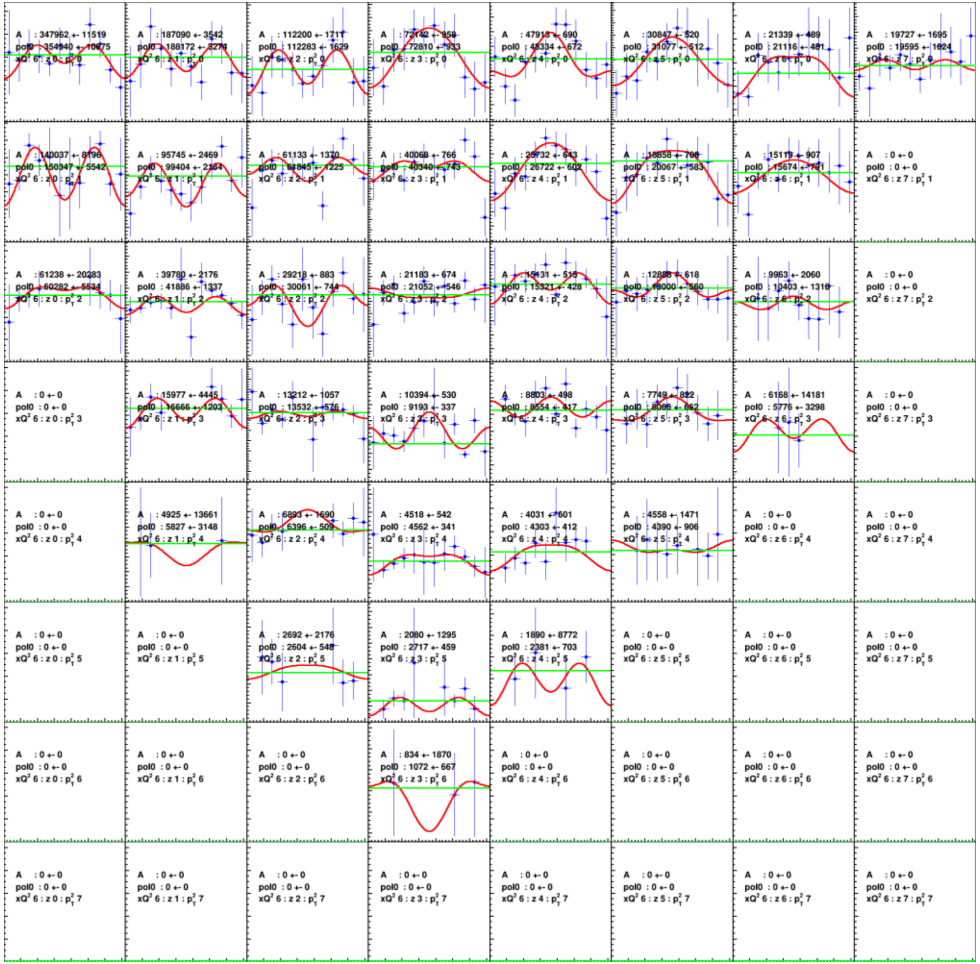

X-Q^2 Bin 8 : $\varphi_H(z, p_T^2)$

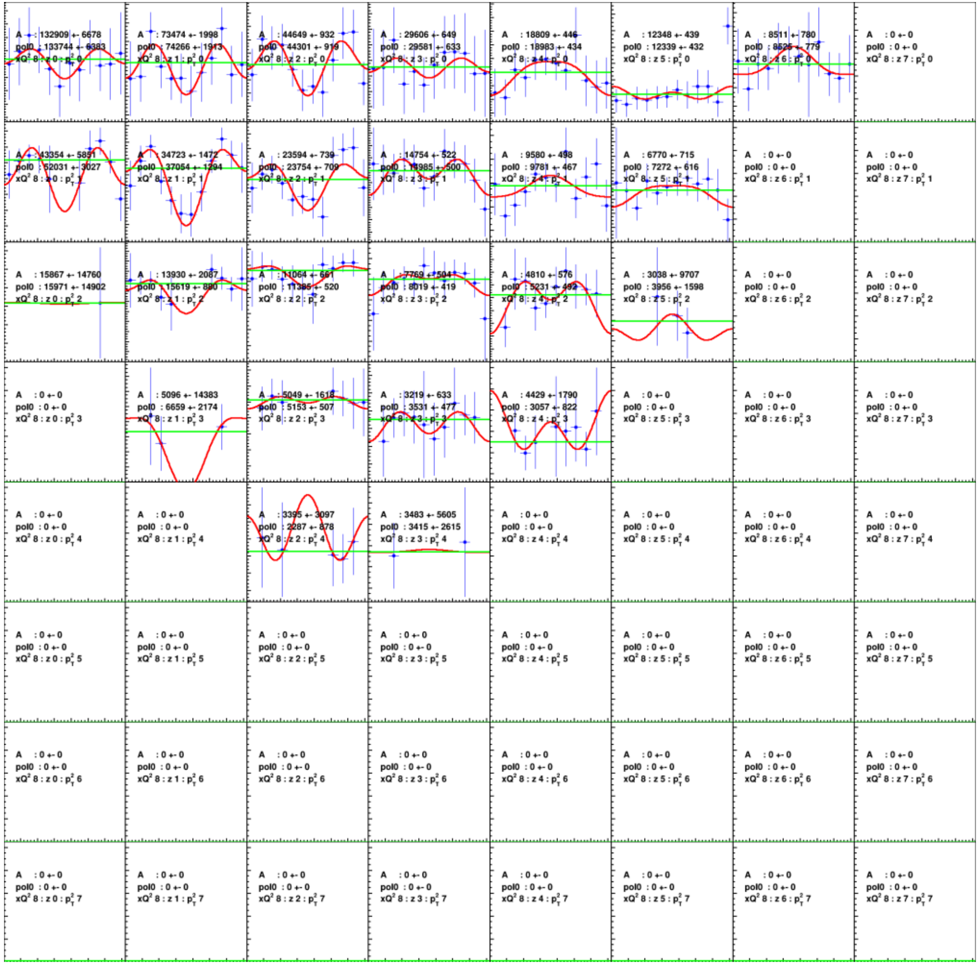

A(z) IN x-Q^2 BIN 1

- To the right is the acceptance of the z distributions.
- The uncut distributions are in blue, $M_x > 1.5$ in red, and $M_x > 1$ in green.

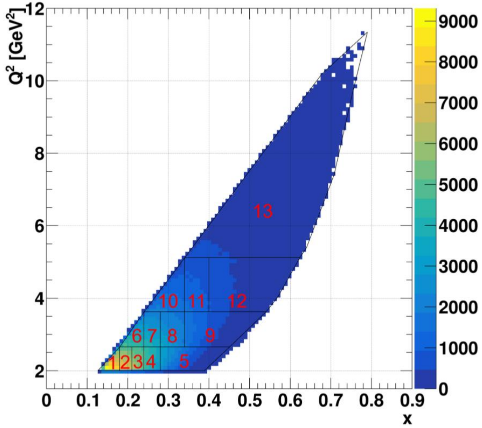

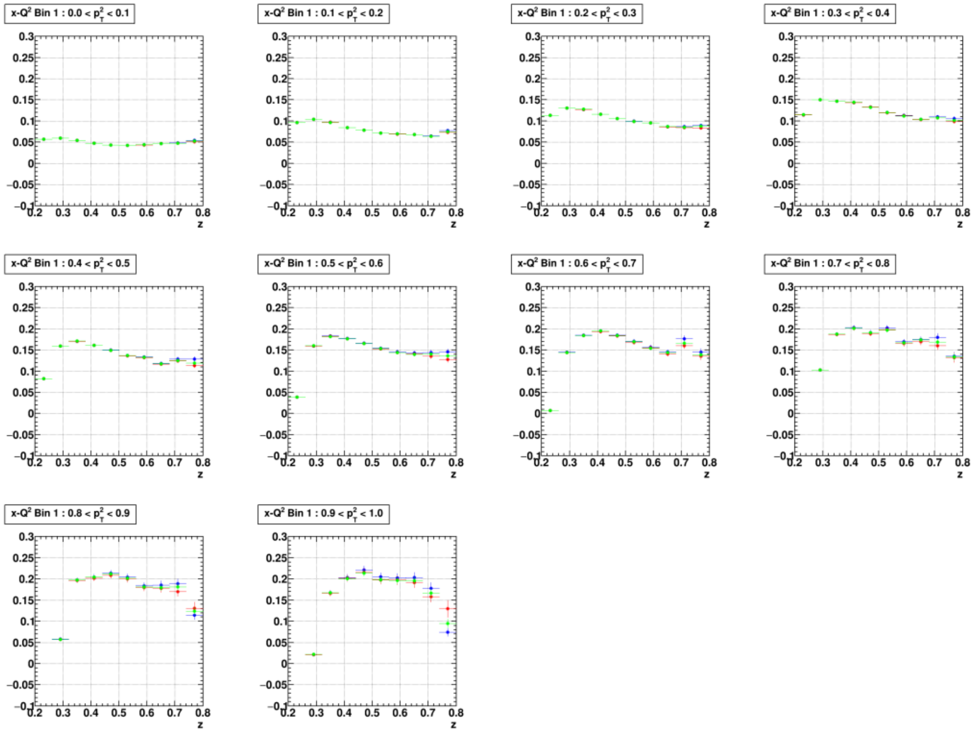

A(z) in x-Q^2 bin 2

- To the right is the acceptance of the z distributions.
- The uncut distributions are in blue, $M_x > 1.5$ in red, and $M_x > 1$ in green.

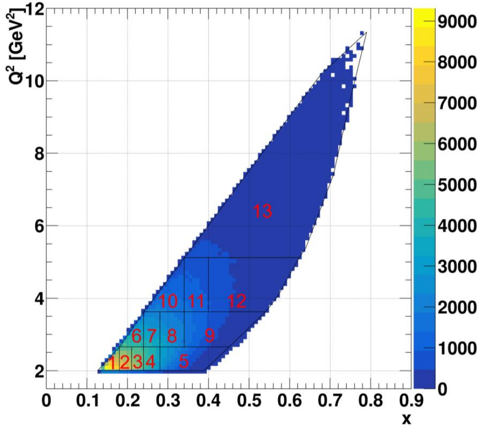

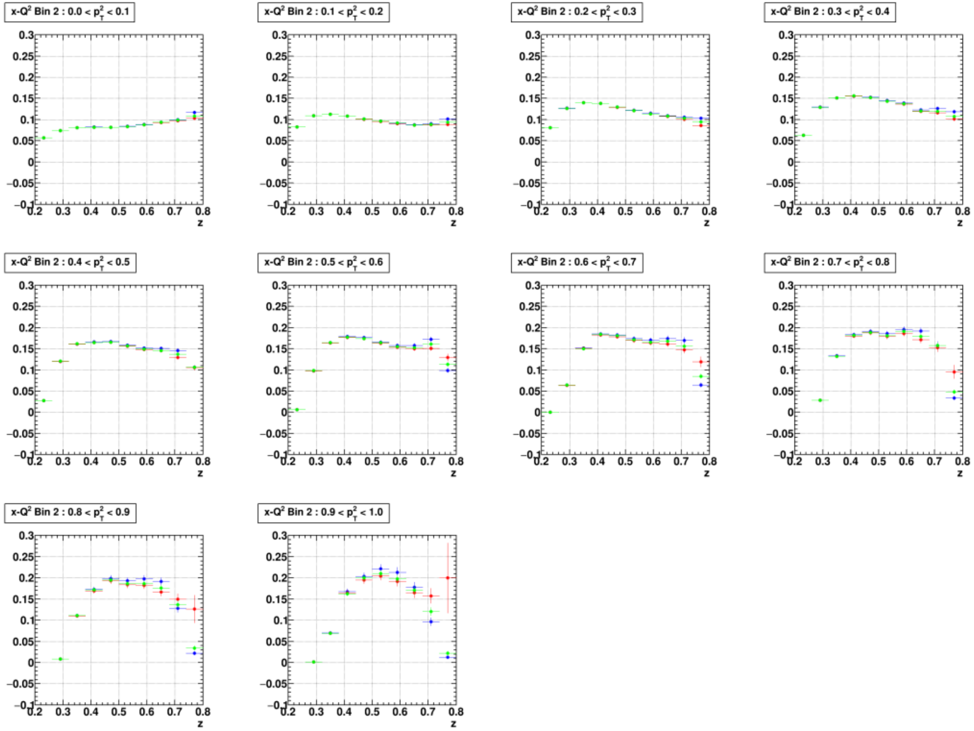

A(z) in x-Q^2 bin 3

- To the right is the acceptance of the z distributions.
- The uncut distributions are in blue, $M_x > 1.5$ in red, and $M_x > 1$ in green.

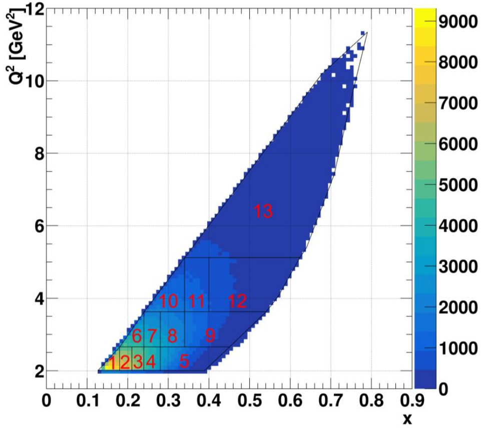

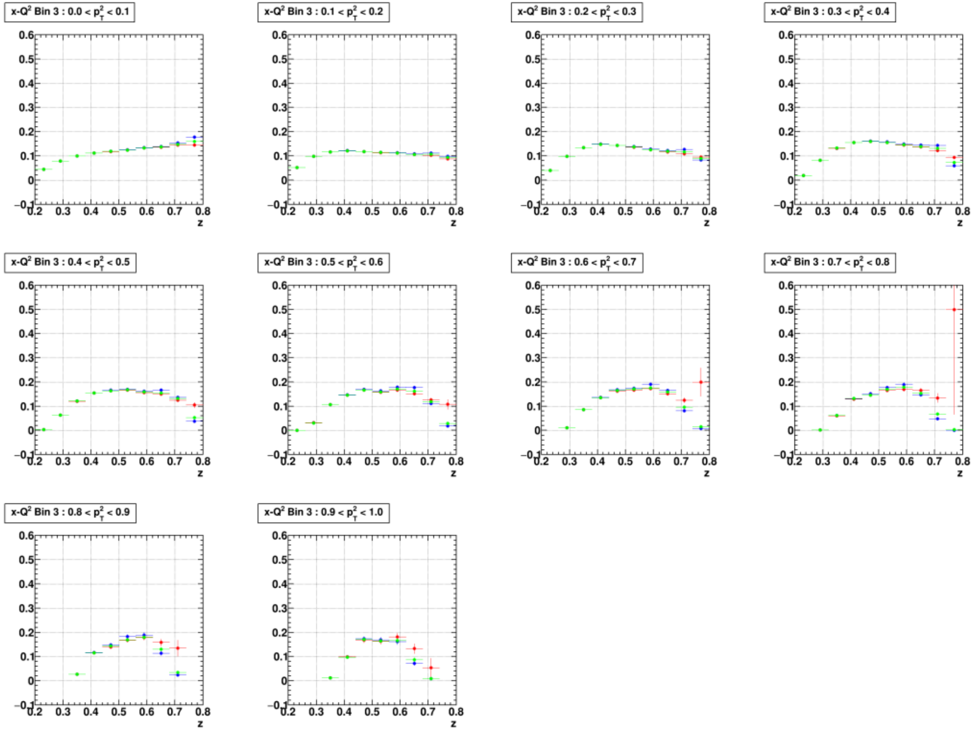

A(z) in x-Q^2 bin 4

- To the right is the acceptance of the z distributions.
- The uncut distributions are in blue, $M_x > 1.5$ in red, and $M_x > 1$ in green.

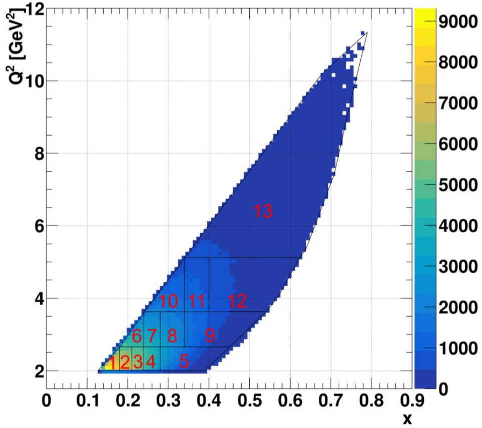

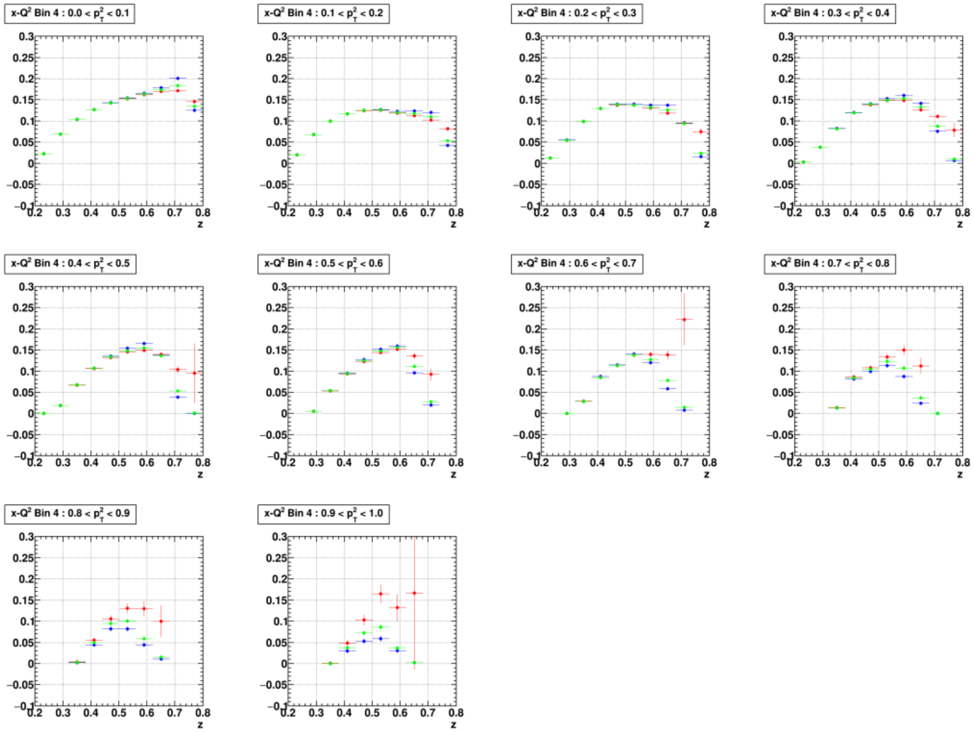

A(z) IN x-Q^2 BIN 5

- To the right is the acceptance of the z distributions.
- The uncut distributions are in blue, M_x > 1.5 in red, and M_x > 1 in green.

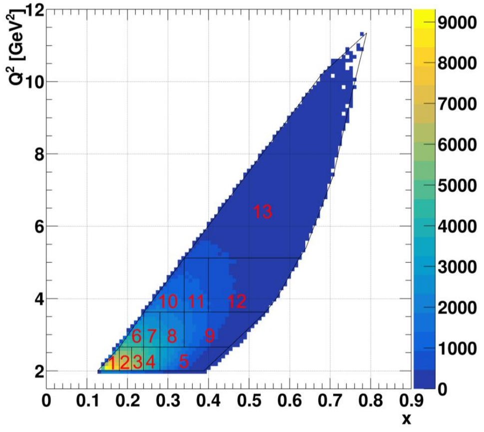

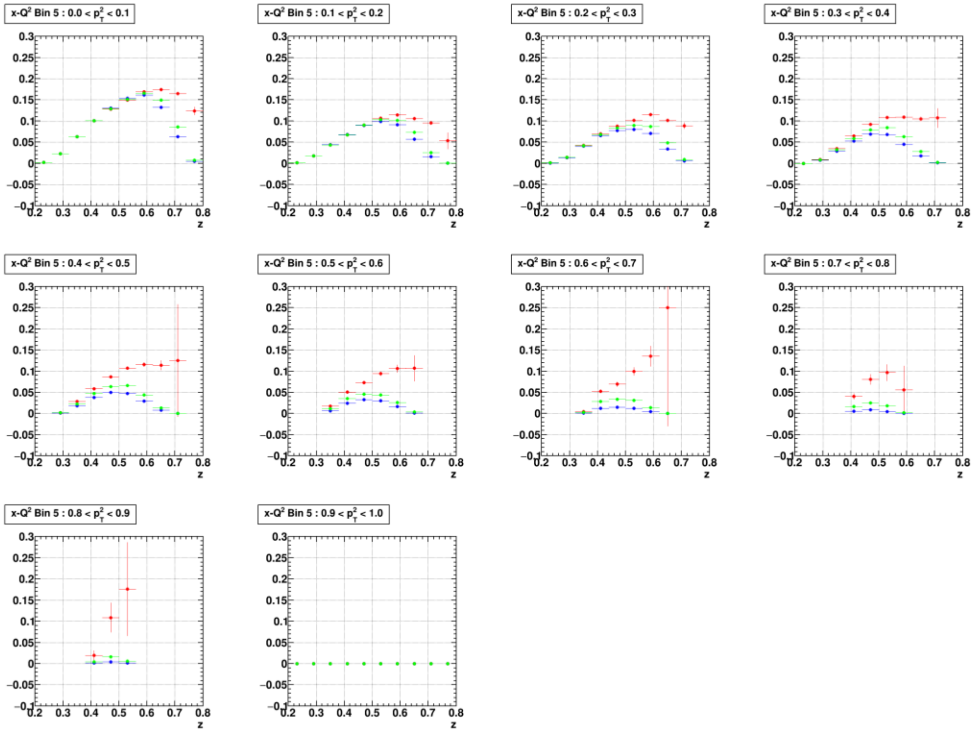

A(z) IN x-Q^2 BIN 6

- To the right is the acceptance of the z distributions.
- The uncut distributions are in blue, $M_x > 1.5$ in red, and $M_x > 1$ in green.

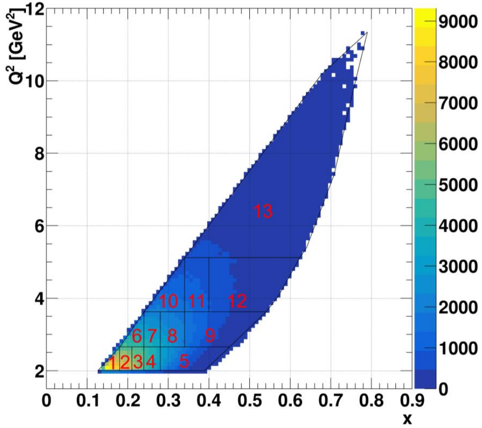

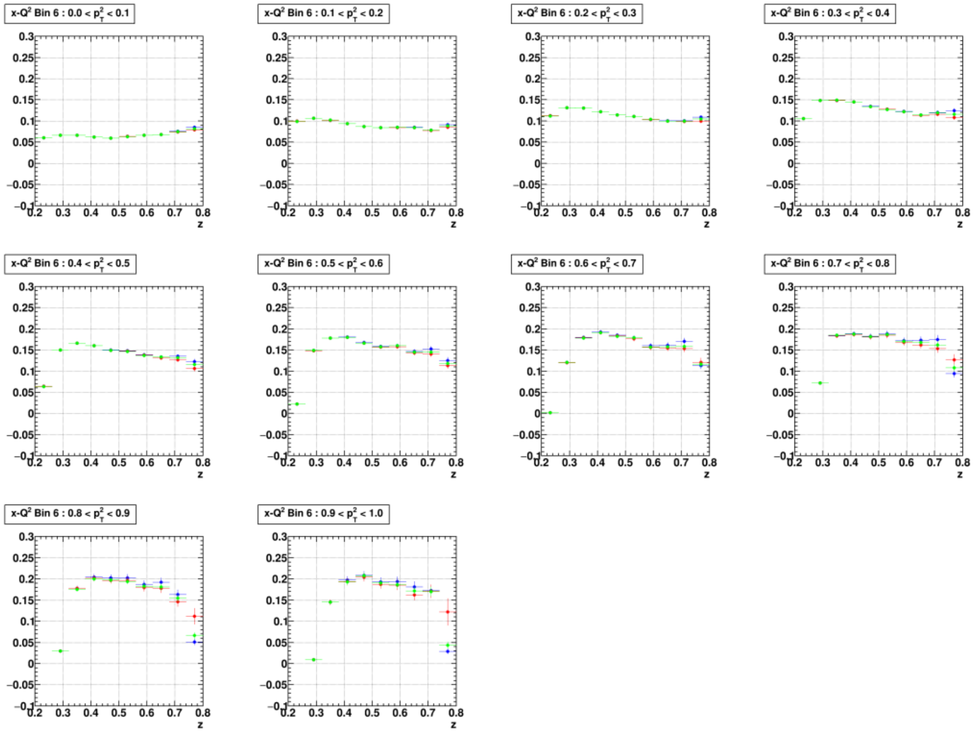

A(z) IN x-Q^2 BIN 7

- To the right is the acceptance of the z distributions.
- The uncut distributions are in blue, $M_x > 1.5$ in red, and $M_x > 1$ in green.

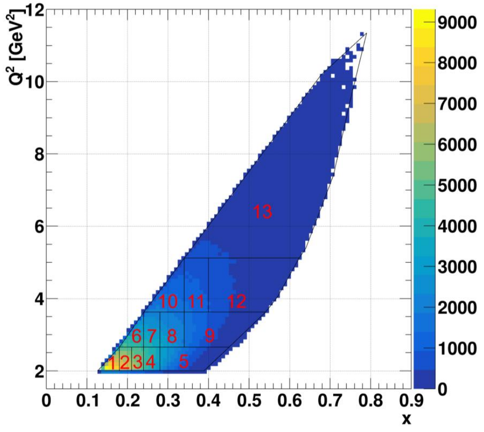

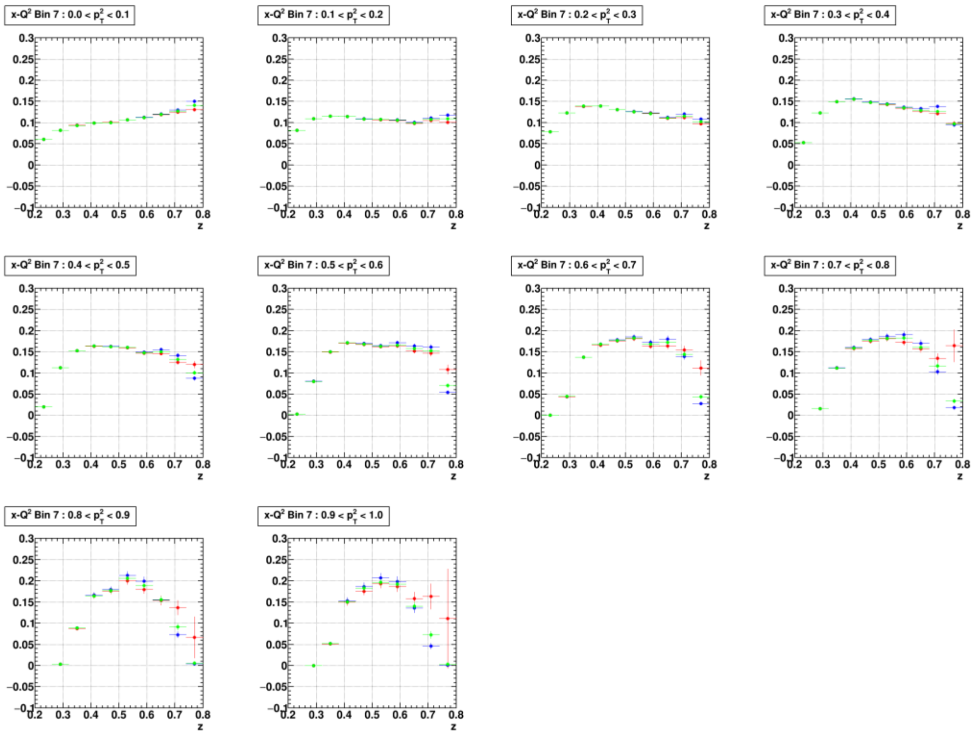

A(z) in x-Q^2 bin 8

- To the right is the acceptance of the z distributions.
- The uncut distributions are in blue, $M_x > 1.5$ in red, and $M_x > 1$ in green.

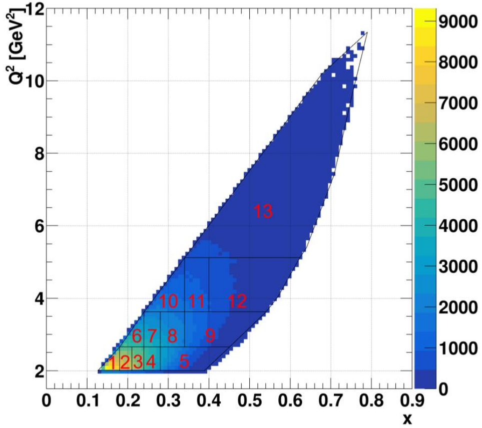

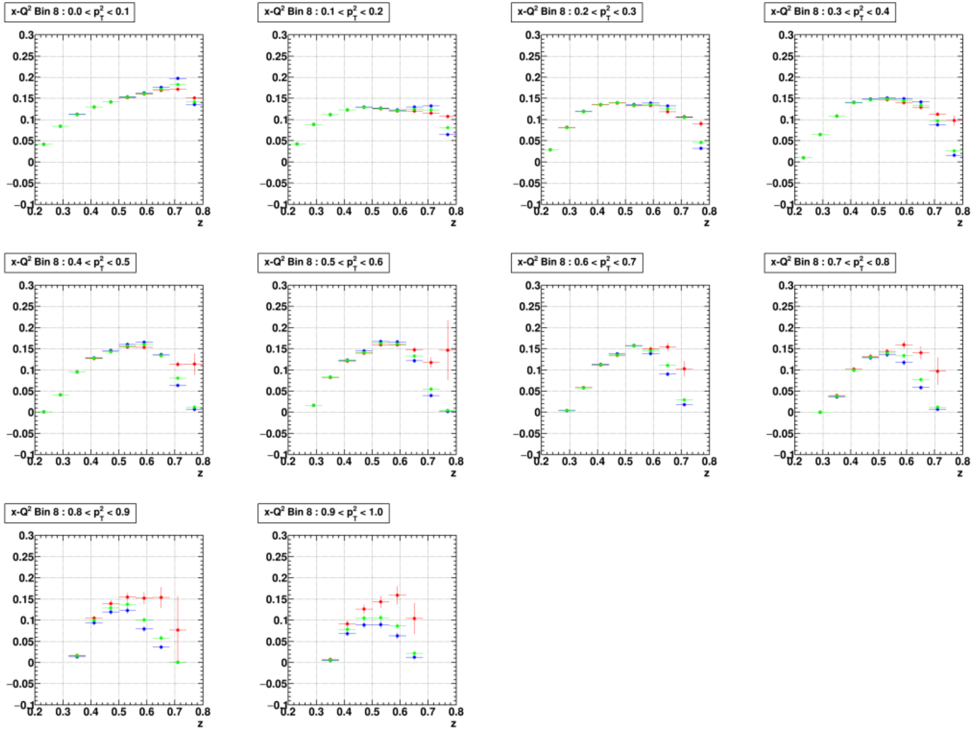

A(z) in x-Q^2 bin 9

- To the right is the acceptance of the z distributions.
- The uncut distributions are in blue, $M_x > 1.5$ in red, and $M_x > 1$ in green.

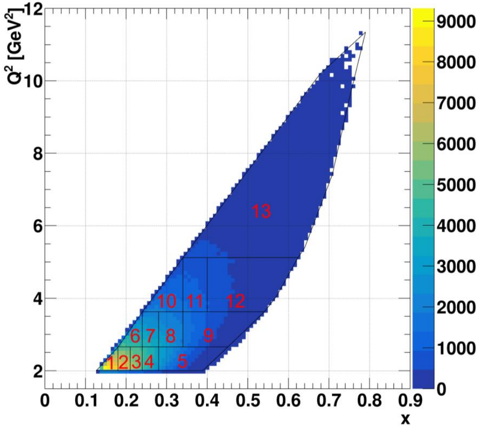

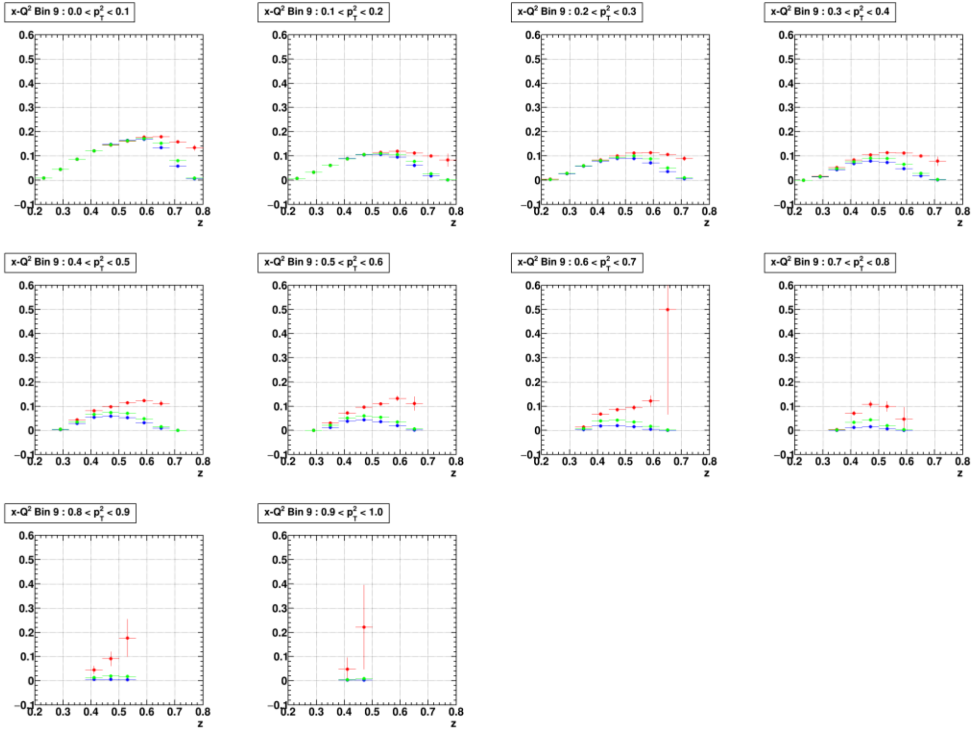

A(z) in x-Q^2 bin 10

- To the right is the acceptance of the z distributions.
- The uncut distributions are in blue, $M_x > 1.5$ in red, and $M_x > 1$ in green.

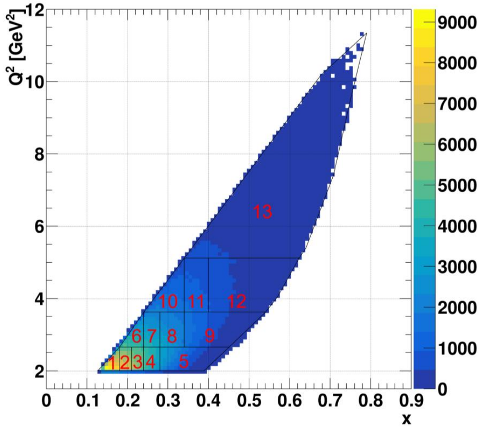

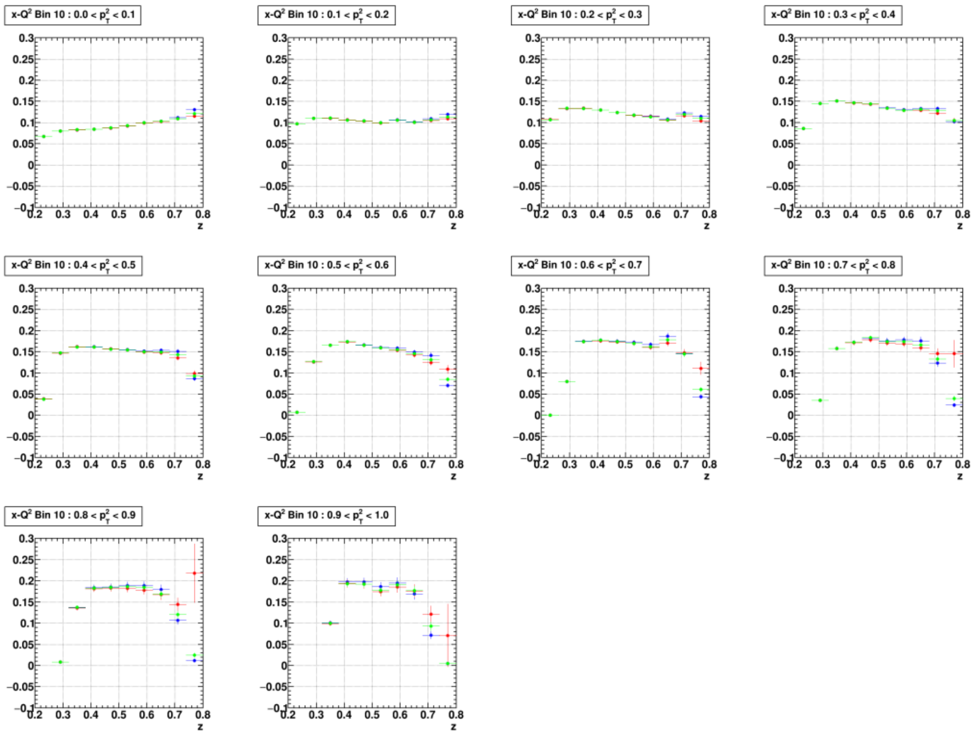

A(z) in x-Q² bin 11

- To the right is the acceptance of the z distributions.
- The uncut distributions are in blue, $M_x > 1.5$ in red, and $M_x > 1$ in green.

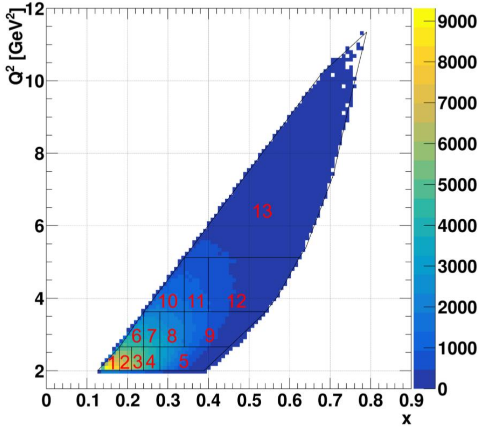

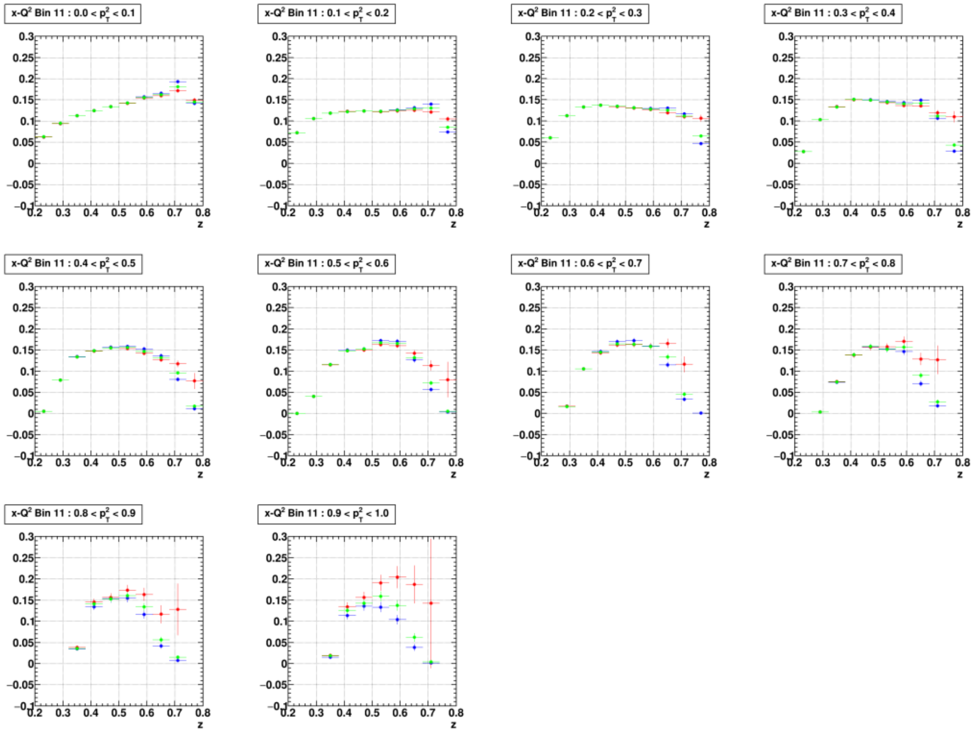

A(z) in x-Q^2 bin 12

- To the right is the acceptance of the z distributions.
- The uncut distributions are in blue, $M_x > 1.5$ in red, and $M_x > 1$ in green.

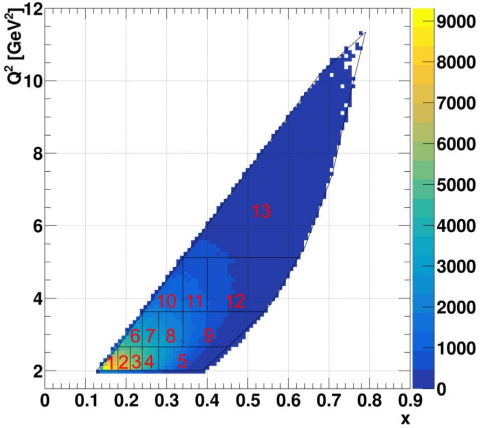

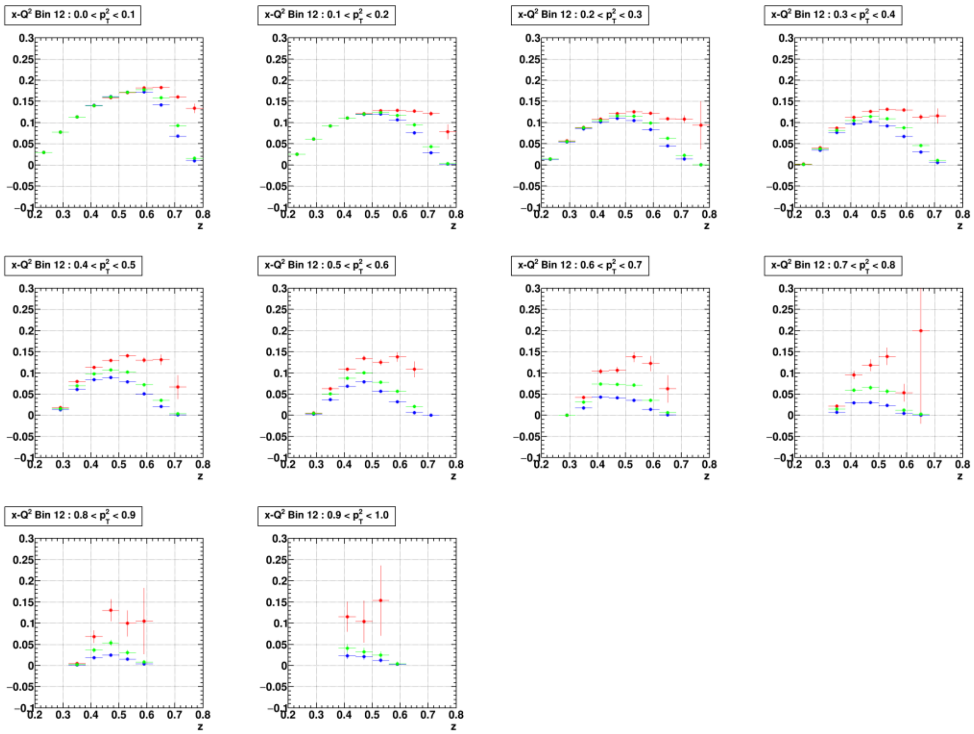

A(z) in x-Q^2 bin 13

- To the right is the acceptance of the z distributions.
- The uncut distributions are in blue, $M_x > 1.5$ in red, and $M_x > 1$ in green.